

**PRELIMINARY UPDATED GROUNDWATER FLOW AND
TRANSPORT MODELING REPORT FOR MARSHALL STEAM
STATION, TERRELL, NORTH CAROLINA**

November 2018

Prepared for
Duke Energy Carolinas, LLC

Investigators

Ronald W. Falta, Ph.D. – Falta Environmental, LLC
Regina Graziano, M.S. – SynTerra Corporation
Johnathan Ebenhack, M.S. – SynTerra Corporation
Rong Yu, Ph.D. – SynTerra Corporation
Lawrence C. Murdoch, Ph.D. – FRx, Inc.

TABLE OF CONTENTS

EXECUTIVE SUMMARY	ES-1
1.0 INTRODUCTION.....	1
1.1 General Setting and Background	1
1.2 Study Objectives	4
2.0 CONCEPTUAL MODEL	6
2.1 Aquifer System Framework	6
2.2 Groundwater Flow System	6
2.3 Hydrologic Boundaries	7
2.4 Hydraulic Boundaries	7
2.5 Sources and Sinks	8
2.6 Water Budget	8
2.7 Modeled Constituents of Interest	8
2.8 Constituent Transport.....	9
3.0 COMPUTER MODEL	10
3.1 Model Selection	10
3.2 Model Description	10
4.0 GROUNDWATER FLOW AND TRANSPORT MODEL CONSTRUCTION	11
4.1 Model Domain and Grid	11
4.2 Hydraulic Parameters.....	13
4.3 Flow Model Boundary Conditions.....	14
4.4 Flow Model Sources and Sinks.....	15
4.5 Flow Model Calibration Targets	17
4.6 Transport Model Parameters.....	17
4.7 Transport Model Boundary Conditions	19
4.8 Transport Model Sources and Sinks	20
4.9 Transport Model Calibration Targets.....	21
5.0 MODEL CALIBRATION TO CURRENT CONDITIONS	22
5.1 Flow Model.....	22
5.2 Flow Model Sensitivity Analysis.....	25
5.3 Historical Transport Model Calibration.....	25
5.4 Transport Model Sensitivity	27
6.0 PREDICTIVE SIMULATIONS OF CLOSURE SCENARIOS.....	29
6.1 Interim Period with Ash Basin Pond Decanted	30
6.2 Excavation Scenario.....	30
6.3 Final Cover Scenario.....	32
6.4 Hybrid Design Scenario.....	34
6.5 Conclusions Drawn from the Predictive Simulations.....	36
7.0 REFERENCES.....	38

LIST OF TABLES

- Table 5-1. Comparison of observed and computed heads for the calibrated flow model.
- Table 5-2. Calibrated hydraulic parameters.
- Table 5-3. Flow model sensitivity. The normalized root mean square error (NRMSE) is shown.
- Table 5-4. Ash basin boron source concentrations ($\mu\text{g/L}$) used in historical transport model from 1965 through 2018.
- Table 5-5. Ash landfill (Phase I and II) and PV Structural Fill boron source concentrations ($\mu\text{g/L}$) used in historical transport model.
- Table 5-6. Comparison of observed and simulated boron concentrations ($\mu\text{g/L}$) in monitoring wells.
- Table 5-7. Transport model sensitivity to the boron K_d values. The calibrated model has a normalized root mean square error (NRMSE) of 1.61%. Boron concentrations are shown for the calibrated model, and for models where the K_d is increased and decreased by a factor of 5.

LIST OF FIGURES

Figure ES-1. Simulated Boron concentrations transition zone, excavation, final cover, and hybrid simulations.

Figures ES-2. Boron time vs. concentration plots transition zone, excavation, final cover, and hybrid simulations.

Figure 1-1. Site location map, Marshall Steam Station, Terrell, NC.

Figure 4-1. Numerical model domain.

Figure 4-2. Fence diagram of the 3D hydrostratigraphic model used to construct the model grid.

Figure 4-3. Numerical grid used for flow and transport modeling viewed from the southeast.

Figure 4-4. Hydraulic conductivity measured in slug tests performed in coal ash at 14 sites in North Carolina.

Figure 4-5. Hydraulic conductivity measured in slug tests performed in saprolite at 10 Piedmont sites in North Carolina.

Figure 4-6. Hydraulic conductivity measured in slug tests performed in the transition zone at 10 Piedmont sites in North Carolina.

Figure 4-7. Hydraulic conductivity measured in slug tests performed in bedrock at 10 Piedmont sites in North Carolina.

Figure 4-8. Distribution of recharge zones in the model.

Figure 4-9. Surface water features included in the model outside of the ash basin area (the ash basin area is shown in Figure 4.10).

Figure 4-10. Surface water features included in the model in the ash basin area.

Figure 4-11. Location of water supply wells in the model area.

Figure 5-1. Zones used to define horizontal hydraulic conductivity and horizontal to vertical anisotropy in the ash.

Figure 5-2. Zones used to define horizontal hydraulic conductivity and horizontal to vertical anisotropy in the saprolite.

Figure 5-3. Zones used to define horizontal hydraulic conductivity and horizontal to vertical anisotropy in the transition zone.

Figure 5-4. Zones used to define horizontal hydraulic conductivity and horizontal to vertical anisotropy in the upper bedrock.

Figure 5-5. Zones used to define horizontal hydraulic conductivity and horizontal to vertical anisotropy in the upper bedrock.

Figure 5-6. Zones used to define horizontal hydraulic conductivity and horizontal to vertical anisotropy in the upper bedrock.

Figure 5-7. Zones used to define horizontal hydraulic conductivity and horizontal to vertical anisotropy in the upper bedrock.

Figure 5-8. Zones used to define horizontal hydraulic conductivity and horizontal to vertical anisotropy in the mid-depth bedrock.

Figure 5-9. Zones used to define horizontal hydraulic conductivity and horizontal to vertical anisotropy in the lower bedrock.

Figure 5-10. Comparison of observed and computed heads from the calibrated steady state flow model.

Figure 5-11. Simulated heads in the transition zone.

Figure 5-12. Simulated heads in the second fractured bedrock model layer.

Figure 5-13. Groundwater divide and flow directions at the MSS.

Figure 5-14. COI source zones in the ash basin for the historical transport model.

Figure 5-15. COI source zones in the ash landfills and structural fill for the historical transport model.

Figure 5-16a. Simulated July 2018 boron concentrations ($\mu\text{g/L}$) in the transition zone.

Figure 5-16b. Simulated July 2018 boron concentrations ($\mu\text{g/L}$) in the upper bedrock.

Figure 6-1. Simulated hydraulic heads in the transition zone after ash basin pond decanting.

Figure 6-2. Simulated boron concentrations in the transition zone in 2038 for a simulation where the ash basin lake has been decanted.

Figure 6-3. Drain network used in excavation simulations to represent springs and streams that may form.

Figure 6-4. Simulated hydraulic heads for excavation case.

Figure 6-5 a,b,c,d. Simulated boron concentrations in the transition zone (layer 8) in 2050 (a), 2100 (b), 2200 (c), and 2300 (d) for the excavation scenario.

Figure 6-6 a,b,c,d. Simulated boron concentrations in the upper bedrock (layer 9) in 2050 (a), 2100 (b), 2200 (c), and 2300 (d) for the excavation scenario.

Figure 6-7. Locations for boron time-series plots.

Figure 6-8. Predicted boron concentrations at point 1 near Lake Norman for the excavation case.

Figure 6-9. Predicted boron concentrations at point 2 east of the Phase I ash landfill for the excavation case.

Figure 6-10. Proposed ash basin underdrain system for the final cover simulations.

Figure 6-11. Simulated hydraulic heads for the final cover case.

Figure 6-12 a,b,c,d. Simulated boron concentrations in the transition zone (layer 8) in 2050 (a), 2100 (b), 2200 (c), 2300 (d) for the final cover scenario.

Figure 6-13 a,b,c,d. Simulated boron concentrations in the upper bedrock (layer 9) in 2050 (a), 2100 (b), 2200 (c), 2300 (d) for the final cover scenario.

Figure 6-14. Predicted boron concentrations at point 1 near Lake Norman for the final cover case.

Figure 6-15. Predicted boron concentrations at point 2 east of the Phase I ash landfill for the final cover case.

Figure 6-16. Hybrid closure design used in simulations (from AECOM, 2015).

Figure 6-17. Drains used in the hybrid design simulation.

Figure 6-18. Simulated hydraulic heads for the hybrid scenario.

Figure 6-19 a,b,c,d. Simulated boron concentrations in the transition zone (layer 8) in 2050 (a), 2100 (b), 2200 (c), 2300 (d) for the hybrid scenario.

Figure 6-20 a,b,c,d. Simulated boron concentrations in the upper bedrock (layer 9) in 2050 (a), 2100 (b), 2200 (c), 2300 (d) for the hybrid scenario.

Figure 6-21. Predicted boron concentrations at point 1 near Lake Norman for the hybrid case.

Figure 6-22. Predicted boron concentrations at location 2 east of the Phase I ash landfill for the hybrid case.

Figure 6-23. Comparison of closure options for the transition flow zone - Model years 2050 and 2100.

Figure 6-24. Comparison of closure options for the transition flow zone - Model years 2200 and 2300.

Figure 6-25. Comparison of closure options for the upper bedrock flow zone - Model years 2050 and 2100.

Figure 6-26. Comparison of closure options for the upper bedrock flow zone - Model years 2200 and 2300.

EXECUTIVE SUMMARY

Duke Energy Carolinas, LLC (Duke Energy) owns and operates the Marshall Steam Station (MSS, Plant, or Site) in Terrell, Catawba County, North Carolina. MSS began operation in 1965 and currently operates four coal-fired units. The first two units began operation in 1965 and 1966 with a capacity of 350 MW each. The second two units began operation in 1969 and 1970 with a capacity of 648 MW each. The current electric generating capacity is 2090 MW. Coal combustion residuals (CCR) have historically been managed in the Site's ash basin, on-site landfills, and as structural fills. Inorganic compounds in the ash have dissolved and transported in groundwater in the vicinity of the ash basin.

Preliminary numerical simulations of groundwater flow and transport have been calibrated to current conditions and used to evaluate different scenarios being considered as options for closure of the ash basin. The predictive simulations presented herein are not intended to represent a final detailed closure design. These simulations use conceptual designs that are subject to change as new data are evaluated and the closure plans are finalized. The simulations are intended to show the key characteristics of groundwater flow and mobile constituent transport that are expected to result from the closure actions under consideration. It should be noted that for groundwater modeling purposes, a reasonable assumption was made for initiation dates for each of the closure options. The assumed dates were based on information provided by Duke Energy that is currently evolving and may vary from dates provided in contemporary documents. The potential variance in closure dates presented in the preliminary groundwater model is inconsequential to the results of the model as it does not produce substantial changes in the modeled scenarios. This preliminary model report is intended to provide basic model development information and simulations of conceptual basin closure designs. A more detailed model report is planned for inclusion in the groundwater corrective action plan (CAP) scheduled for submittal in December 2019.

The model simulations were developed using flow and transport models MODFLOW and MT3DMS. Boron was the constituent of interest (COI) selected to estimate the time to achieve compliance because it is highly mobile in groundwater and tends to have the largest extent of

migration. The less mobile, more reactive constituents (i.e. arsenic, selenium, chromium, etc.) will follow the same flow path as boron; however, they generally are not present at concentrations greater than the 15A NCAC 02L .0202 Groundwater Quality Standard (2L standard) beyond the compliance boundary.

The results of the model simulations indicate the boron plume configuration over time is different for the three closure scenarios: excavation, final cover (closure-in-place), and hybrid (Figure ES-1 and ES-2)¹. The differences are caused by changes to the groundwater flow field that would occur following excavation in the excavation and hybrid closure scenarios. Without any additional corrective action, it is expected that the three scenarios will take hundreds of years for boron to be below the 2L standard at the closure-specific compliance boundaries near Lake Norman. These times would likely be reduced if groundwater extraction wells were used to control the boron plume. Boron concentrations shown in groundwater beneath Lake Norman do not represent surface water concentrations in Lake Norman. In the simulations no public or private wells are impacted. Three closure-specific compliance boundaries² were used to evaluate the results:

- Excavation scenario is evaluated using a compliance boundary that is 250 feet (ft) from the current waste boundary.
- Final Cover scenario is evaluated using a compliance boundary that is 500 ft from the current waste boundary.
- Hybrid scenario is evaluated using a compliance boundary 250 ft from the final waste boundary.

Two reference locations (point 1 and point 2) near the current compliance boundary were also used to evaluate changes in boron concentrations with time for the three closure designs, in the absence of any additional corrective action. These points are located along the eastern side of the current compliance boundary near Lake Norman where boron concentrations greater than the 2L standard extend out farthest from the compliance boundary and were chosen as conservative locations to track boron beyond the compliance boundary. The simulated boron concentrations exceeded the 2L standard at point 1 and point 2 during historical operation of the ash basin. The

¹ It is noted that these modeled scenarios do not include any active form of groundwater remediation. The relative benefits of various groundwater remediation alternatives will be addressed in the CAP.

² These compliance boundaries are based upon retention of the NPDES permit for the Final Cover scenario and the proposed North Carolina CCR Rules for the Excavation and Hybrid scenarios.

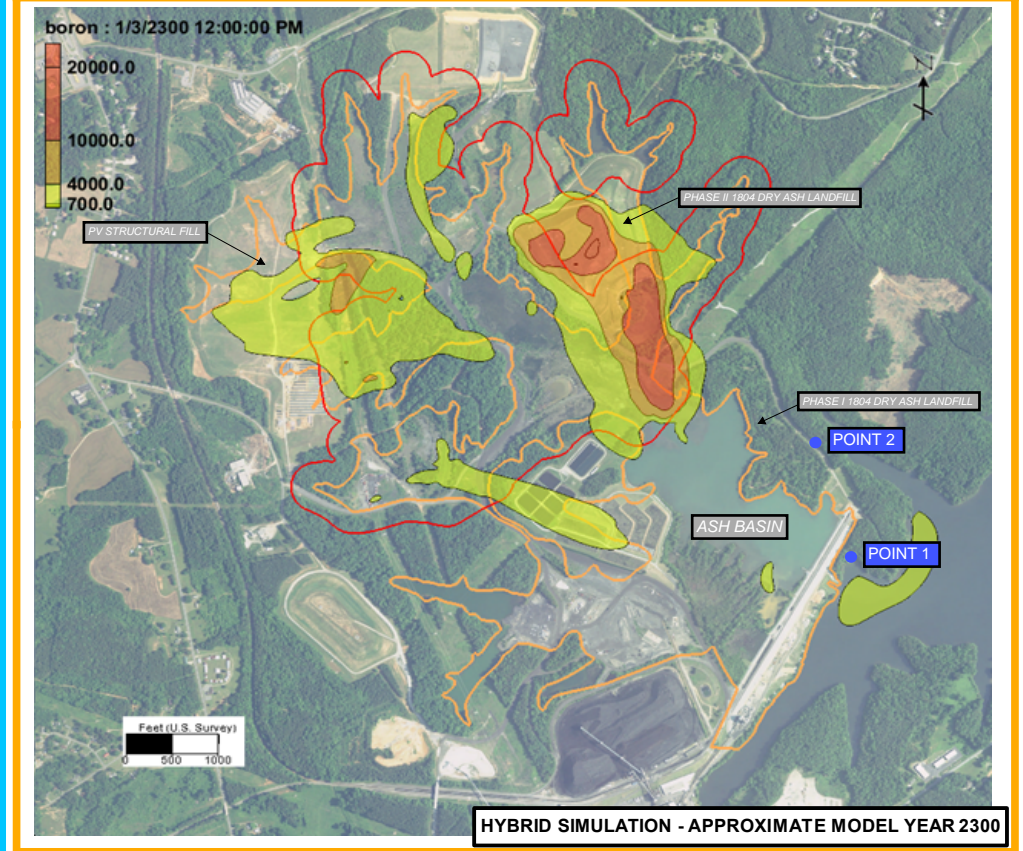
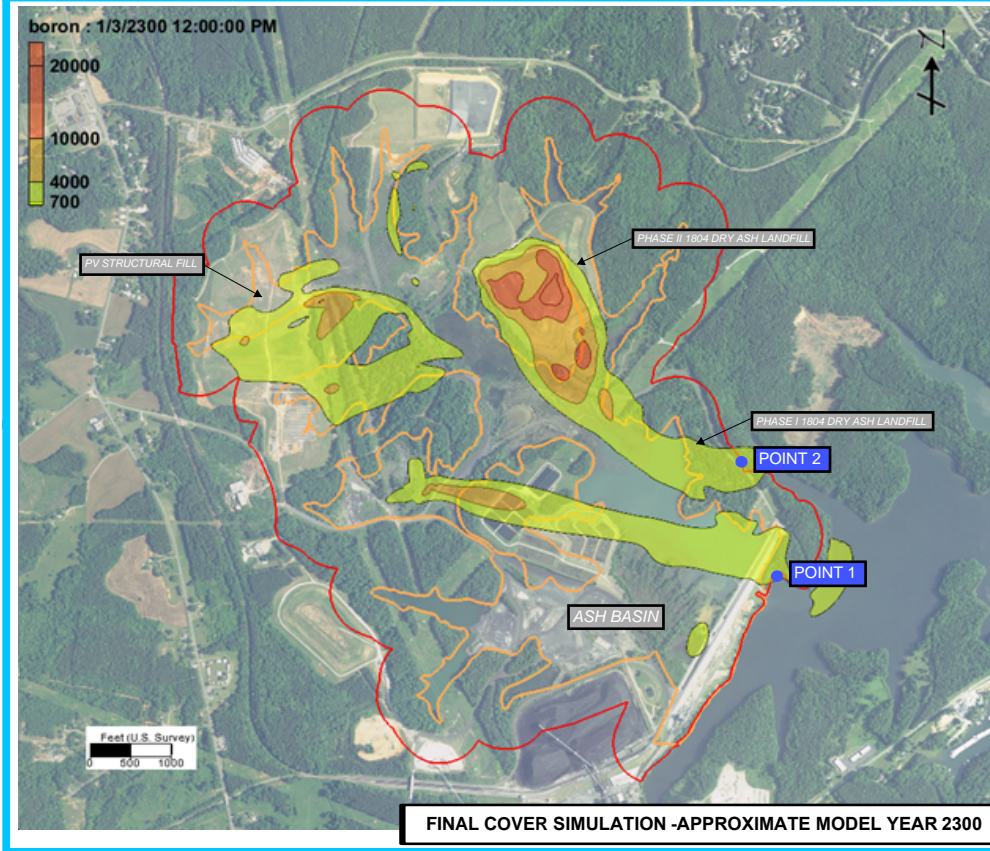
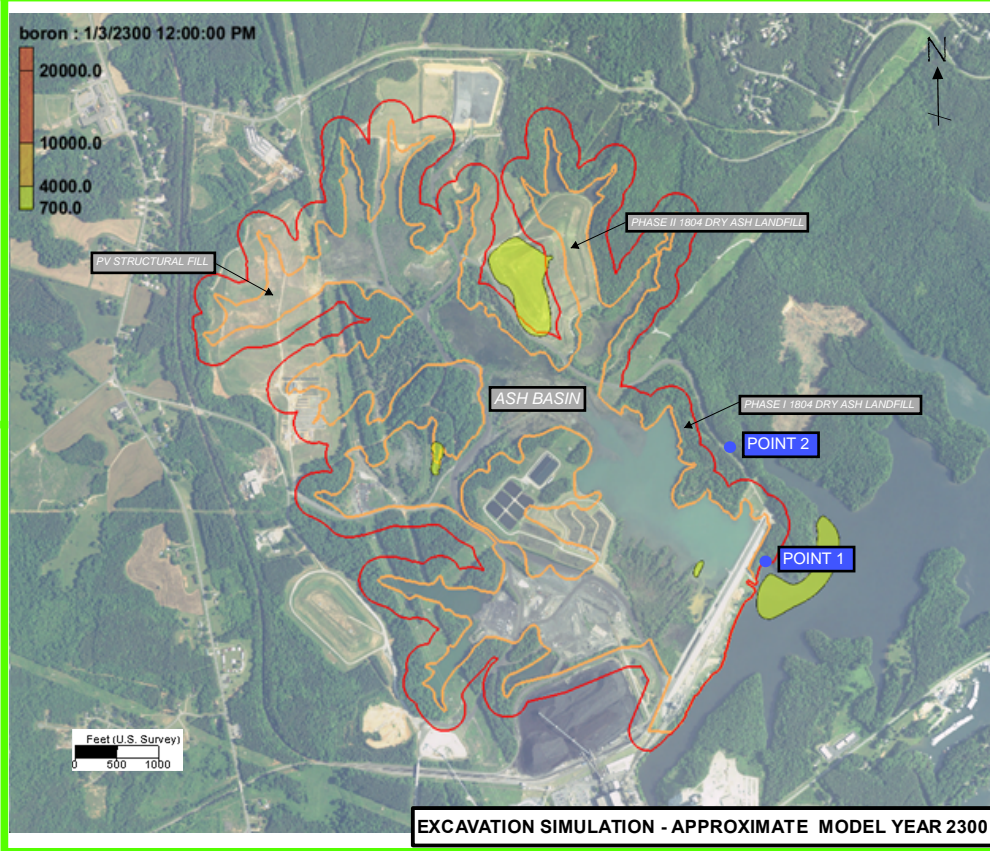
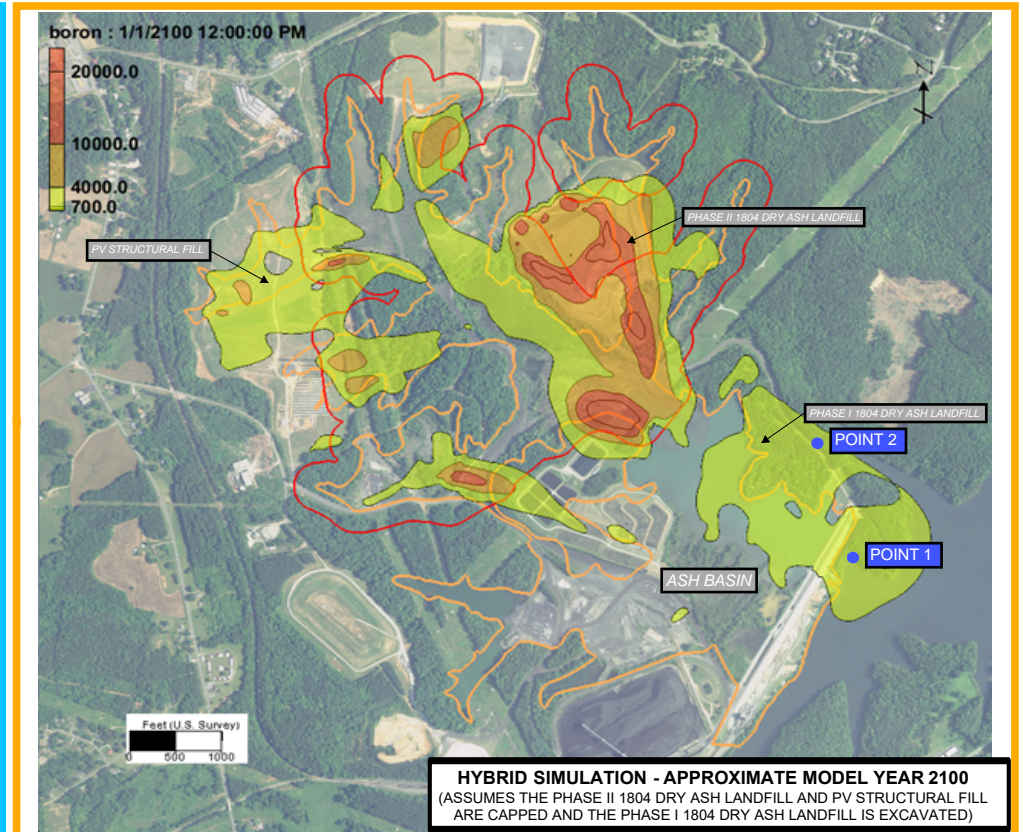
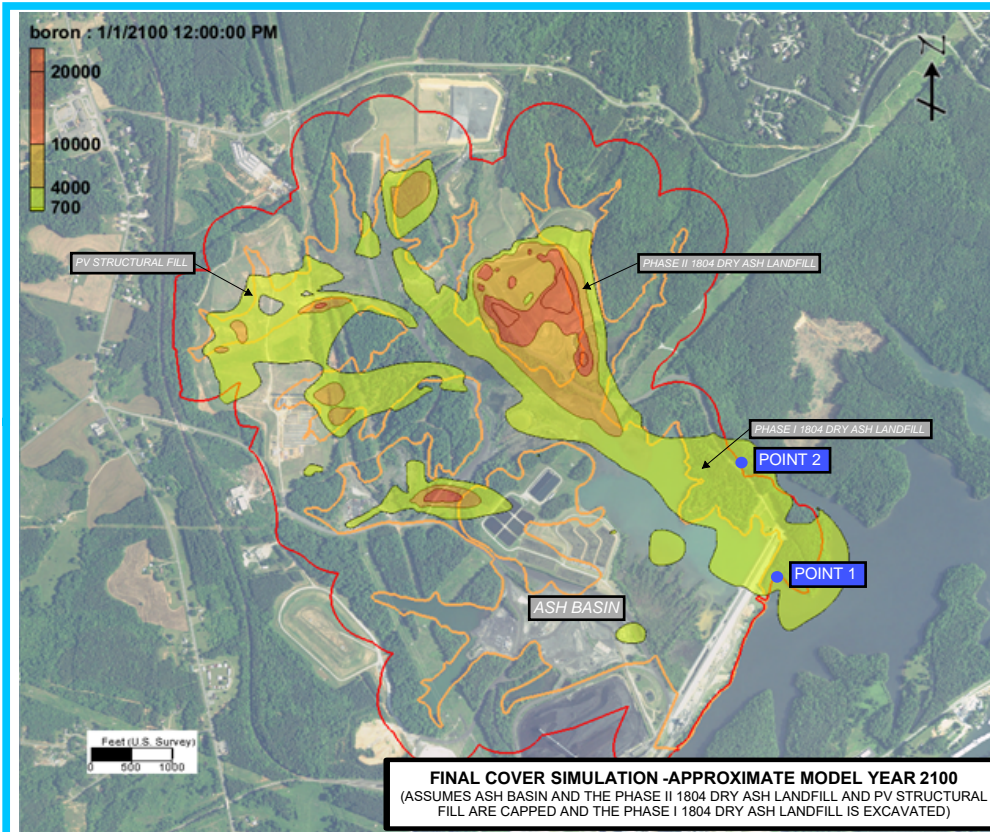
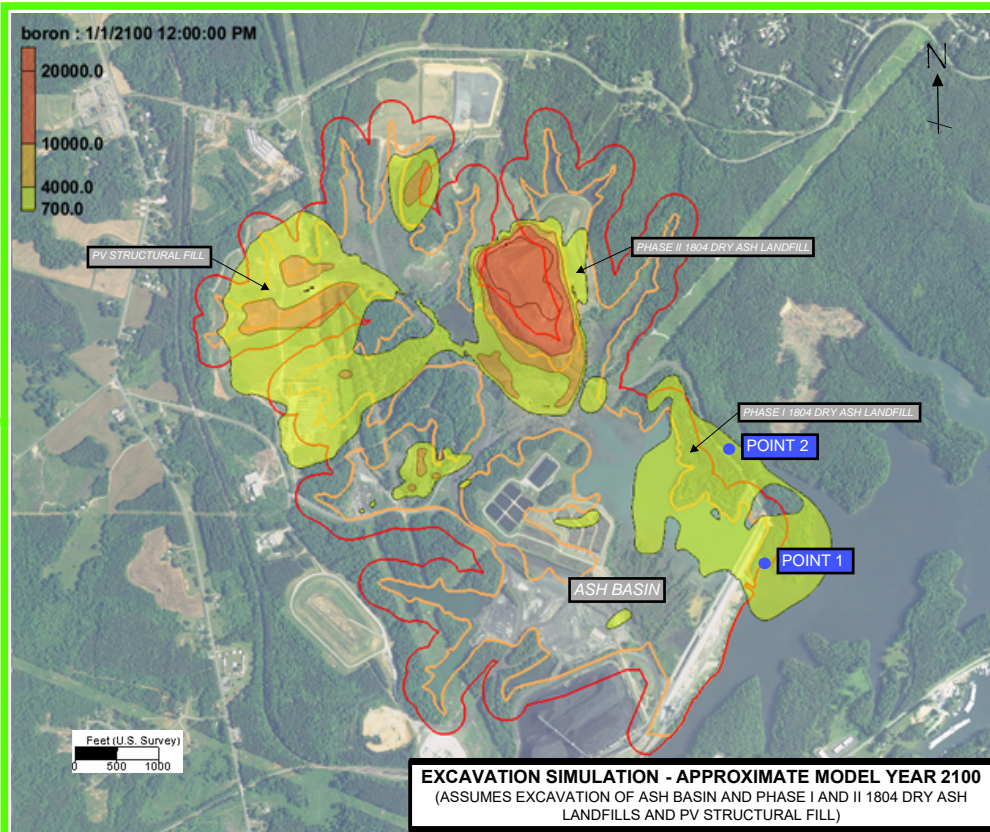
boron concentrations decrease over the next 100-700 years with boron receding behind the current compliance boundary at these locations by about 2200 for excavation, 2750 with final cover, and 2200 with the hybrid design (Figure ES-2).

Data from recent ash basin and underlying saprolite pumping tests and planned deep bedrock wells within and near the ash basin dam will reduce model uncertainty, and these results will be incorporated into the next version of this model.

Water supply wells and private wells near the Marshall Plant are outside the groundwater flow system of the ash basin. In the simulations, boron is not found in public or private wells, which is consistent with water sampling from domestic and water supply wells where no constituents released from ash were detected. Future modeling projections for all three closure scenarios predict private and public water wells will not be impacted by boron.

¹ It is noted that these modeled scenarios do not include any active form of groundwater remediation. The relative benefits of various groundwater remediation alternatives will be addressed in the CAP.

² These compliance boundaries are based upon retention of the NPDES permit for the Final Cover scenario and the proposed North Carolina CCR Rules for the Excavation and Hybrid scenarios.



LEGEND

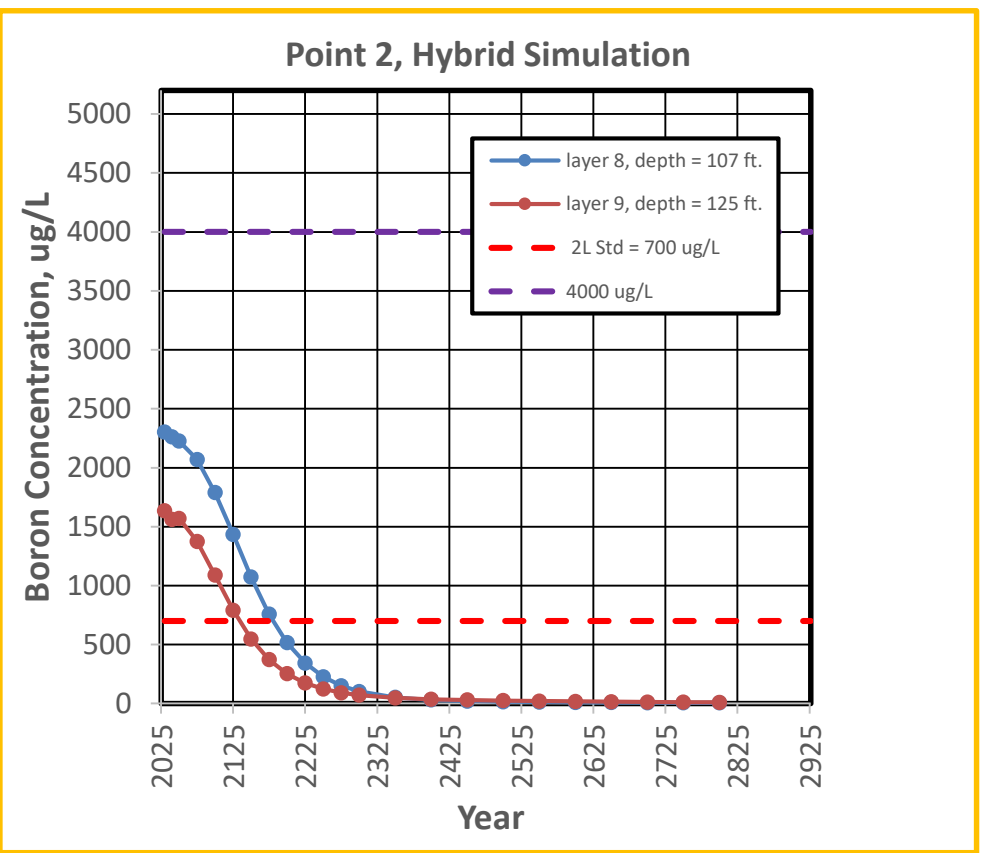
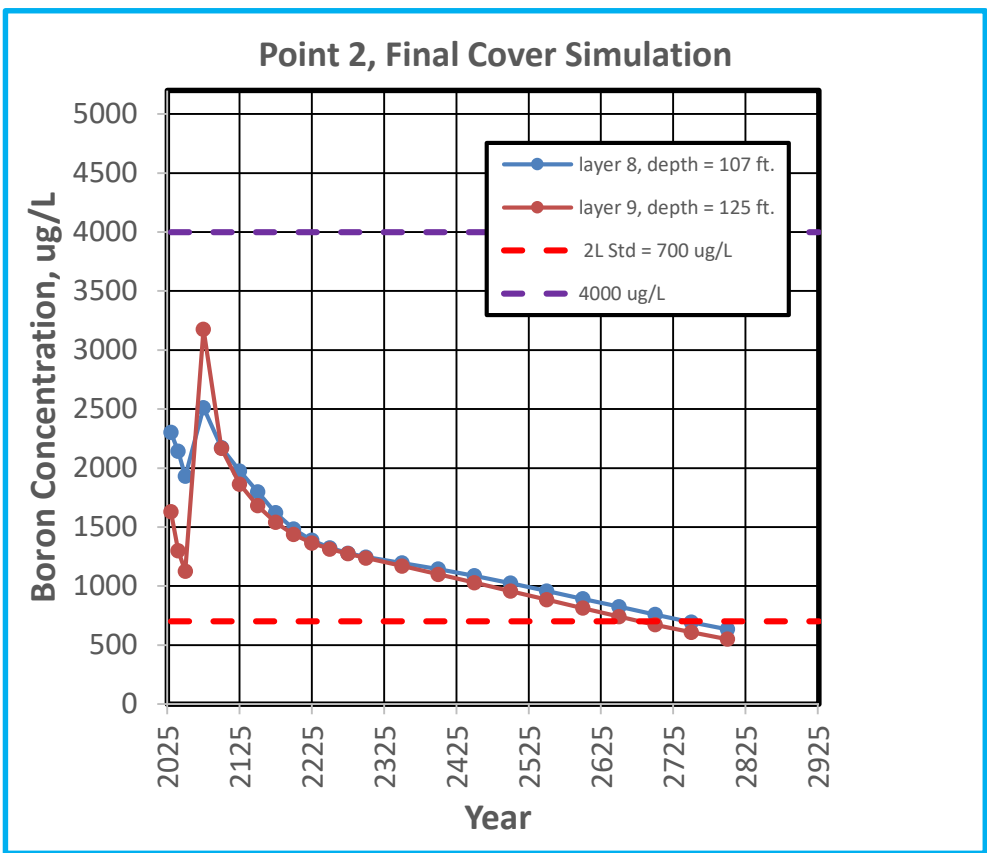
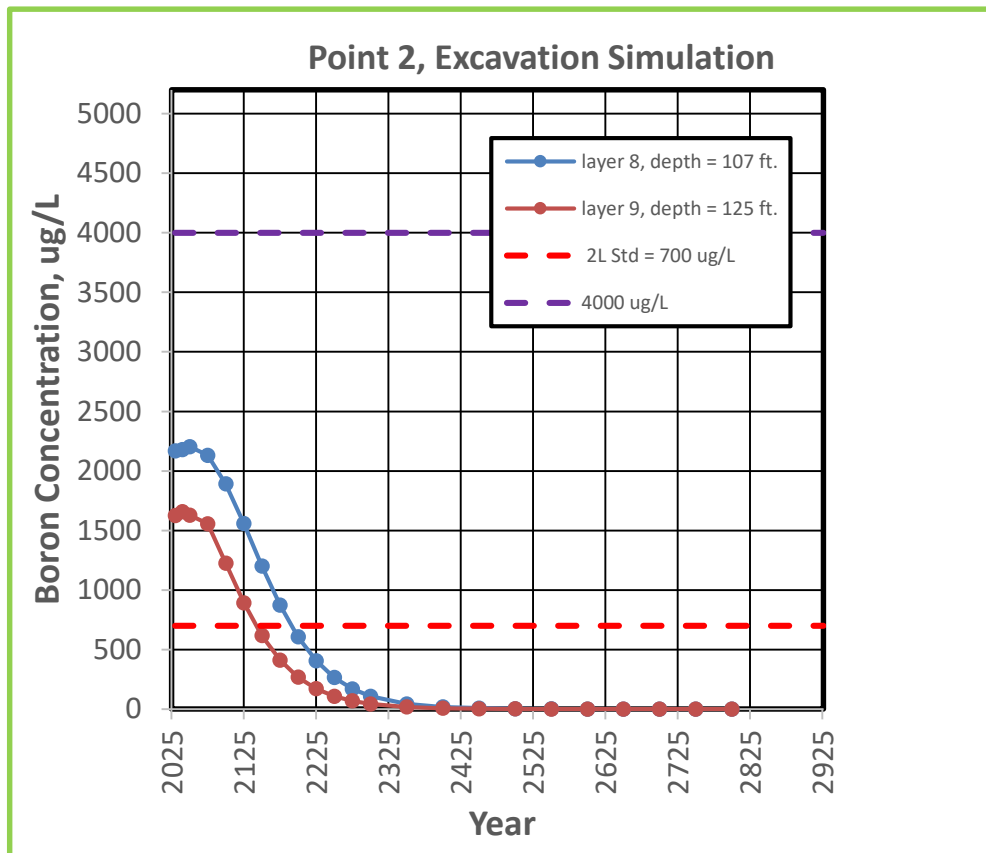
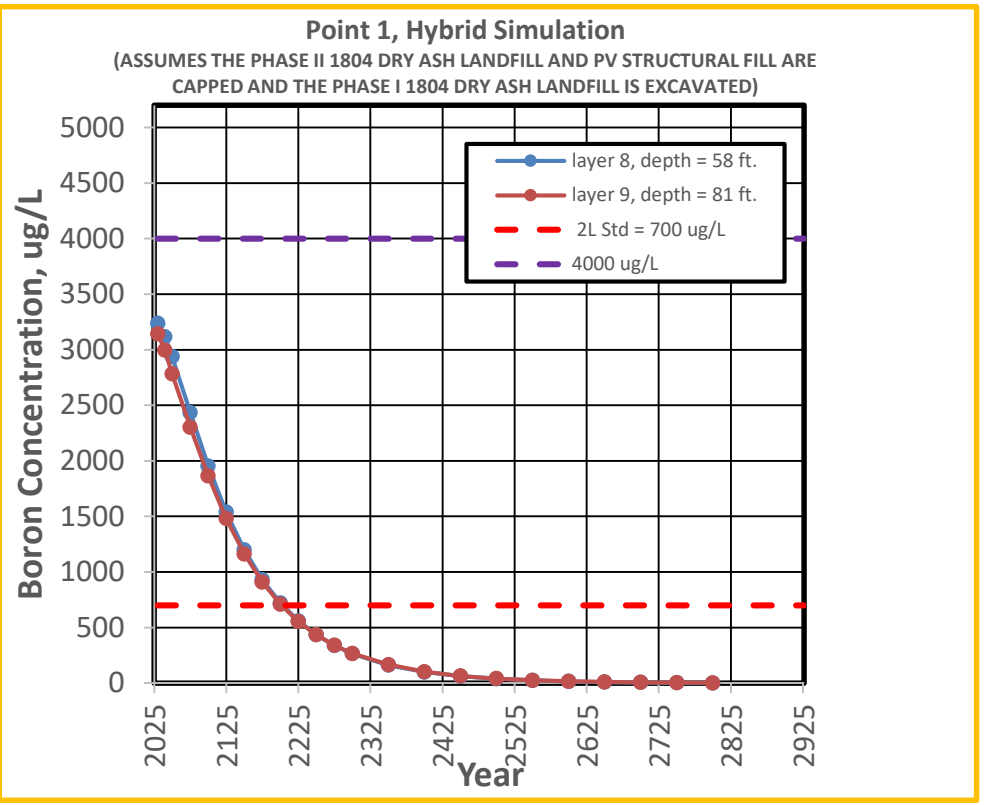
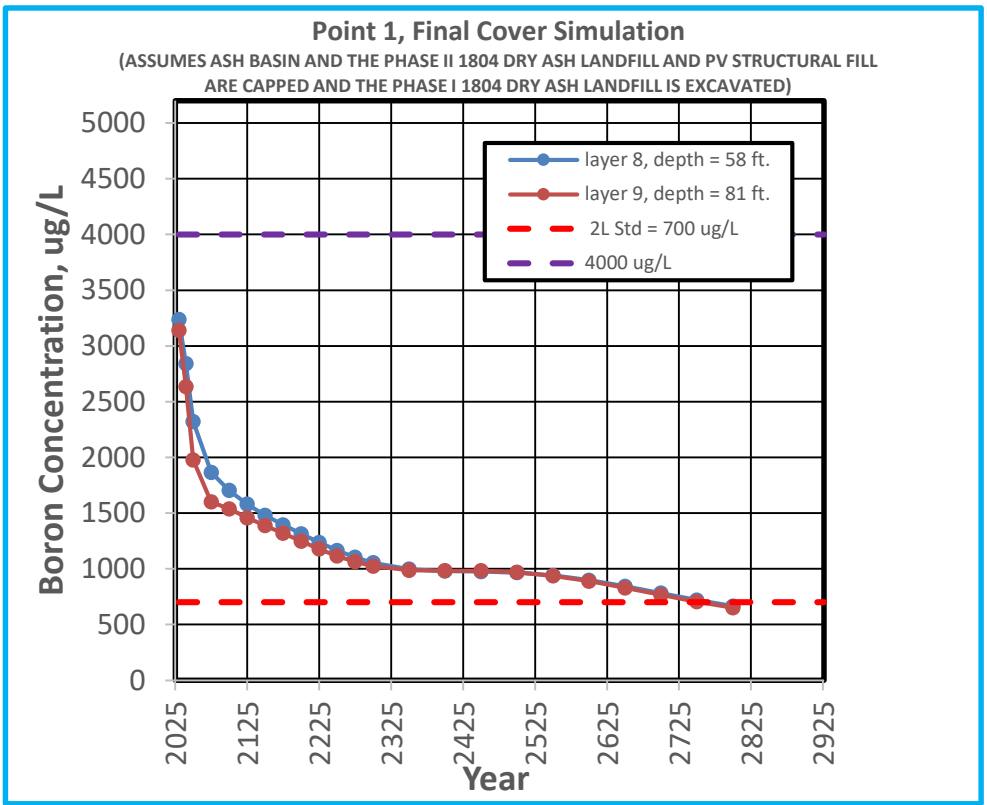
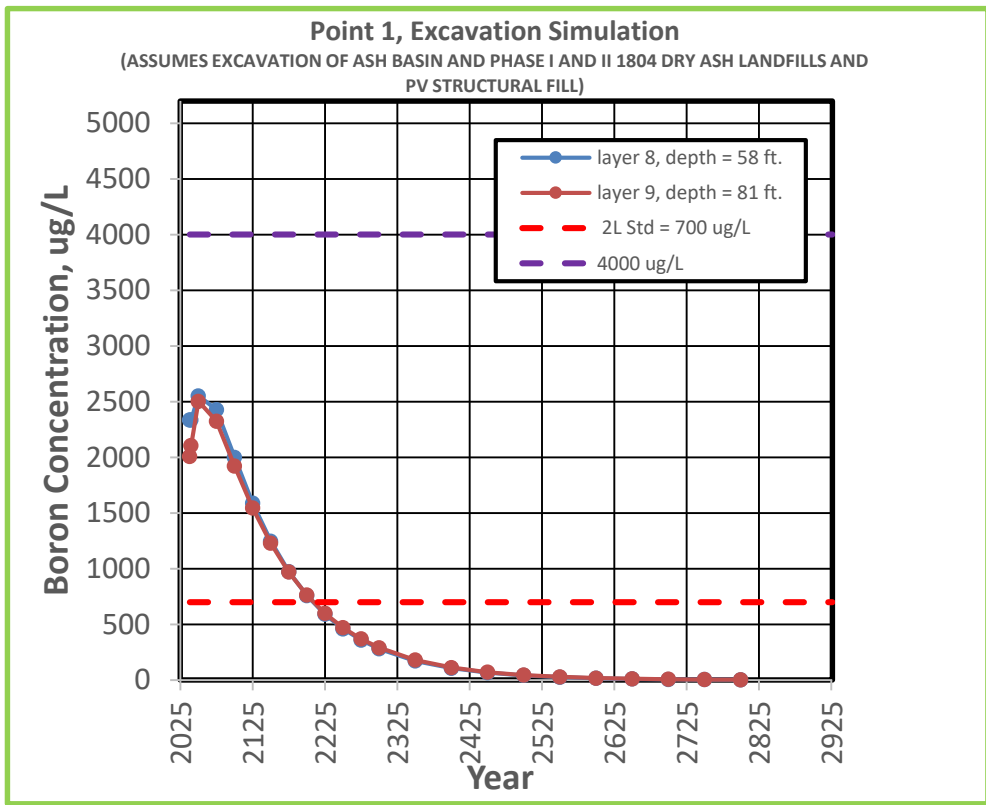
- █ BORON CONCENTRATION RANGE (> 10,000 µg/L)
- █ BORON CONCENTRATION RANGE (4,000 - 10,000 µg/L)
- █ BORON CONCENTRATION RANGE (700 - 4,000 µg/L)
- █ ASH BASIN WASTE BOUNDARY
- █ POTENTIAL ASH BASIN COMPLIANCE BOUNDARY

NOTES:

- 1) THE MODELED TIME TO RETURN TO COMPLIANCE WITH 2L GROUNDWATER STANDARDS FOR THE ASH BASIN CANNOT BE PREDICTED DUE TO THE PLUME BEING COMINGLED WITH THAT FROM THE LANDFILLS USING BORON IN THE TRANSITION ZONE AS THE BASIS FOR THE EVALUATION.
- 2) TRANSITION ZONE RESULTS SHOWN SINCE THIS REPRESENTS THE MOST TRANSMISSIVE ZONE.
- 3) THREE CLOSURE-SPECIFIC COMPLIANCE BOUNDARIES WERE USED TO EVALUATE THE RESULTS:
 - a) EXCAVATION SIMULATION IS EVALUATED USING A COMPLIANCE BOUNDARY THAT IS 250 FT FROM THE CURRENT WASTE BOUNDARY.
 - b) FINAL COVER SIMULATION IS EVALUATED USING A COMPLIANCE BOUNDARY THAT IS 250 FT FROM THE CURRENT WASTE BOUNDARY FOR BASINS WITHOUT NPDES PERMITS.
 - c) HYBRID SIMULATION IS EVALUATED USING A COMPLIANCE BOUNDARY 250 FT FROM THE FINAL WASTE BOUNDARY.

- 4) THE THREE MODEL SIMULATIONS ARE BASED ON THE COMPLETION DATES FOR THOSE ACTIVITIES. THESE DATES ARE:
EXCAVATION - YEAR 2030
FINAL COVER - YEAR 2038
HYBRID - YEAR 2030
- 5) SEE FIGURE 2 FOR TIME VS. CONCENTRATION PLOTS OF BORON AT POINT 1 AND POINT 2.
- 6) FINAL COVER EXTENT AND HYBRID WASTE BOUNDARY PROVIDED BY AECOM, INC.
- 7) AERIAL PHOTOGRAPHY OBTAINED FROM DIGITALGLOBE VIA ESRI ARCGIS ONLINE. IMAGE COLLECTED ON OCTOBER 3, 2017.
- 8) DRAWING HAS BEEN SET WITH A PROJECTION OF NORTH CAROLINA STATE PLANE COORDINATE SYSTEM FIPS 3200 (NAD83).

FIGURE ES-1
SIMULATED BORON CONCENTRATIONS
TRANSITION ZONE
EXCAVATION, FINAL COVER, AND HYBRID SIMULATIONS
MARSHALL STEAM STATION
DUKE ENERGY CAROLINAS, LLC
TERRELL, NORTH CAROLINA



NOTES:
 THE START DATES FOR THE THREE MODEL SIMULATIONS ARE BASED ON THE COMPLETION DATES FOR THOSE ACTIVITIES.
 THESE DATES ARE:

- EXCAVATION – YEAR 2038
- FINAL COVER – YEAR 2030
- HYBRID – YEAR 2030

TRANSITION ZONE RESULTS SHOWN

FIGURE ES-2
BORON TIME VS. CONCENTRATION PLOTS
TRANSITION ZONE
EXCAVATION, FINAL COVER, AND HYBRID SIMULATIONS
MARSHALL STEAM STATION
DUKE ENERGY CAROLINAS, LLC
TERRELL, NORTH CAROLINA

1.0 INTRODUCTION

Duke Energy Carolinas, LLC (Duke Energy) owns and operates the Marshall Steam Station (MSS, Plant or Site) in Terrell, Catawba County, North Carolina (Figure 1-1). MSS is a four-unit coal-fired electricity generating plant with a combined capacity of 2,090 megawatts (MW). The station began commercial operations in 1965 with Unit 1 (350 MW) followed by Unit 2 (350 MW) in 1966. Units 3 (648 MW) and 4 (648 MW) began operation in 1969 and 1970. Cooling water for MSS is provided by Lake Norman. Coal combustion residuals (CCR), composed primarily of fly ash and bottom ash, have historically been managed in the Site's ash basin which was constructed in 1965, immediately north of the plant.

The ash basin is located east of a topographic divide along Sherrills Ford Road, and south of a topographic divide along Island Point Road. Dry ash has been stored in other areas at the site including the unlined Dry Ash Landfill Phase I and Phase II (Permit No. 1804-INDUS-1983), the lined FGD Landfill (Permit No. 1809-INDUS-) and the double lined Industrial Landfill No. 1 (Permit No. 1812-INDUS-2008). Ash was used as structural fill in the photovoltaic (PV) Structural Fill (State Permit No. CCB0031), the road next to and within the ash basin leading up to the PV Structural Fill (State Permit No. CCB0030), and was used as structural fill beneath parts of the Industrial Landfill No. 1 (State Permit No. CCB0072). Inorganic compounds in the ash have dissolved and been transported in groundwater in the vicinity of the ash basin. Preliminary numerical simulations of groundwater flow and transport have been calibrated to current conditions and used to evaluate different scenarios being considered as options for closure of the ash basin. The methods and results of those simulations are described in this report.

1.1 General Setting and Background

The MSS is located in the Piedmont region of North Carolina. The topography in the area is hilly with elevations ranging from a high of about 910 feet¹ near the intersection of Sherrills Ford Road and Island Point Road, to a low of about 756 feet at Lake Norman. Lake Norman, which serves as the cooling lake for the Station, has a full pool elevation of 760 feet,

¹ The datum for all elevation information presented in the report is NAVD88.

but the actual water level fluctuates between about 752 feet and 760 feet. Sherrills Ford Road and Island Point Road are located along topographic ridges that act as groundwater divides west and north of the ash basin and landfills. The topography slopes downward toward Lake Norman towards the southeast. The ash basin dam is located immediately adjacent to Lake Norman. The ash basin pond water level is typically maintained at an elevation of 789 feet.

Coal combustion residuals (CCR) were historically sluiced to the ash basin. The ash basin consists of a single cell that was formed by damming the former Holdsclaw Creek near where the creek historically entered the Catawba River. The basin has a dendritic shape with coves of deposited ash. The ash basin waste boundary is approximately 394 acres. All coal ash from the MSS was sluiced to the ash basin from 1965 until 1984. Since 1984, fly ash has mainly been disposed of in the on-site ash landfills. Bottom ash has continued to be sluiced to the ash basin. Wastewater from the ash basin is discharged to Lake Norman by NPDES permitted Outfall 002 (NC0004987).

Two unlined ash landfills, the Phase I and Phase II Dry Ash Landfills, are located near and partially within the ash basin. The Dry Ash Landfill (Phase I) contains about 280,000 tons of fly ash, which was placed from 1984 to 1986. The Dry Ash Landfill (Phase I) is located just east of the ash basin, near the ash basin dam and Lake Norman. Dry Ash Landfill (Phase II) contains about 2,515,000 tons of fly ash and is located in the northeast part of the ash basin. The Dry Ash Landfill (Phase II) received fly ash starting in 1986 and was completed in 1999. The Dry Ash Landfill (Phase II) was built over part of the existing ash basin in the northeast part of the basin. These landfills were closed with a soil cover system.

The PV Structural Fill, consisting of compacted fly ash, was constructed between 2000 and 2013 in the northwestern part of the ash basin. This PV Structural Fill was built over part of the existing ash basin. This fill was closed with a soil cover system. The Industrial Landfill No. 1 is located adjacent to the northern part of the ash basin, south of Island Point Road. This landfill has a three-component liner with leak detection and leachate collection. Stormwater and leachate from the landfill are collected and piped to the ash basin.

The subsurface at the Site is composed of three primary zones. The top zone is residual soil consisting primarily of saprolite, which forms when bedrock is weathered in place. Below the saprolite zone is a transition zone consisting of less weathered and highly fractured bedrock.

Bedrock is present below the transition zone and generally is fractured with decreased fracturing with depth. Typically, the saprolite is partially saturated and the water table fluctuates within it. Water movement is generally preferential through the weathered and fractured bedrock of the transition zone (i.e., enhanced permeability zone). Groundwater within the Site area exists under unconfined, or water table, conditions within the saprolite, transition zone and in fractures and joints of the underlying bedrock. The shallow water table and bedrock water-bearing zones are interconnected. The saprolite, where saturated thickness is sufficient, acts as a reservoir for supplying groundwater to the fractures and joints in the bedrock. Shallow groundwater generally flows from local recharge zones in topographically high areas, such as ridges, toward groundwater discharge zones, such as stream valleys and Lake Norman.

The groundwater flow and transport model for the MSS has been under development since 2015. The development process began with a steady-state groundwater flow model and a transient model of constituent transport that were calibrated to field observations resulting from an intensive drilling campaign in early and mid-2015. The first set of simulations were completed in March 2016 (HDR, 2016). The present model domain has been greatly expanded compared to the 2016 model, and the number of model layers has been doubled. The earlier model was calibrated to hydraulic heads and COI concentrations measured in 2015. Since that time, significant site activities have taken place including the installation of many additional monitoring wells. The current model has been accordingly revised with respect to the 2015 model. These additional data have further improved the predictive capability and reduced uncertainty in the model results. To take advantage of this potential, the model was recalibrated using data from both the new and existing groundwater wells.

The following data sources were used during calibration of the revised groundwater flow and fate and transport model:

- Average site-wide water levels measured in CAMA/CCR/Compliance groundwater monitoring wells through December 2017.
- Groundwater quality data obtained from CAMA/CCR/Compliance sampling events conducted in the second quarter of 2018.
- Hydrogeologic data described in the CSA reports completed in 2015 (HDR, 2015) and 2018 (SynTerra, 2018)

- Surface water elevations provided by Duke Energy
- Water supply well information provided by Duke Energy

This study consists of three main activities: developing a calibrated steady-state flow model of current conditions, developing a historical transient model of boron transport that is calibrated to current conditions, and performing predictive simulations of the possible closure actions at the Site.

The predictive simulations include consideration of three different closure scenarios: final cover (closure-in-place), excavation, and a hybrid scenario. In each of the three closure scenarios ash is excavated from the Dry Ash Landfill (Phase I). In the final cover scenario, a low permeability final cover system is built over the ash in the ash basin, Dry Ash Landfill (Phase II), and PV Structural Fill. In the excavation scenario ash is excavated from the ash basin, Dry Ash Landfill (Phase II), and PV Structural Fill. In the hybrid scenario ash is excavated from the southern portion of the ash basin and placed in the middle portion of the ash basin. The middle of the portion of the ash basin along with the Dry Ash Landfill (Phase II) and PV Structural Fill are covered with a low permeability engineered cover system.

1.2 Study Objectives

The overall objective of the groundwater flow and transport modeling effort is to predict the performance of three closure scenarios. The goal is for these predictions to guide decisions during the selection of closure actions. The flow and transport models have been undergoing a process of continuous improvement and refinement by including new field data. The continuous improvement process is designed to increase the accuracy and reliability of the performance predictions.

The objective of this model is to describe a subset of the overall results of simulations of boron transport in saprolite, the transition zone, and the underlying fractured rock. The predictive simulations shown here are not intended to represent a final detailed closure design. These simulations use conceptual designs that are subject to change as the closure plans are finalized. The simulations are intended to show the key characteristics of groundwater flow and mobile constituent transport that are expected to result from the closure actions. Model simulations and the results presented do not include any active form of groundwater remediation.

The relative benefits of various groundwater remediation alternatives will be addressed in the CAP.

2.0 CONCEPTUAL MODEL

The site conceptual model for the MSS Site is primarily based on the 2015 Comprehensive Site Assessment report (HDR, 2015), and the 2018 Comprehensive Site Assessment Update (2018 CSA) for the MSS (SynTerra, 2018a). The 2018 CSA Update report contains extensive detail and data related to most aspects of the site conceptual model that are used here.

2.1 Aquifer System Framework

The aquifer system at the Site consists of an unconfined aquifer. Depending on the local topography and hydrogeology, the water table surface may exist in the saprolite, the transition zone, or in the fractured bedrock. At some isolated locations along streambeds, the upper unit (saprolite) is absent. At other locations, the upper unit may be unsaturated, with the water table located in deeper units (transition zone and fractured bedrock).

The hydraulic conductivity at the MSS Site has been measured in a series of slug tests in the different units. Twenty-seven slug tests were performed in the coal ash, with measured conductivities ranging from 0.007 ft/d to 199 ft/d. Thirty-eight slug tests performed in saprolite wells yielded hydraulic conductivities ranging from 0.004 ft/d to 137 ft/d. Seventy slug tests performed in transition zone wells gave results ranging from 0.001 ft/d to 35 ft/d. Twenty-six slug tests conducted in bedrock wells gave hydraulic conductivity values ranging from 0.07 ft/d to 38 ft/d. The range of observed conductivity in the saprolite, transition zone and bedrock highlights the large degree of heterogeneity in the multi-unit system.

2.2 Groundwater Flow System

The unconfined groundwater system at the MSS is dominated by flow due to recharge that falls within a watershed roughly defined by Sherrills Ford Road to the west, Island Point Road to the north, and by a ridge to the east of the ash basin. Within this area, groundwater flows towards the ash basin, and then towards Lake Norman, or a nearby small creek, where it ultimately discharges. The ash basin pond is maintained at an elevation of about 789 ft., which is about 33 ft. above the typical water elevation in the adjacent Lake Norman. The higher hydraulic head in the ash basin pond drives some groundwater flow through the small ridge to

the east of the ash basin near the dam. Groundwater flowing through this ridge discharges to the small stream and cove of Lake Norman that are east of the ash basin.

The groundwater system is recharged from infiltrating rainwater, and from water that infiltrates from the ash basin pond. The average value of recharge in the vicinity of the MSS was estimated at 8 inches per year. The North Carolina map of recharge by Haven (2003) does not show values for Catawba County, but the average value in nearby counties is consistent with this estimate. A reduced rate of recharge (1 inch per year) was assumed for the power plant, and an infiltration rate of zero was assumed for the constructed wetland areas (which have an underlying geomembrane) and the lined Industrial and FGD landfills.

There are three public supply wells and 80 private water wells that have been identified within one-half mile of the ash basin compliance boundary (SynTerra, 2018). Most of these wells are located west of the Site, along Sherrills Ford Road, and south of the Site, along NC Highway 150. A few wells are located at residences along Island Point Road, north of the Site. Pumping rates for the private wells were not available, and completion depths were only available for about 20 of the wells.

2.3 Hydrologic Boundaries

The major discharging locations for the shallow water system serve as hydrologic boundaries to the shallow groundwater system. Lake Norman is the major hydrologic boundary in the area.

2.4 Hydraulic Boundaries

The shallow groundwater system does not appear to contain impermeable barriers or boundaries in the study area, but it does include hydraulic boundaries between zones of different hydraulic conductivity. The degree of fracturing, and thus the hydraulic conductivity, is expected to decrease with depth in metamorphic rock. This will result in blocks of unfractured rock where the hydraulic conductivity is quite low to negligible. However, isolated fractures may occur that result in large local hydraulic conductivities, and the locations of these fractures are difficult to predict or to comprehensively map. It was assumed that the rock was impermeable below the depth of the bottom modeled layer, and a no-flow boundary was used to represent this condition.

2.5 Sources and Sinks

Groundwater flow from areal recharge (rainfall infiltration) and flow out of the ash basin pond are sources of water to the groundwater system. Groundwater in the model domain discharges to Lake Norman, and to small streams and drainages. These small streams and drainages are located primarily outside of the ash basin around the periphery of the model. The water supply wells within the model area remove only a small amount of water from the overall hydrologic system.

2.6 Water Budget

Over the long term, the rate of water inflow to the study area is equal to the rate of water outflow from the study area. Water enters the groundwater system from recharge and the ash basin pond. Water leaves the system through discharge to Lake Norman, several small creeks and through water supply wells.

2.7 Modeled Constituents of Interest

Antimony, arsenic, barium, beryllium, boron, cadmium, chloride, chromium (hexavalent and total), cobalt, iron, manganese, molybdenum, nickel, radium 226 and 228, selenium, strontium, sulfate, TDS (total dissolved solids), thallium, and vanadium have been identified as constituents of interest (COIs) for groundwater at the MSS (SynTerra, 2018a, SynTerra, 2018b).

Boron is the best (most conservative, or proxy) constituent for tracking historical and future plume migration at the Site because it is present in plumes from CCR releases at concentrations higher than background. Boron is also not subject to chemical attenuation under normal aquifer conditions (due to its low reactivity and low K_d).

Boron is present at significant concentrations in the ash basin and near and beneath the Phase I and Phase II Dry Ash Landfills, and the PV Structural Fill. A small boron plume extends to monitoring wells south and east of the ash basin near the ash basin dam. Boron is found in monitoring wells screened in the saprolite, the transition zone, and the bedrock. Boron concentrations in background monitoring wells are below the 15A NCAC 02L .0202 Groundwater Quality Standard for boron (2L standard) and are generally less than the laboratory detection limit. Other conservative constituents from the ash (*i.e.*, chloride, sulfate, and TDS) have similar K_d values but are not present in such large concentrations in the source area or are

present naturally in regional groundwater. Attenuation for these conservative COIs primarily occurs through physical means (i.e., dispersion and dilution). This preliminary model report will focus exclusively on boron because boron is the dominant mobile constituent at the Site.

The remaining constituents were not considered for this modeling exercise for one or more of the following reasons: 1) concentrations in the ash pore water do not greatly exceed likely background levels; 2) there is no discernable plume of the constituent extending downgradient from the ash basin; and 3) the reactive, non-conservative parameters subject to chemical attenuation have relatively high K_d values (i.e., greater than 10 L/kg) under all probable pH and E_H conditions at MSS. The relatively high K_d values are due to sorption, ion exchange, and (co)precipitation. Therefore, their migration potential is significantly limited, meaning that the plumes are small and sometimes discontinuous.

2.8 Constituent Transport

The COIs that are present in the coal ash dissolve into the ash pore water. As water infiltrates through the ash, water containing COIs can enter the groundwater system. Once in the groundwater system, the COIs are transported by advection and dispersion, subject to retardation due to sorption to solids. If the COIs reach a hydrologic boundary or water sink, they are removed from the groundwater system, and they enter the surface water system, where in general, they are greatly diluted.

3.0 COMPUTER MODEL

3.1 Model Selection

The numerical groundwater flow model was developed using MODFLOW (McDonald and Harbaugh, 1988), a three-dimensional (3D) finite difference groundwater model created by the United States Geological Survey (USGS). The chemical transport model is the Modular 3-D Transport Multi-Species (MT3DMS) model (Zheng and Wang, 1999). MODFLOW and MT3DMS are widely used in industry and government and are considered to be industry standards. The models were assembled using the Aquaveo GMS 10.3 graphical user interface (<http://www.aquaveo.com/>).

3.2 Model Description

MODFLOW uses Darcy's law and the conservation of mass to derive water balance equations for each finite difference cell. MODFLOW considers 3D transient groundwater flow in confined and unconfined heterogeneous systems, and it can include dynamic interaction with pumping wells, recharge, evapotranspiration, rivers, streams, springs, lakes, and swamps.

This study uses the MODFLOW-NWT version (Niswonger, et al., 2011). The NWT version of MODFLOW provides improved numerical stability and accuracy for modeling systems with variable water tables. That improved capability is helpful in the present work where the position of the water table in the ash basin can fluctuate depending on the conditions under which the basin is operated and the various closure scenario simulations.

Some of the Marshall flow models were challenging to run due to the topography and layers that become unsaturated in the model. It was found that using the NWT solver options "MODERATE" with the xMD matrix solver could overcome these difficulties.

MT3DMS uses the groundwater flow field from MODFLOW to simulate 3D advection and dispersion of the dissolved COIs including the effects of retardation due to COI adsorption on the soil and rock matrix.

4.0 GROUNDWATER FLOW AND TRANSPORT MODEL CONSTRUCTION

The flow and transport model for the Site was built through a series of steps.

- Step 1: Build a 3D model of the site hydrostratigraphy based on field data.
- Step 2: Determine the model domain and construct the numerical grid.
- Step 3: Populate the numerical grid with initial estimates of flow parameters
- Step 4: Calibrate the steady-state flow model to current hydraulic heads with adjustments of the flow parameters
- Step 5: Develop a transient model of historical flow and transport to provide time-dependent constituent transport development.
- Step 6: Calibrate the historical flow and transport model to recent boron concentration field data to ensure the model reproduces the observed boron plumes.

The process of revising the model involved using an initial updated model as a starting point and following an iterative process of adjusting parameters until the model adequately predicted the observed heads and concentrations.

4.1 Model Domain and Grid

The initial steps in the model grid generation process were the determination of the model domain, and the construction of a 3D hydrostratigraphic model. The model has dimensions of about three miles by three miles and is oriented in a North-South orientation (Figure 4-1). The model is generally bounded to the east by Lake Norman, which also forms part of the northern and southern boundary. To the west, the model boundary is more than a half-mile from the ash basin, and it is separated from the ash basin by a major topographic ridge that runs along Sherrills Ford Road, and by creek drainages located west of Sherrills Ford Road. The northern boundary is located beyond the topographic ridge that runs along Island Point Road, and it extends either to Lake Norman, or to a location beyond a creek drainage that runs into Lake Norman. The southern boundary is nearly a mile from the ash basin, and it extends to Lake Norman on both the eastern and the extreme western sides. The distance to the boundary from the ash basin is large enough to prevent boundary conditions from artificially affecting the results near the basin.

The ground surface of the model was developed by HDR and was interpolated from the North Carolina Floodplain Mapping Program's 2010 Light Detection and Ranging (LiDAR) elevation data. These data were supplemented by on-site surveys conducted by Duke Energy in 2014. The elevations used for the top of the ash surface in the ash basin were modified from the topographic and bathymetric data to provide a model surface that can accommodate planned regrading of ash for the final cover or hybrid closure options. For current conditions simulations, the portions of the ash basin that have ponded water above the ash are given a large hydraulic conductivity to represent the open water conditions.

The hydrostratigraphic model (called a solids model in GMS) consists of five units: ash, saprolite, transition zone, upper fractured bedrock, and deeper bedrock. The contact elevations between these units were determined from boring logs from previous studies by HDR (2016). The contact elevations were estimated by HDR for locations where well logs were not available by extrapolation of the borehole data using the Leapfrog Hydro geologic modeling tool. This program was used by HDR to develop surfaces defining the top of the saprolite, transition zone, and bedrock. While the contacts between the upper units (ash, saprolite, transition zone, bedrock) are well defined, the division of the bedrock into an upper fractured zone, a mid-depth bedrock zone and deeper bedrock was subjective. For the purposes of model construction, the upper fractured mid-depth zones are both 150 feet thick. The deeper bedrock extends another 250 feet below the mid-depth zone for a total bedrock thickness of 550 feet in the model. The upper and mid-level bedrock zones in the model were given a heterogeneous hydraulic conductivity distribution to represent more and less fractured zones.

Figure 4-2 shows a fence diagram of the 3D hydrostratigraphic unit viewed from the southeast, with a vertical exaggeration of 4x. The light grey material corresponds to the ash in the basin, the light tan material is the saprolite, the orange material is the transition zone, the brown material is the upper fractured part of the bedrock, and the dark grey material is the deep bedrock.

The numerical model grid is shown in Figure 4-3. The grid is discretized in the vertical direction using the solids model (Figure 4-2) to define the numerical model layers. The top 4 model layers represent the ash basin, including the dam that forms the basin, the Dry Ash Landfill (Phase II), and the PV Structural Fill. Model layers 5-7 represent the saprolite except in

the Dry Ash Landfill (Phase I) area, where model layer 5 represents ash. Model layer 8 represents the transition zone. Model layers 9-12 represent the upper fractured part of the bedrock, while model layers 13-15 represent mid-depth parts of the fractured bedrock. The deep bedrock (which may also be fractured) is represented by model layers 16-20. The model varies in thickness from about 630 to 720 ft.

The discretization in the horizontal direction is variable with smaller grid cells in and around the ash basin area. The minimum horizontal grid spacing in the finely divided areas is about 30 ft., while the maximum grid spacing near the outer edges of the model is about 200 ft. The grid contains a total of 979,760 active cells in 20 layers.

4.2 Hydraulic Parameters

The horizontal hydraulic conductivity and the horizontal to vertical hydraulic conductivity anisotropy ratio are the main hydraulic parameters in the model. The distribution of these parameters is based primarily on the model hydrostratigraphy, with additional horizontal and vertical variation. Most of the hydraulic parameter distributions in the model were heterogeneous across a model layer. The geometries and parameter values of the heterogeneous distributions were determined during the flow and transport model calibration process. Initial estimates of parameters were based on experience at other Piedmont sites in North Carolina, literature values, results of slug and core tests, and simulations performed using a preliminary flow model. The hydraulic parameter values were adjusted during the flow model calibration process described in Section 5.0 to provide a best fit to observed water levels in observation wells and were further refined during calibration of the transport model. Slug test data from hundreds of wells at the Duke Energy coal ash basin sites in North Carolina are shown in Figures 4-4 through 4-7.

The hydraulic conductivity of coal ash measured at 14 sites in North Carolina ranges over about 4 orders of magnitude, with a median value of about 1.6 ft/d (Figure 4-4). Ash hydraulic conductivity values measured in slug tests at Marshall ranged from 0.007 ft/d to 199 ft/d. The current conditions flow model is not very sensitive to the ash conductivity, but the predicted heads in the final cover simulations are more sensitive to the ash hydraulic conductivity. Four pumping tests were recently conducted within the ash basin including the underlying saprolite in June 2018 to help refine the value of these unit specific parameters. Results of these tests are

expected to yield an estimate of the ash properties that is more representative of site conditions. The simulations will be revised when the data from the pumping tests have been evaluated. Results from the revised simulations will be presented in future versions of the flow and transport model.

The hydraulic conductivities from hundreds of slug tests performed in saprolite wells at 10 Piedmont sites are shown in Figure 4-5. These also range over 4 or more orders of magnitude, and have a median value of 1.0 ft/d. Saprolite slug tests performed at Marshall ranged from 0.004 ft/d to 137 ft/d. Transition zone hydraulic conductivities from hundreds of slug tests at 10 Piedmont sites are shown in Figure 4-6. These range over 6 orders of magnitude, with a median value of 0.97 ft/d. The measured values at Marshall range from 0.001 ft/d to 35 ft/d.

Slug test results from bedrock from hundreds of wells at 10 Piedmont sites in North Carolina (Figure 4-7) range over more than 6 orders of magnitude, with a median value of 0.5 ft/d. It is possible that this median value is larger than the true average value for deep bedrock for three reasons. First, the bedrock wells at these sites are almost all screened in the uppermost few tens of feet of the bedrock, which is expected to be more highly fractured than deeper bedrock zones. Second, the wells are typically screened in zones with visible flowing fractures, rather than in zones with intact unfractured rock. Finally, wells that do not produce water are not slug tested. These factors may bias the slug test data to higher values than may be representative of the deeper bedrock as a whole. At Marshall, the measured values from slug tests in shallow bedrock ranged from 0.07 ft/d to 38 ft/d.

4.3 Flow Model Boundary Conditions

Lake Norman forms a hydraulic boundary east of the ash basin. The lake is treated as a high conductance general head boundary in the uppermost active model layer with an elevation of 756 feet. The lake wraps around the northeastern and southeastern parts of the model. The western model boundary does not align with any clearly defined hydraulic features. This boundary is located more than a half mile from the ash basin, and there is a major topographic ridge between the model boundary and the basin along with two deep creek drainages located west of the ridge. Most of the western boundary is treated as a low conductance general head boundary with the head set to an elevation of 15 feet below the top of the saprolite, except in stream valleys, where

a no flow boundary is used perpendicular to the streams. The flow in these valleys is dominated by flow towards the streams, which are modeled as drains. The southwestern boundary is treated as a no flow boundary as it crosses stream valleys approximately perpendicular to the streams, which are treated as drains in the model. This boundary is also almost a mile away from the ash basin. Model boundaries were set at appropriate distances from the study area to ensure that boundary effects did not impact the simulation results in the vicinity of the ash basins.

4.4 Flow Model Sources and Sinks

The flow model sources and sinks consist of Lake Norman, the ash basin pond, recharge, wells, streams, ponds and wet areas that are assumed to directly drain into the ash basin pond.

Recharge is a significant hydrologic parameter in the model, and the distribution of recharge zones in the model is shown in Figure 4-8. As described in Section 2.2, the recharge rate for the MSS Site was estimated to be 8 inches/year. The recharge rate for the MSS Plant was set to 1 inch per year due to the large areas of roof and pavement. The ash basin pond and other ponds in the model are treated as high conductance general head boundaries. The recharge rate was set to zero in the constructed wetlands areas. The recharge rate through the lined FGD and Industrial landfill covers was set to zero.

Lake Norman, the ash basin pond, and several smaller ponds were treated as specified general head zones in the model (Figures 4-9 and 4-10). With this condition, the hydraulic head is specified, along with a conductance. For large values of conductance, this condition acts like a specified head boundary condition. The general head condition was used here because the GMS software can perform external water balance calculations with the general head boundary condition that it cannot perform with the specified head condition. Lake Norman is maintained at an elevation of 756 ft. and the ash basin pond is maintained at an elevation of 789 ft.

The many creeks exert a significant local control on the hydrology in the model. These features are shown as green lines in Figure 4-9. The position of these creeks was determined mainly from the topographic map (Figure 1-1), supplemented by a site visit where each drainage feature near the ash basin was inspected. The elevation of locations along the creeks were determined from the surface LiDAR elevations, and were assumed to be 2 feet below the ground

surface. The creeks were simulated using the DRAIN feature in MODFLOW with a high conductance value ($100 \text{ ft}^2/\text{d}/\text{ft}$).

The outer “fingers” of the ash basin contains several areas of standing water, along with the main sluicing channel. Most of these surface water features were treated as general head boundaries (Figure 4-10). With this condition, the water bodies may add or remove water from the groundwater system, depending on the hydraulic heads in the groundwater flow system. Two marshy areas in the ash basin near the Dry Ash Landfill (Phase II) were simulated as drains.

Figure 4-11 shows the location of public and private water supply wells in the model area. There are three public supply wells in the model domain. One well is located at the Plant and is operated by Duke Energy. This well is open from an elevation of 727 ft. to 214 ft. and it pumps at an average rate of 20,000 gallons per day. A second public supply well is operated by the Boathouse Restaurant on NC Highway 151, across the lake from the Plant. This well is open from an elevation of 716 ft. to 520 ft., and it was assumed to pump 3,000 gallons per day. A third public supply well is located at The Old Country Church, on NC Highway 150. This well is screened from an elevation of 722 to 702 ft. and was assumed to pump 280 gallons per day on average. This pumping rate is similar to that of a household and was selected based on the assumption that the church is mainly occupied on Sunday mornings, but is vacant during most of the remainder of the week.

There are 80 private wells inside the model boundary, five of which are known to be abandoned. Where depth data were available, the private wells were open over the known depths. In most cases, the well depths were unknown, and the wells were assumed to be open in the upper part of the bedrock in model layer 9. The pumping rates from the wells were unknown, and the model assumed a pumping rate of 280 gals/day, which is an average water use for a family of four (Treece et al. 1990; North Carolina Water Use, 1987, and 1995). Septic return was assumed to be 94% of the pumping rate, based on Treece et al. (1990), Daniels et al. (1997) and Radcliffe et al. (2006). The septic return was injected into layer 6 (saprolite) in the model.

4.5 Flow Model Calibration Targets

The steady state flow model calibration targets were water level measurements made in 172 observations wells through the 4th quarter of 2017. The water level data for wells with multiple measurements were averaged to account for seasonal variations. All sampled wells are included in the calibration. These wells include wells screened in each of the hydrostratigraphic units, including many sets of nested wells.

4.6 Transport Model Parameters

The transport model uses a time-dependent MODFLOW simulation to provide the time-dependent groundwater velocity field. The MODFLOW simulation started January 1965, and it continued through July 2018. The transient flow field is approximated as a series of flow fields that correspond to conditions at different times as the Industrial and FGD landfills were constructed. The transient flow field was modeled as four successive steady state flow fields; one corresponding to the site conditions before the Industrial and FGD landfills were constructed, one corresponding to conditions after the eastern cell of the Industrial landfill was completed, one after the FGD landfill was completed, and one after the western cell of the Industrial landfill was completed. These steps all represent minor changes to the groundwater flow field, and they are simulated by adjusting the recharge rate at the landfills from the background value of 8 inches per year to zero once the landfills were completed. Neither of these landfills are considered to be a source of COIs at the Site.

The key transport model parameters (besides the flow field) are the boron source concentrations in the ash, and the boron soil-water distribution coefficient (K_d). Other parameters are the longitudinal, transverse, and vertical dispersivity, and the effective porosity. The boron source concentrations in the ash basin, Phase I and II Dry Ash Landfills, and the PV Structural Fill were initially estimated from the ash pore water concentrations and from concentrations in nearby wells. During the transport model calibration process, the basin and other source areas were subdivided, and different concentrations were assigned to different zones at different times. The timing of boron sources appearing in the Phase I and II Dry Ash Landfills and the PV Structural Fill locations correspond to the time when they became active (1984, 1986, and 2000, respectively). The ash basin source zones become active when the model starts (1965). In areas where landfills or structural fill was built over the ash basin, the ash basin areas

were activated first (in 1965) followed by the landfill or structural fill at the appropriate time. Once they are activated, source concentrations of the boron are held constant at the specified levels in the ash layers during the historical transport simulation, but they are allowed to vary in time during the predictive simulations that follow. Changes in concentration within the source zones during the predictive simulations are controlled by flow in these regions and the chemical transport parameters (i.e. K_d values).

The numerical treatment of adsorption in the model requires special consideration because part of the system is a porous media (ash, saprolite, and transition zone) with a relatively high porosity, while the bedrock is a fractured media with very low matrix porosity and permeability. As a result, transport in the fractured bedrock occurs almost entirely through the fractures. The MODFLOW and MT3DMS flow and transport models used here simulated the fractured bedrock as an equivalent porous media. With this approach, an effective hydraulic conductivity is assigned to the fractured rock zones so that it produces the correct Darcy flux (volume of water per area of media per time) for a given hydraulic gradient. However, because the water flows almost entirely through the fractures, this approach requires that a small effective porosity value (~0.01 or less) be used for the transport calculations to compute a realistic flow velocity as with other sites.

The COI retardation factor is computed internally in the MT3DMS code using a conventional approach:

$$R = 1 + \frac{\rho_b K_d}{\phi}$$

Where ρ_b is the bulk density and ϕ is the porosity. If typical porous media values are used for the bulk density and K_d , the resulting retardation factor in the fractured media becomes unrealistically large due to the low porosity value. In the current model, the calibrated boron K_d value was 0.5 mL/g for the saprolite and transition zone. Considering the fractured bedrock, with a bulk density of 1.6 g/mL and a porosity of 0.01, a K_d value of 0.5 mL/g (which is the calibrated value used in the saprolite) results in a retardation factor of 81, which is unrealistically high for boron transport. To avoid this problem, the boron was assigned a much lower K_d value in the bedrock layers of the model so that it would have a reasonable retardation factor during transport through the fractured media.

Ash leaching tests were performed on 5 samples from the Marshall ash basin using US EPA (LEAF) Method 1316. The leaching data were analyzed to develop a K_d (partition coefficient) value for boron in the coal ash. The average of those test values was 0.77 mL/g. The modeling approach for the predictive simulations of future boron transport allows the boron concentration in the ash to vary with time in response to water infiltrating and flowing through the ash, dissolving boron, and flowing out of the source areas. Using the K_d value that is derived from ash leaching tests ensures that the model response of the boron in the ash to water flowing through the source areas is realistic.

The K_d value for the boron outside of the ash basin was treated as a calibration parameter. Boron is expected to be mobile, and to have a low K_d value. The calibrated K_d values for the saprolite and transition zone layers were 0.5 mL/g. In the fractured bedrock, a much lower value was used as described above of 0.02 mL/g. These values were derived by calibrating the K_d value to groundwater boron concentrations in observation wells.

The longitudinal dispersivity was assigned a value of 20 ft., the transverse dispersivity was set to 2 ft., and the vertical dispersivity was set to 0.2 ft. The dispersivities are model parameters that are used to describe the diffusion-like spreading of plumes that occurs in addition to transport with the bulk groundwater flow. Dispersivity values are both model and scale-dependent. The longitudinal dispersivity is typically found to be between 1/200 and 1/10 of the constituent plume travel distance. Transverse and vertical dispersivities are typically on the order of 1/10 and 1/100 of the longitudinal value, respectively. The dispersivities used in this study are consistent with these literature values. The transport model is not very sensitive to the dispersivities within a reasonable range of values.

The effective porosity was set to a value of 0.3 in the unconsolidated layers, and to 0.01 in all the bedrock layers. The soil dry bulk density was set to 1.6 g/mL.

4.7 Transport Model Boundary Conditions

The transport model boundary conditions are no flow on the exterior edges of the model except where constant or general head boundaries exist, where they are specified as a concentration of zero. All the specified general head water bodies (Lake Norman, ash basin pond, small ponds and sluicing channel), have a fixed concentration of zero for any water

entering the model. As water containing dissolved constituents leaves the model through these flow source/sink zones, the dissolved mass is removed from the model. The infiltrating rainwater is assumed to be clean and enters from the top of the model. The ash basin pond is handled differently because it is considered a source of boron in the model. In the ash basin pond, the water level is maintained using a constant general head hydraulic boundary, and the boron concentration is specified in model cells below the water surface. The water entering the model from the general head boundary does not contain boron, but as it infiltrates through the ash layers it equilibrates with the specified boron concentrations in those layers.

The initial condition for the current conditions transport model (back in 1965) is one of zero concentration of boron everywhere in the model. No background concentrations are considered.

4.8 Transport Model Sources and Sinks

The ash basin, Phase I and II Dry Ash Landfills, and the PV Structural Fill are the source of boron in the model. During the historical transport simulation, these sources are simulated by holding the boron concentration constant in cells located inside the ash in these zones, which simulates a continuous replenishing of source material in these zones. The boron concentrations from the historical transport simulation form the initial condition for the predictive simulations of future transport at the Site. The predictive simulations do not hold the boron concentrations constant in the ash source zones because no additional source material is being added to the ash source zones, and this mobile constituent can wash out of the ash over time. The boron K_d value used for the ash was measured in ash leaching tests using ash from the Site to ensure that the simulated boron leaching rate is realistic.

Impacted soil and rock at the Site can continue to serve as a source for groundwater contamination by boron. This potential is fully accounted for in the model by continuously tracking the boron concentrations in time in the saprolite, transition zone, and rock materials throughout the model. The historical transport model simulates the migration of boron through the soil and rock from the ash basin, and these results are used as the starting concentrations for the predictive simulations. Therefore, even if all the coal ash is excavated, the transport model predicts ongoing impacts to groundwater from the contaminated soil beneath the ash.

The transport model sinks are the general head or drain conditions used to simulate the lake, ponds, and creeks. As groundwater enters these features, it is removed along with any dissolved boron mass. Similarly, if water containing boron were to encounter a pumping well, the boron would be removed with the water.

4.9 Transport Model Calibration Targets

The transport model calibration targets are boron concentrations measured in 159 monitoring wells in the 2nd quarter of 2018. All sampled wells are included in the calibration.

5.0 MODEL CALIBRATION TO CURRENT CONDITIONS

5.1 Flow Model

The flow model was calibrated in stages starting with a relatively simple layered model. All calibration was done by trial and error, simultaneously matching the recent water levels measured in all observation wells (Table 5-1). Additional flow model calibration was required to also match the current conditions boron distribution. The primary calibration parameters are the three-dimensional distribution of hydraulic conductivity. Each model layer has been subdivided into hydraulic conductivity zones. These model conductivity zones are shown in Figures 5-1 through 5-9, and the calibrated hydraulic conductivity values assigned to each zone in each layer are listed in Table 5-2.

Starting at the top, in layers 1-4, the layers represent both the coal ash and the ash basin dam. It was important to calibrate the conductivity of the dam fill material in these layers separately (Figure 5-1) in order to match the head values in wells located in and near the dam. The dam fill material has a calibrated conductivity of 0.03 ft/d.

In the current steady-state flow model, a high hydraulic conductivity (100 ft/d) was applied to the ash basin pond to represent open water (Figure 5-1). The hydraulic conductivity of the ash was assumed to be 2.0 ft/d. The current conditions flow model is relatively insensitive to the ash conductivity because the water levels around the ash basin are largely controlled by the ash basin pond and other surface water bodies. The value of 2.0 ft/d that was used is close to the median of more than 200 slug tests performed at 14 coal ash basin sites in North Carolina shown in Figure 4-4, and it falls within the range of values measured at Marshall. Although the current conditions model is not sensitive to this parameter, the predictive final cover simulation is more sensitive to the ash conductivity. Pumping tests in the Marshall ash basin were recently performed to improve the understanding of the coal ash hydraulic conductivity at the MSS. These data will be incorporated into an updated version of this model at a later date.

The calibrated background hydraulic conductivity for the saprolite (layers 5-7) was 1.0 ft/d, which is equal to the median value for slug tests performed in saprolite at 10 coal ash basin sites in the Piedmont of North Carolina, and near the median for slug tests performed at Marshall (Figure 4-5). This material is heterogeneous and zones of both higher and lower conductivity

were required to match the hydraulic heads and boron transport in and around the ash basin (Figure 5-2 and Table 5-2). The range of saprolite conductivity in the model goes from 0.05 ft/d to 4.0 ft/d, which falls within the range of values measured in slug tests in the 10 Piedmont Sites shown in Figure 4-5.

The calibrated background conductivity for the transition zone (layer 8) was 1.5 ft/d. This value falls near the average value for slug tests performed in the transition zone at 10 Piedmont Sites in North Carolina (Figure 4-6). The transition zone is heterogeneous, with values ranging from 0.05 ft/d to 1.5 ft/d (Figure 5-3 and Table 5-2). The low conductivity zones are mainly located in areas where there are topographic ridges or hills. The lower conductivity values are required in order to match the higher hydraulic heads observed in wells in these locations.

The upper bedrock zone in the model includes layers 9-12, and it is 150 feet thick. It was necessary to adjust model conductivity values separately in each of these layers in order to match the observed hydraulic heads and boron concentrations in observation wells. The background conductivity value used in the model of 0.7 ft/d is close to the median of values measured from slug tests at 10 Piedmont sites in North Carolina, and in slug tests performed at Marshall (Figure 4-7).

The upper bedrock conductivity ranges from 0.005 ft/d to 8 ft/d in the model (Figures 5-4 to 5-7 and Table 5-2). The low values were used to better match high hydraulic heads that are observed in wells located on ridges and other topographically high areas. Higher conductivity values were needed in places to match the lower observed hydraulic heads, and in some cases, to match the observed boron transport. A fairly complicated three-dimensional pattern of conductivity was required beneath the Dry Ash Landfill (Phase II) to match the heads in shallow and bedrock wells in this area (Figure 5-6). The wells AL-4D and AL-4BR screened beneath the landfill have average heads of about 811 ft., while the deeper AL-4BRL has a head of only 798 ft. Matching these heads is accomplished by placing a low permeability zone above AL-4BRL and connecting a highly permeable fracture zone to AL-4BRL (Figure 5-6). This combination also provides a good match with the boron data in this area.

The mid-depth bedrock includes model layers 13-15 (Figure 5-8 and Table 5-2) and is 150 feet thick. The background value of 0.2 is somewhat lower than the shallower bedrock

value. It is expected that the degree of fracturing, and hence the average conductivity should decrease with depth. The conductivity of these layers range from 0.01 to 5.0. The high conductivity value is located around well AL-02BRLL, beneath the Phase II Dry Ash Landfill. This well is about 350 feet deep, and it is screened at an elevation of about 570 ft. This deep well intersects a productive fracture zone that consistently indicates high boron concentrations ($>10,000 \mu\text{g/L}$). The high conductivity zone in layers 13-15 was used to represent a highly fractured zone in this location, and it was needed to reproduce the high observed boron concentrations in this well. A pumping test is planned for this well to help better characterize the hydraulic properties of the fracture zone. This information will be incorporated into a future version of the model.

The deep bedrock layer extends over the bottom 250 feet (layers 16-20) of the model and was assigned a uniform value of 0.01 ft/d (Figure 5-9). The flow model calibration is relatively insensitive to this value, but the model conductivity is high enough to allow some water flow in the deep bedrock. The combination of the low rock porosity (0.01) and the high mobility of boron results in some deeper predicted migration of boron in parts of the model. Additional deeper bedrock wells are planned in the vicinity of the ash basin dam and Dry Ash Landfill (Phase II). Hydraulic and COI concentration data from those wells will be used to refine the calibration of bedrock parameters in a future version of the flow and transport model.

The final calibrated flow model has a mean head residual of -0.44 ft., a root mean squared error (RMSE) of 2.37 ft., and a normalized root mean square error (NRMSE) of 2.08%. The range of heads at the site is about 114 ft. with a maximum of 870.23 ft. and a minimum of 756.27 ft. A comparison of the observed and simulated water levels is listed in Table 5-1 and the observed and simulated levels are cross-plotted in Figure 5-10. Table 5-2 lists the best-fit hydraulic parameters from the calibration effort.

The computed heads in the transition zone (model layer 8) are shown in Figure 5-11. Figure 5-12 shows the simulated heads in the second fractured bedrock model layer (model layer 10). These are similar to the shallower heads. The calibration wells are also shown in this figure (many of the nested wells plot on top of each other). The green and yellow bars indicate the magnitude of model error at each well. The green color indicates that the difference is less than

5 ft. and the yellow color indicates a difference of 5 to 10 ft. Almost all the wells have a model error of less than 5 feet.

The groundwater flow divide around the ash basin is shown in Figure 5-13 as the yellow line. This divide wraps around the west, north, and east part of the ash basin area. Inside of this divide, groundwater flows towards the ash basin and Lake Norman (blue arrows), while outside of the divide, groundwater flows away from the ash basin.

5.2 Flow Model Sensitivity Analysis

A parameter sensitivity analysis was performed by varying the main hydraulic parameters (recharge, ash conductivity, saprolite conductivity, transition zone conductivity, and upper, mid-depth, and lower bedrock conductivity) in the current conditions flow model. Starting with the calibrated model, each parameter was halved and doubled to evaluate the model sensitivity. Only the main background conductivity values were varied in this study. Table 5-3 shows the results of the flow parameter sensitivity study. The model is very sensitive to the recharge rate, and is moderately sensitive to the saprolite, and transition zone conductivities. The model is strongly sensitive to the conductivity of the upper 150 feet of bedrock (the upper bedrock layers 9-12), and it is moderately sensitive to the mid-depth bedrock conductivity. The model is not very sensitive to the ash conductivity or to the conductivity of the deeper bedrock, although reducing the ash conductivity resulted in a larger error. As discussed earlier, additional testing of the ash and deeper bedrock units from pumping tests and geophysical testing has recently taken place, or will take place in the near future, and these results will be incorporated into a later version of this model.

5.3 Historical Transport Model Calibration

The transient flow field was modeled as four successive steady state flow fields; one corresponding to the site conditions before the Industrial and FGD landfills were constructed, one corresponding to conditions after the eastern cell of the Industrial landfill was completed, one after the FGD landfill was completed, and one after the western cell of the Industrial landfill was completed. These steps all represent small changes to the groundwater flow field, and they are simulated by adjusting the recharge rate from the background value of 8 inches per year to zero once the landfills were built. Neither of these landfills are considered to be a source of

COIs at the Site because they are lined landfills with negligible infiltration contributing boron concentrations to the groundwater.

The boron distribution in and around the ash basin is extremely complex. Dissolved boron concentrations in some locations at the Site are high, reaching levels between 50,000 and 100,000 $\mu\text{g/L}$. At other nearby locations, the boron concentration can be much lower, in the hundreds of $\mu\text{g/L}$. Boron is found as deep as 250 feet below the original ground surface at well AL-02BRLL. Reproducing this complex pattern of boron distribution required the use of many different specified boron source concentration zones (Figures 5-14 and 5-15 and Tables 5-4 and 5-5).

The ash basin was subdivided into 20 different zones with specified boron concentrations (Figure-5-14 and Table 5-4). These sources are activated at the start of the simulation, in 1965. At some locations the boron concentration was not specified in all 4 of the ash layers; this was done to improve the calibration with transition zone and shallow bedrock wells in those areas. At two locations, the Dry Ash Landfill (Phase II) and the PV Structural Fill, ash was later placed on top of part of the ash basin. Monitoring wells in these locations sometimes indicate higher boron concentrations than surrounding wells, and this is reflected in the specified source concentrations.

The remaining parts of the Dry Ash Landfills Phase I and Phase II and PV Structural Fill were described using 4 specified concentration zones (Figure 5-15 and Table 5-5). These boron source zones were activated when the respective landfill or structural fill became active.

The calibrated K_d values for the boron was 0.5 in the saprolite and transition zone materials, and 0.02 in the bedrock. The effective porosity was set to 0.3 in the unconsolidated layers, and 0.01 in the bedrock layers.

Table 5-6 compares measured (2nd quarter, 2018) and simulated current conditions boron concentrations. The simulated boron concentrations in the transition zone (model layer 8) and the upper part of the bedrock (model layer 9), are shown in Figure 5-16a, b. The model predicts boron transport above the 2L standard beyond the current compliance boundary from the ash basin and Dry Ash Landfill (Phase I) to the south and east near the ash basin dam. This boron migration appears to mainly occur in the saprolite, transition zone, and shallow bedrock, but

transport in the mid-depth bedrock is also predicted. A deep well was recently installed at the AB-01 location and sampling appears to confirm this predicted transport. The model also predicts relatively deep boron transport beneath the Dry Ash Landfill (Phase II), and it shows significant boron concentrations at the AL-02BRLL location at an elevation of about 570 ft. An additional deep well is being installed in this area to better define concentrations in this region.

The simulation shows boron concentrations above the 2L standard to the east of the northern portion of the dam near monitoring wells MW-10S and MW-10D. Boron concentrations are non-detect in groundwater samples from these wells and this could not be reproduced in the simulation while still matching concentrations in surrounding wells. A potential cause of the inconsistency between the simulation and the groundwater sample results could be that the monitoring wells are in direct hydraulic communication with Lake Norman. The water level in Lake Norman fluctuates over about an 8 ft. range, and these water level fluctuations may cause mixing and dilution in subsurface where the wells are screened. This effect is not captured by the model, which assumes a constant average water level for Lake Norman.

Overall, the simulated boron concentrations appear to reasonably match the observed concentrations in most areas, and the model simulated boundary where the 2L standard is exceeded is similar to the observed locations. The normalized root mean square error of the predicted boron values is 1.61%. The simulation results are consistent with the monitoring well data that show no impacts to water supply wells from the ash basin, structural fill, or landfills.

5.4 Transport Model Sensitivity

After the source concentration, the most important transport model parameter for the boron is the K_d . The effective porosity affects transport velocity, but it also appears in the denominator of the retardation factor equation. Considering a Darcy velocity of V , the actual COI velocity, V_c is affected by both the porosity and the retardation factor:

$$V_c = \frac{V}{\phi R} = \frac{V}{\phi + \rho_b K_d}$$

The denominator of this relationship tends to be dominated by the K_d term unless it is very small. This is the reason why a small K_d value is assigned to the bedrock, where the

effective porosity is due to the fractures, and is low. The transport model sensitivity to the K_d values was evaluated by running the boron transport simulation with K_d values that were 5 times smaller, and 5 times larger than the calibrated values (0.5 mL/g in the saprolite and transition zone, and 0.02 mL/g in the bedrock). The results of this study are shown in Table 5-7. The simulation results are seen to be sensitive to the K_d value range tested here. The calibrated value produces a normalized root mean square error of 1.61%. This increases to 5.33% and 2.33% for the low K_d and high K_d cases, respectively. In terms of the boron plume behavior, the low K_d simulation over-predicts the extent of boron migration, while the high K_d simulation under-predicts the extent of boron migration.

6.0 PREDICTIVE SIMULATIONS OF CLOSURE SCENARIOS

The simulated July 2018 boron distribution was used as the initial condition in closure simulations of future flow and transport at the MSS. There are three main simulated scenarios: one in which all of the ash in the ash basin, the Dry Ash Landfill (Phase II), and the PV Structural Fill is excavated and removed from the Site; one in which a final cover system is installed over the ash basin, Dry Ash Landfill (Phase II) and the PV Structural Fill; and a hybrid design where part of the ash is excavated and moved to the central of the ash basin where it is capped with a final cover system, along with capping of the Dry Ash Landfill (Phase II) and the PV Structural Fill. The Dry Ash Landfill (Phase I) is excavated in all 3 closure options.

The current plans call for the MSS ash basin pond to be decanted (drained of free-standing water) beginning in 2019. The decanting of the ash basin pond is expected to take one to two years. Ash basin pond decanting will have an effect on the groundwater flow field, because the pond level will be lowered by about 17 feet, removing free-standing water.

After the ash basin pond decanting, the final site closure activities will start and will continue for several years. The final cover system and hybrid designs are expected to take 8-9 years to complete, while excavation is expected to take about 17 years to complete.

The predictive simulations are run in two steps. The first step is a simulation that starts in 2020 and uses the groundwater flow field after the ash basin pond is decanted. The starting boron distribution for this simulation is the simulated July 2018 concentration distribution. This simulation step continues for a period of 18 years (for excavation) or 10 years (for the final cover system and hybrid design) ending in either 2038 or 2030. The second step assumes that construction activities have been completed and uses the final excavation, hybrid, or final cover system flow field for transport simulations. These simulations start in 2038 or 2030 and continue for 800 years or until the boron concentrations beyond the current compliance boundary decrease below 2L standards. New potential compliance boundaries have recently been developed¹ for the excavation and hybrid closure actions, and these potential boundaries are shown on the related figures in this report. These potential compliance boundaries for the excavation and hybrid scenarios are located at 250 feet from the waste, or at 50 feet inside the property line,

¹ These compliance boundaries are based upon retention of the NPDES permit for the Final Cover scenario and the proposed North Carolina CCR Rules for the Excavation and Hybrid scenarios.

whichever is closer to the waste. For the final cover scenario, the compliance boundary is 500 feet from the waste boundary, or 50 feet inside the property line.

6.1 Interim Period with Ash Basin Pond Decanted

This simulation represents an interim period after the pond is decanted, but before closure action construction is completed. Decanting of the pond is simulated by removing the specified head zone that represents the pond in the current conditions flow simulation and replacing it with a small specified general head area at an elevation of 772 ft., which is 17 feet below the current ash basin free water surface. The specified head area is located in the deepest part of the current ash basin pond (Figure 6-1). Several small ponds in the southern part of the ash basin, and the sluice channel were converted from a general head boundary condition to a drain condition. Recharge at a rate of 8 inches per year is added to the ash basin, and boron initial conditions come from the historical transport simulation. Boron concentrations in the ash are no longer held constant, and the boron can leach from the ash according to its K_d value (which was derived from ash leaching tests). Boron present in the underlying soil and rock is mobile and moves in response to the groundwater flow with adsorption occurring according to the soil or rock K_d value. The surface drains in the southern part of the ash basin remain in this simulation. Figure 6-1 shows the simulated steady-state hydraulic heads after the pond is decanted. Figure 6-2 shows the simulated boron distribution in the transition zone in 2038 with the ash basin decanted prior to excavation.

6.2 Excavation Scenario

This simulation begins in 2038 using the boron distribution from the decanted pond simulation described above. Excavation is simulated by setting the boron concentration in the ash layers in the ash basin, ash landfills, and PV Structural Fill to zero. The concentrations of boron in the remaining impacted soil underneath the ash basin are set to the values from the decanted pond simulation. The ash layers are given a very high hydraulic conductivity (they are now excavated), and the previous ash basin surface water features are removed. Recharge occurs in the ash basin footprint at the background level of 8 inches per year. Ash is present in the ash basin below the elevation of Lake Norman. After the ash is excavated from the basin, a stormwater pond will be present in the excavated area in the southern part of the ash basin. This excavated stormwater pond is shown in blue in Figure 6-3. A small stream network is added to

the ash basin, following the original drainages along the top of the saprolite surface, and draining towards the excavated stormwater pond (Figure 6-3). This drain network simulates the springs and streams that will form in the basin. The stormwater pond is treated as a general head boundary with a high conductance and a head equal to that of Lake Norman (756 ft.).

The steady-state hydraulic heads in the transition zone are shown in Figure 6-4. The groundwater now flows towards the excavated stormwater pond, where it discharges. Dissolved boron that discharges into the stormwater pond from groundwater is likely to be greatly diluted in the pond. If this excavation scenario is selected, the discharge from the drainage system may need to be collected, treated and discharged per the NPDES permit for a period of time.

The simulated boron concentrations in the transition zone (model layer 8) are shown for the years 2050, 2100, 2200, and 2300 for the excavation case in Figure 6-5a, b, c, d. The predicted boron concentrations in the shallow bedrock (model layer 9) are shown for the years 2050, 2100, 2200, and 2300 in Figure 6-6a, b, c, d. The red line in these figures is the potential compliance boundary following ash basin excavation. This simulation suggests that in the absence of any further corrective action, boron may continue to be above the 2L standard in groundwater beyond the current compliance boundary near Lake Norman for several hundred years. The simulated boron concentrations are persistent under Lake Norman in the transition zone and bedrock throughout the future projections due to the low hydraulic gradients under the lake. Boron concentrations shown in groundwater beneath Lake Norman do not represent surface water concentrations in Lake Norman. The boron concentration in groundwater that is beyond the current or potential compliance boundary never exceeds the US EPA tap water standard of 4,000 $\mu\text{g/L}$. The simulation shows that water supply wells in the area are not impacted by boron at any time in the future.

Two locations were chosen to produce boron concentration versus time (time-series) plots (Figure 6-7). Point 1 is located at the current compliance boundary immediately east of the Dry Ash Landfill (Phase I). Location 2 is on the current compliance boundary below the ash basin dam on the edge of Lake Norman. At these points, boron concentrations greater than the 2L standard extend out farthest from the compliance boundary and were chosen as conservative locations to track boron beyond the compliance boundary.

The predicted concentrations in the transition zone and shallow bedrock at point 1 are shown in Figure 6-8. The concentrations are predicted to gradually decrease over time, dropping below the 2L standard in about 100-200 years. Similar behavior is observed at location 2, shown in Figure 6-9. The boron concentration at both locations is always below the EPA Regional Screening tap water level of 4,000 µg/L at these locations.

6.3 Final Cover Scenario

The final cover simulations begin in 2030 using the boron distribution from the decanted basin simulations described above. The ash basin cover design used in the model is based on a draft closure plan design developed by AECOM (2018). Following ash basin pond decanting, this draft design calls for the ash to be regraded inside the basin to form a gentle slope from north to south towards the dam. Shallow swales are built that approximately trace the original surface water drainage patterns in the basin footprint, with ditches at the center of each swale. The cover system consists of an impermeable geomembrane, covered with about 2 feet of soil and a grass surface. The surface drainage ditches follow the centers of the final cover swales and converge to a single channel that discharges into Lake Norman just north of the existing dam. An underdrain system is proposed to collect ash pore water below the cap. The current conceptual design for this subsurface drainage system calls for the installation of drains 5 feet below the elevation of the cover system in a network that corresponds to the cover surface water drainage system. Figure 6-10 shows the drain network that was used in the final cover simulation to simulate this underdrain system. The numbered nodes along the drain arcs are locations where the drain elevation was specified using the draft design from AECOM (2018). Drain elevations between these nodes were interpolated along the arcs. The drains are simulated using the MODFLOW DRAIN feature, using a relatively high conductance of 10.0 ft²/d/ft. Groundwater flow into these drains is removed from the model. If the final cover design is selected, the discharge from the drainage system may need to be collected, treated and discharged per the NPDES permit for a period of time.

The final cover system is simulated by removing all of the original ash basin surface water features and replacing them with this underdrain network. The ash properties are adjusted to reflect regrading of the ash in the area near the dam (a conductivity of 2 ft/d), and the recharge rate through the cover is set to 0.00054 inches per year. This value is based on landfill cover

simulations performed using the Hydrologic Evaluation of Landfill Performance program (HELP) by AECOM. The plans call for excavation of the Dry Ash Landfill (Phase I), and three of the northern ash basin fingers near the Industrial landfill (these three fingers are being removed to install the temporary stormwater ponds for stormwater being rerouted around the PV Structural Fill). The Dry Ash Landfill (Phase II) and the PV Structural Fill are capped in this simulation. The recharge rate through the cover of these fills is set to 0.00054 inches per year.

The boron initial conditions for this simulation come from the dewatered ash basin pond simulation in the year 2030. The boron concentrations in the ash are variable in time, and the K_d value in the ash was set to a value measured in ash leaching tests performed with ash from the basin (0.77 mL/g).

The steady-state hydraulic heads in the transition zone are shown in Figure 6-11. The groundwater flow field changes slightly from current conditions, and it continues to be dominated by strong groundwater divides to the west, north, and east, with flow towards Lake Norman. The simulation predicts that the underdrain system would remove about 130 gpm of groundwater.

The simulated boron concentrations in the transition zone (model layer 8) are shown for the years 2050, 2100, 2200, and 2300 for the final cover simulation in Figure 6-12a, b, c, d. The predicted boron concentrations in the shallow bedrock (model layer 9) are shown for the years 2050, 2100, 2200, and 2300 in Figure 6-13a, b, c, d. As in the case of the excavation simulation, this final cover simulation also suggests that in the absence of corrective action, that boron may be present above the 2L standard beyond the current compliance boundary near Lake Norman for several hundred years. Boron concentrations shown in groundwater beneath Lake Norman do not represent surface water concentrations in Lake Norman. The dissolved boron concentration in groundwater that is beyond the current or potential compliance boundary never exceeds the US EPA tap water standard of 4,000 $\mu\text{g/L}$. The simulation shows that water supply wells in the area are not impacted by boron at any time in the future.

The simulated transport in the final cover scenario differs from the excavation case because groundwater containing boron is not intercepted by the excavated stormwater pond. Over time, plumes of dissolved boron that originate upgradient in the ash basin, Dry Ash Landfill (Phase II), and to a lesser extent, the PV Structural Fill are predicted to migrate to the

southeast towards Lake Norman. As in the excavation simulation, the simulated boron concentrations are persistent under Lake Norman in the transition zone and bedrock throughout the future projections due to the low hydraulic gradients under the lake.

As before, two locations were chosen to produce boron concentration versus time (time-series) plots (Figure 6-7). Point 1 is located at the current 2L compliance boundary immediately east of the Phase 1 ash landfill. Location 2 is on the current 2L compliance boundary below the ash basin dam on the edge of Lake Norman.

The predicted boron concentrations in the transition zone and shallow bedrock at point 1 are shown in Figure 6-8. The boron concentrations are predicted to slowly decrease over time, dropping below the 2L standard after about 400 years. Similar behavior is observed at location 2, shown in Figure 6-9.

As described above, these predictions differ from the excavation case because in that simulation, the boron plume is intercepted by the excavated stormwater pond. The time to achieve boron below the 2L concentrations outside the current compliance boundary would be greatly reduced if some corrective action was taken. The boron concentration at both locations is always below the EPA tap water standard of 4,000 $\mu\text{g/L}$ at these locations in this simulation.

6.4 Hybrid Design Scenario

The hybrid design simulation begins in 2030 using the boron distribution from the decanted basin simulation described previously. The hybrid design is based on a draft closure plan option developed by AECOM in 2015. This design, illustrated in Figure 6-16 (from AECOM, 2015), involves complete excavation of the coal ash from the southern part of the ash basin following decanting of the ash basin. This ash would be placed in the center part of the ash basin, forming a large mound or stack. The 2015 design results in a maximum ash stack elevation of 920 ft., and ash in the northern fingers of the basin would be capped in a manner similar to the final cover design. The excavation of ash in the southern part of the ash basin would extend below the elevation of Lake Norman resulting in a stormwater pond that would form within the footprint of the excavated area (shown in blue in Figures 6-16 and 6-17).

The regraded ash would be covered with an impermeable geomembrane, soil, and a grass surface. The center elevated ash stack will be surrounded by a perimeter ditch that drains

towards the excavated area. A stabilized ash zone with lower permeability is proposed along the northern edge of the excavated area at the base of the ash stack. This stabilized ash zone could potentially be created using a deep mixing technique, and it is included in the model as a 50 foot wide zone of lower ash conductivity (0.2 ft/d) at the southern edge of the ash stack.

An underdrain system has been included in this simulation to collect water in the ash below the cap. These drains are located 5 feet below the elevation of the cover system in a network that follows the surface drainage ditches from the ash basin fingers, towards the central perimeter ditch that drains water around the main ash stack (Figure 6-17). The underdrain node elevations were estimated from the final cover design, and from current ground surface elevations in the area. If the hybrid scenario is selected, the discharge from the underdrains and reformation of streams in the former ash basin footprint may need to be collected, treated and discharged per the NPDES permit for a period of time.

The cover system over the ash extends to the PV Structural Fill and the Dry Ash Landfill (Phase II) and is simulated by setting the recharge rate to 0.00054 inches per year. The excavated part of the ash basin is simulated by increasing the hydraulic conductivity of the ash to a very high value, by restoring the recharge to the background level of 8 inches per year, by adding the excavated stormwater pond as a general head boundary, and by adding a drain network along the base of the excavation in former valleys. This drain network is intended to simulate springs and streams that will form in the excavated area (Figure 6-17). Boron concentrations in the excavated ash layers are set to zero, while initial boron concentrations in the deeper layers come from the decanted ash basin pond simulation.

The boron initial conditions in the remaining ash come from the decanted ash basin pond simulation. The boron concentrations in the ash are variable in time, and the K_d value in the ash is set to the value measured in ash leaching tests performed with ash from the basin (0.77 mL/g).

The steady-state hydraulic heads in the transition zone are shown in Figure 6-18. This design is similar to the excavation scenario in that the groundwater now discharges to the excavated stormwater pond. Boron dissolved in groundwater discharging into this pond would be greatly diluted after it entered the pond.

The simulated boron concentrations in the transition zone (model layer 8) are shown for the years 2050, 2100, 2200, and 2300 for the hybrid case in Figure 6-19a, b, c, d. The predicted boron concentrations in the shallow bedrock (model layer 9) are shown for the years 2050, 2100, 2200, and 2300 in Figure 6-20a, b, c, d. The red line in these figures is a potential compliance boundary for the hybrid closure action. The predicted boron transport is similar to the excavation case, except that boron from the ash basin, landfill, and structural fill migrate somewhat further to the southeast before being intercepted by the excavated stormwater pond. The simulated boron concentrations are persistent under Lake Norman in the transition zone and bedrock throughout the future projections due to the low hydraulic gradients under the lake. Boron concentrations shown in groundwater beneath Lake Norman do not represent surface water concentrations in Lake Norman.

As in the excavation and final cover simulations, this simulation also suggests that in the absence of corrective action, that boron may be beyond the current compliance boundary near Lake Norman for several hundred years. The boron concentration in groundwater that is beyond the current or potential compliance boundary never exceeds the US EPA tap water standard of 4,000 $\mu\text{g/L}$. The simulation shows that water supply wells in the area are not impacted by boron at any time in the future.

The same two locations were chosen to produce boron concentration versus time (time-series) plots (Figure 6-7). Point 1 is located at the current 2L compliance boundary immediately east of the Dry Ash Landfill (Phase 1). Location 2 is on the current 2L compliance boundary below the ash basin dam on the edge of Lake Norman.

The predicted boron concentrations in the transition zone and shallow bedrock at Point 1 are shown in Figure 6-21. The concentrations are similar to the excavation case, and are predicted to gradually decrease over time, dropping below the 2L standard in about 100 years. Similar behavior is observed at location 2, shown in Figure 6-22. The boron concentration is always below the EPA tap water standard of 4,000 $\mu\text{g/L}$ at these locations.

6.5 Conclusions Drawn from the Predictive Simulations

The simulated boron concentrations in the transition zone and shallow bedrock from the 3 model scenarios are compared side-by-side in Figures 6-23 through 6-26 for the years 2050,

2100, 2200, and 2300. Based on the simulations described in this report, the following conclusions are drawn:

- Water supply wells and domestic wells in the area are not impacted by boron currently or at any time in the future for any of the scenarios.
- Predicted future boron concentrations at and beyond the current compliance boundary vary for the excavation, final cover system, and hybrid design closure simulations. In all cases a low concentration (but above 2L) plume of boron is predicted to continue to migrate south and east towards Lake Norman.
- These simulations do not include remedial measures associated with groundwater corrective action. It is expected that straightforward engineered measures, such as ground water pumping, could control the boron plume in each scenario.
- In the absence of remedial measures associated with corrective action, boron is predicted to exceed the 2L standard at the current compliance boundary near Lake Norman for hundreds of years.
- Recent ash basin pumping tests and the installation of deep bedrock wells near the ash basin dam will reduce model uncertainty, and results will be incorporated into the next version of this model.

7.0 REFERENCES

- AECOM, 2015, Closure Option #1 Hybrid Closure #1 Plan View, Drawing Number B2-1, December 23, 2015.
- AECOM, 2018, Duke Energy Marshall Steam Station 2018 Closure Plan Updates – (Draft 60%) Ash Basin Closure, August 24, 2018.
- Daniel, C.C., D. G. Smith, and J. L. Eimers, 1997, Hydrogeology and Simulation of Groundwater Flow in the Thick Regolith-Fractured Crystalline Rock Aquifer System of Indian Creek Basin, North Carolina, USGS Water-Supply 2341.
- Haven, W. T. 2003. Introduction to the North Carolina Groundwater Recharge Map. Groundwater Circular Number 19. North Carolina Department of Environment and Natural Resources. Division of Water Quality, 8 p.
- HDR, 2015a Comprehensive Site Assessment Marshall Steam Station Ash Basin- September 8, 2015. Terrell, NC.
- HDR, 2015b, Corrective Action Plan Part 1 Marshall Steam Station Ash Basin- December 7, 2015. Terrell, NC.
- HDR, 2016, Corrective Action Plan Part 2 Marshall Steam Station Ash Basin – March 3, 2016. Terrell, NC
- McDonald M.G. and A.W. Harbaugh, 1988, A Modular Three-Dimensional Finite-Difference Ground-Water Flow Model, U.S. Geological Survey Techniques of Water Resources Investigations, book 6, 586 p.
- Niswonger, R.G., S. Panday, and I. Motomu, 2011, MODFLOW-NWT, A Newton formulation for MODFLOW-2005, U.S. Geological Survey Techniques and Methods 6-A37, 44-.
- North Carolina Water Supply and Use, in “National Water Summary 1987 - Hydrologic Events and Water Supply and Use”. USGS Water-Supply Paper 2350, p. 393-400.
- North Carolina; Estimated Water Use in North Carolina, 1995, USGS Fact Sheet FS-087-97
- Radcliffe, D.E., L.T. West, L.A. Morris, and T. C. Rasmussen. 2006. Onsite Wastewater and Land Application Systems: Consumptive Use and Water Quality, University of Georgia.
- SynTerra, 2018a, 2018 Comprehensive Site Assessment Update, January 31, 2018.
- SynTerra, 2018b, CSA Update Report Comments-Response to Comments, August 31, 2018.
- Treece, M.W, Jr., Bales, J.D., and Moreau, D.H., 1990, North Carolina water supply and use, in National water summary 1987 Hydrologic events and water supply and use: U.S. Geological Survey Water-Supply Paper 2350, p. 393-400.
- Zheng, C. and P.P. Wang, 1999, MT3DMS: A Modular Three-Dimensional Multi-Species Model for Simulation of Advection, Dispersion and Chemical Reactions of Contaminants in Groundwater Systems: Documentation and User’s Guide, SERDP-99-1, U.S. Army Engineer Research and Development Center, Vicksburg, MS.

TABLES

Table 5-1. Comparison of observed and computed heads for the calibrated flow model.

Well	Observed Head	Computed Head	Residual Head
AB-10BR	790.42	791.18	-0.76
AB-10D	790.04	791.11	-1.07
AB-10S	790.94	790.76	0.18
AB-10SL	790.07	790.94	-0.87
AB-11D	795.32	796.90	-1.58
AB-11S	794.57	796.53	-1.96
AB-12BR	794.16	791.95	2.21
AB-12D	791.25	791.97	-0.72
AB-12S	790.31	791.95	-1.64
AB-12SL	790.39	791.94	-1.55
AB-13D	797.87	801.92	-4.05
AB-13S	797.69	800.75	-3.06
AB-14D	809.95	812.41	-2.46
AB-14S	809.77	812.69	-2.92
AB-15BR	806.46	804.31	2.15
AB-15D	803.36	804.41	-1.05
AB-15S	805.28	804.78	0.50
AB-15SL	800.94	804.32	-3.38
AB-16D	815.02	813.43	1.59
AB-16S	815.36	813.41	1.95
AB-17D	819.76	822.34	-2.58
AB-17S	819.1	823.02	-3.92
AB-18D	818.18	818.17	0.01
AB-18S	818.13	818.38	-0.25
AB-1BR	772.29	770.24	2.05
AB-1BRL	774.29	770.13	4.16
AB-1D	768.81	769.90	-1.09
AB-1S	765.97	769.18	-3.21
AB-20D	826.72	828.65	-1.93
AB-20S	828.55	828.88	-0.33
AB-21D	792.83	793.88	-1.05
AB-21S	791.45	793.98	-2.53
AB-2D	767.09	764.64	2.45
AB-2S	761.02	762.70	-1.68
AB-3D	796.69	793.65	3.04
AB-3S	797.54	794.45	3.09
AB-4D	794.54	796.54	-2.00
AB-4S	798.93	796.69	2.24
AB-4SL	798.67	796.56	2.11
AB-5BR	799.16	801.70	-2.54

AB-5D	799.53	801.71	-2.18
AB-5S	799.48	802.04	-2.56
AB-6BR	817.69	818.35	-0.66
AB-6BRA	818	818.64	-0.64
AB-6BRL	816.47	817.83	-1.36
AB-6D	818.49	819.50	-1.01
AB-6S	820.4	820.21	0.19
AB-7D	813.95	815.24	-1.29
AB-7S	815.11	815.60	-0.49
AB-8D	791.74	795.23	-3.49
AB-8S	791.18	794.65	-3.47
AB-9BR	790.26	790.40	-0.14
AB-9D	789.53	790.43	-0.90
AB-9S	790.08	790.35	-0.27
AL-1BR	776.97	776.71	0.26
AL-1D	773.98	776.87	-2.89
AL-1S	779.11	776.97	2.14
AL-2BR	803.23	797.98	5.25
AL-2BRL	799.48	798.07	1.41
AL-2BRLL	798.65	798.08	0.57
AL-2D	801.46	798.14	3.32
AL-2S	800.19	798.26	1.93
AL-3BR	803.57	806.14	-2.57
AL-3D	805.5	806.29	-0.79
AL-3S	806.55	806.65	-0.10
AL-4BR	809.5	810.96	-1.46
AL-4BRL	796.76	798.16	-1.40
AL-4D	812.37	811.18	1.19
BG-1BR	801.23	806.04	-4.81
BG-1BRA	801.78	806.14	-4.36
BG-1D	804.98	807.82	-2.84
BG-1S	807.23	809.22	-1.99
BG-2BR	807.6	810.37	-2.77
BG-2S	809.15	812.07	-2.92
BG-3BR	830.93	830.03	0.90
BG-3D	835.19	831.46	3.73
BG-3S	833.29	832.60	0.69
GWA-10D	767.54	766.27	1.27
GWA-10S	764.68	765.09	-0.41
GWA-11BR	763.78	767.37	-3.59
GWA-11D	763.8	767.58	-3.78
GWA-11S	766.11	768.36	-2.25
GWA-12BR	857.45	861.61	-4.16

GWA-12D	858.4	861.61	-3.21
GWA-12S	870.23	865.27	4.96
GWA-13D	860.44	863.31	-2.87
GWA-13DA	859.57	863.20	-3.63
GWA-13S	865.96	865.69	0.27
GWA-14D	867.58	863.73	3.85
GWA-14S	867.61	864.78	2.83
GWA-15S	757.92	760.21	-2.29
GWA-1BR	764.38	765.13	-0.75
GWA-1D	761.8	765.19	-3.39
GWA-1S	760.98	765.30	-4.32
GWA-2D	803.16	797.87	5.29
GWA-2DA	801.42	797.73	3.69
GWA-2S	802.54	798.84	3.70
GWA-3D	832.95	834.90	-1.95
GWA-3S	830.27	834.96	-4.69
GWA-4D	843.73	844.67	-0.94
GWA-4S	843.3	845.66	-2.36
GWA-5D	811.3	813.27	-1.97
GWA-5S	812.58	814.57	-1.99
GWA-6D	802.2	801.86	0.34
GWA-6S	802.39	801.93	0.46
GWA-7D	800.95	796.62	4.33
GWA-7S	798.37	798.37	0.00
GWA-8D	816.42	814.72	1.70
GWA-8S	817.5	817.21	0.29
GWA-9BR	846.71	844.73	1.98
MS-10	833.46	834.03	-0.57
MS-11	825.46	823.65	1.81
MS-12	813.28	814.22	-0.94
MS-13	810.79	812.99	-2.20
MS-14	806.81	808.16	-1.35
MS-15	811.1	809.31	1.79
MS-16	811.24	814.67	-3.43
MS-8	826.35	823.71	2.64
MS-9	824.05	820.57	3.48
MW-1	772.58	777.31	-4.73
MW-10D	756.27	757.66	-1.39
MW-10S	754.59	757.61	-3.02
MW-11D	840.17	837.44	2.73
MW-11S	840.01	839.50	0.51
MW-12D	856.61	857.78	-1.17
MW-12S	857.58	859.71	-2.13

MW-13D	843.45	844.29	-0.84
MW-13S	841.8	844.50	-2.70
MW-14BR	774.22	774.95	-0.73
MW-14D	772.77	774.70	-1.93
MW-14S	773.32	774.77	-1.45
MW-2	790.7	792.05	-1.35
MW-3	804.63	805.77	-1.14
MW-4	828.92	830.84	-1.92
MW-4D	829.28	831.22	-1.94
MW-5	796.82	797.85	-1.03
MW-6D	771.62	767.32	4.30
MW-6S	769.04	767.36	1.68
MW-7D	769.4	766.37	3.03
MW-7S	762.13	765.52	-3.39
MW-8D	759.92	760.21	-0.29
MW-8S	757.88	758.94	-1.06
MW-9D	758.8	759.00	-0.20
MW-9S	760.38	757.77	2.61
OB-1	804.33	805.40	-1.07
OB-1 (WLO)	776.93	780.08	-3.15
OB-2	810.5	813.38	-2.88
OB-3	812.71	816.77	-4.06
CCR-1S	796.79	797.03	-0.24
CCR-1D	795.36	796.76	-1.40
CCR-2S	794.61	791.87	2.74
CCR-2D	794.81	791.69	3.12
CCR-3S	758.4	759.87	-1.47
CCR-3D	758.95	760.25	-1.30
CCR-4S	760.23	760.34	-0.11
CCR-4D	761.24	760.68	0.56
CCR-5S	760.68	759.71	0.97
CCR-5D	762.15	760.02	2.13
CCR-9S	766.56	769.25	-2.69
CCR-9DA	770.04	768.77	1.27
CCR-11S	787.46	787.76	-0.30
CCR-11D	787.47	785.91	1.56
CCR-12S	788.22	788.42	-0.20
CCR-12D	788.2	787.79	0.41
CCR-13S	787.13	785.50	1.63
CCR-13D	787.04	785.23	1.81
CCR-14S	787.07	787.07	0.00
CCR-14D	787.2	786.42	0.78
CCR-15S	794.32	792.03	2.29

CCR-15D	794.3	791.96	2.34
CCR-16S	806.1	802.59	3.51
CCR-16D	797.44	800.59	-3.15

Table 5-2. Calibrated hydraulic parameters.

Hydrostratigraphic Unit	Model Layers	Spatial Zones (number corresponds to Figures 5-1 through 5-7)	Horizontal Hydraulic Conductivity, ft/d	Anisotropy ratio, $K_h \cdot K_v$
Ash Basin, Landfills, Structural Fill	1-4	#2, 6, 10, 11 coal ash	2.0	10
Ash Basin (pond)	1-4	#5 pond	100	1
Ash Basin Dam	1-4	#1 ash basin dam	0.03	5
Saprolite	5-7	#13 saprolite main model	1.0	1
	5-7	#1	0.1	1
	5-7	#2	4.0	1
	5-7	#3	0.1	1
	5-7	#4	0.1	1
	5-7	#5	0.2	1
	5-7	#6	0.1	1
	5-7	#7	0.05	1
	5-7	#8	1.0	1
	5-7	#9	0.3	1
	5-7	#10	0.3	1
	5-7	#11	0.05	1
	5-7	#12	0.1	1
Transition zone	8	#8 TZ main model	1.5	1
	8	#1	0.1	1
	8	#2	0.1	1
	8	#3	0.1	1
	8	#4	0.05	1
	8	#5	1.0	1
	8	#6	0.1	1
	8	#7	0.05	1
Bedrock (upper)	9	#9 main model	0.7	1
	9	#1	0.02	1
	9	#2	0.01	1
	9	#3	0.03	1
	9	#4	0.01	1
	9	#5	4.0	1
	9	#6	2.0	1
	9	#7	0.01	1
	9	#8	0.01	1
	10	#9 main model	0.7	1
	10	#1	0.02	1
	10	#2	0.01	1
	10	#3	0.005	1
	10	#4	0.01	1
	10	#5	7.0	1
	10	#6	3.0	1

	10	#7	0.01	1
	10	#8	0.01	1
	11	#10 main model	0.7	1
	11	#1	0.02	1
	11	#2	0.01	1
	11	#3	8.0	1
	11	#4	0.005	1
	11	#5	0.01	1
	11	#6	7.0	1
	11	#7	3.0	1
	11	#8	0.01	1
	11	#9	0.01	1
	12	#9 main model	0.7	1
	12	#1	0.02	1
	12	#2	0.01	1
	12	#3	0.005	1
	12	#4	0.01	1
	12	#5	7.0	1
	12	#6	3.0	1
	12	#7	0.01	1
	12	#8	0.01	1
Bedrock (mid-depth)	13-15	#5 main model	0.2	1
	13-15	#1	0.01	1
	13-15	#2	5.0	1
	13-15	#3	0.01	1
	13-15	#4	0.01	1
Bedrock (lower)	16-20	#1 main model	0.01	1

Table 5-3. Flow model sensitivity. The normalized root mean square error (NRMSE) in the calculated heads is shown.

Parameter	Decrease by 1/2	Calibrated	Increase by 2
Recharge (8 in/yr)	6.79%	2.08%	10.05%
Ash K_h (2.0 ft/d)	2.32%	2.08%	2.06%
Saprolite K_h (1.0 ft/d)	2.30%	2.08%	2.21%
TZ K_h (1.5 ft/d)	2.12%	2.08%	2.12%
Upper Bedrock K_h (0.7 ft/d)	2.96%	2.08%	2.92%
Mid-depth Bedrock K_h (0.2 ft/d)	2.19%	2.08%	2.18%
Lower Bedrock K_h (0.01 ft/d)	2.12%	2.08%	2.09%

Table 5-4. Ash basin boron source concentrations (ug/L) used in historical transport model from 1965 through 2018.

Concentration Zone #	Boron Concentration	Model Layers
1	3,900	1-5
5	500	1-4
6	100	1-4
7	20,000	1-4
8 (Now Phase II Landfill)	5,000 (1965-1986)	1-4
	10,000 (1986-2018)	
9	3,900	1-3
10	100	1-4
11	94,600	1-4
12	100	1-4
14	100	1-3
15	1,000	1-4
16	28,000	1-3
17	900	1-2
18	18,000	1-4
19	1,000	1-4
20	11,000	1-2
21	3,000	1-2
22	5,000	1-4
23 (Now PV Structural Fill)	5,000 (1965-2000)	1-4
	20,000 (2000-2018)	
24 (Now PV Structural Fill)	5,000 (1965-2000)	1-3
	70,000 (2000-2018)	

Table 5-5. Dry Ash Landfill (Phase II) and PV Structural Fill boron source concentrations (ug/L) used in historical transport model.

Date	Phase 1 LF (#1)	Phase II LF (#4)	Phase II LF (#5)	PV Structural Fill (#8)
1965-1984	0	0	0	0
1984-1986	3,000	0	0	0
1986-2000	3,000	40,000	77,000	0
2000-2018	3,000	40,000	77,000	20,000

Table 5-6. Comparison of observed and simulated boron concentrations (ug/L) in monitoring wells.

Well	Observed boron concentration (ug/L)	Simulated boron concentration (ug/L)
AB-01BR	2,250	3,183
AB-01BRL	2,080	3,516
AB-01D	1,090	3,045
AB-01S	4,210	1,170
AB-02D	405	465
AB-02S	ND	49
AB-03D	158	249
AB-03S	687	1,000
AB-04D	374	505
AB-04S	316	1,000
AB-04SL	583	754
AB-05BR	ND	442
AB-05D	ND	442
AB-05S	1,850	1,000
AB-06BRA	644	56
AB-06BRL	ND	28
AB-06D	5,180	167
AB-06S	514	5,000
AB-07D	ND	103
AB-07S	18,300	18,000
AB-08D	31	8
AB-08S	405	1,000
AB-09BR	ND	37
AB-09D	ND	60
AB-09S	46	965
AB-10BR	267	637
AB-10D	1,360	2,336
AB-10S	27,000	20,000
AB-10SL	14,100	20,000
AB-11D	ND	183
AB-11S	ND	57
AB-12BR	ND	179
AB-12D	1,160	504
AB-12S	94,600	94,600
AB-12SL	3,000	2,434
AB-13D	ND	649
AB-13S	869	900
AB-14D	404	2,002
AB-14S	11,600	11,000
AB-15BR	ND	791

AB-15D	30	1,359
AB-15S	2,720	2,603
AB-15SL	1,430	1,414
AB-16D	ND	44
AB-16S	35	71
AB-17D	ND	273
AB-17S	27,600	28,000
AB-18D	ND	727
AB-18S	2,050	2,488
AB-20D	ND	451
AB-20S	69,400	70,000
AB-21D	ND	850
AB-21S	3,560	3,022
AL-01BR	521	1,986
AL-01D	2,850	2,471
AL-01S	3,720	2,709
AL-02BR	3,760	4,834
AL-02BRL	1,780	5,484
AL-02BRLL	10,700	5,441
AL-02D	10,400	4,284
AL-02S	12,500	13,122
AL-03BR	1,070	6,922
AL-03D	5,070	6,789
AL-03S	76,700	77,000
AL-04BR	8,720	2,931
AL-04BRL	ND	874
AL-04D	2,570	2,931
BG-01BRA	ND	0
BG-01D	ND	0
BG-01S	ND	0
BG-02BR	ND	0
BG-02S	ND	0
BG-03BR	ND	0
BG-03D	ND	0
BG-03S	ND	0
GWA-01BR	ND	103
GWA-01D	ND	41
GWA-01S	ND	0
GWA-02DA	40	19
GWA-02S	ND	0
GWA-03D	ND	0
GWA-03S	ND	0
GWA-04D	43	0
GWA-04S	57	0
GWA-05D	ND	0

GWA-06D	ND	0
GWA-06S	ND	0
GWA-07D	ND	0
GWA-07S	31	0
GWA-08D	ND	0
GWA-08S	ND	0
GWA-09BR	ND	0
GWA-10D	ND	68
GWA-10S	89	20
GWA-11BR	ND	1,943
GWA-11D	997	2,272
GWA-11S	2,740	2,623
GWA-12BR	ND	0
GWA-12D	ND	0
GWA-12S	ND	0
GWA-13DA	ND	0
GWA-13S	ND	0
GWA-14D	ND	0
GWA-14S	ND	0
GWA-15S	1,640	2,399
MS-08	ND	0
MS-10	ND	0
MS-11	ND	0
MS-13	ND	0
MW-01	187	2,858
MW-02	2,900	2,311
MW-03	ND	120
MW-04	ND	0
MW-04D	ND	0
MW-05	ND	277
MW-06D	172	162
MW-06S	285	4
MW-07D	353	3,575
MW-07S	3,520	1,954
MW-08D	258	869
MW-08S	220	378
MW-09D	466	478
MW-09S	ND	329
MW-10D	ND	1,658
MW-10S	ND	12
MW-11D	ND	0
MW-11S	ND	0
MW-12D	ND	0
MW-12S	ND	0
MW-13D	ND	0

MW-13S	ND	0
MW-14BR	126	853
MW-14D	2,030	765
MW-14S	2,430	839
OB-01 (Ash Basin)	ND	0
CCR-01D	5	98
CCR-01S	3	99
CCR-02D	137	456
CCR-02S	168	901
CCR-03D	4	67
CCR-03S	5	3
CCR-04D	6	212
CCR-04S	279	42
CCR-05D	5	361
CCR-05S	168	214
CCR-09DA	21	1,363
CCR-09S	4,410	3,209
CCR-11D	2,800	2,225
CCR-11S	5,070	3,000
CCR-12D	12	1,720
CCR-12S	4,160	3,000
CCR-13D	190	1,518
CCR-13S	4,160	1,900
CCR-14D	2,300	2,046
CCR-14S	4,310	3,000
CCR-15D	3	36
CCR-15S	5	3
CCR-16D	4	1
CCR-16S	8	2

Table 5-7. Transport model sensitivity to the boron K_d values. The calibrated model has a normalized root mean square error (NRMSE) of 1.61%. Boron concentrations are shown for the calibrated model, and for models where the K_d is increased and decreased by a factor of 5.

Well	Observed boron concentration (ug/L)	Boron model calibrated	Model, low K_d	Model, high K_d
	NRMSE	1.61%	5.33%	2.23%
AB-01BR	2,250	3,183	3,185	2,869
AB-01BRL	2,080	3,516	3,523	3,061
AB-01D	1,090	3,045	3,049	2,670
AB-01S	4,210	1,170	1,346	127
AB-02D	405	465	499	309
AB-02S	0	49	60	11
AB-03D	158	249	594	11
AB-03S	687	1,000	1,000	1,000
AB-04D	374	505	924	18
AB-04S	316	1,000	1,000	1,000
AB-04SL	583	754	959	237
AB-05BR	0	442	835	16
AB-05D	0	442	812	18
AB-05S	1,850	1,000	1,000	1,000
AB-06BRA	644	56	238	1
AB-06BRL	0	28	166	0
AB-06D	5,180	167	926	3
AB-06S	514	5,000	5,000	5,000
AB-07D	0	103	1,467	0
AB-07S	18,300	18,000	18,000	18,000
AB-08D	31	8	18	4
AB-08S	405	1,000	1,000	1,000
AB-09BR	0	37	157	13
AB-09D	0	60	253	25
AB-09S	46	965	990	944
AB-10BR	267	637	11,964	85
AB-10D	1,360	2,336	13,635	1,239
AB-10S	27,000	20,000	20,000	20,000
AB-10SL	14,100	20,000	20,000	20,000
AB-11D	0	183	784	1
AB-11S	0	57	58	52
AB-12BR	0	179	388	0
AB-12D	1,160	504	1,296	0
AB-12S	94,600	94,600	94,600	94,600
AB-12SL	3,000	2,434	6,118	29

AB-13D	0	649	1,977	28
AB-13S	869	900	900	900
AB-14D	404	2,002	5,265	116
AB-14S	11,600	11,000	11,000	11,000
AB-15BR	0	791	1,529	116
AB-15D	30	1,359	2,050	233
AB-15S	2,720	2,603	2,708	2,462
AB-15SL	1,430	1,414	2,099	316
AB-16D	0	44	96	11
AB-16S	35	71	76	43
AB-17D	0	273	1,330	1
AB-17S	27,600	28,000	28,000	28,000
AB-18D	0	727	1,480	77
AB-18S	2,050	2,488	2,633	1,922
AB-20D	0	451	3,004	5
AB-20S	69,400	70,000	70,000	70,000
AB-21D	0	850	1,810	61
AB-21S	3,560	3,022	3,424	1,622
AL-01BR	521	1,986	2,003	1,452
AL-01D	2,850	2,471	2,480	1,511
AL-01S	3,720	2,709	2,790	690
AL-02BR	3,760	4,834	29,265	21
AL-02BRL	1,780	5,484	29,897	13
AL-02BRLL	10,700	5,441	21,422	17
AL-02D	10,400	4,284	18,231	157
AL-02S	12,500	13,122	27,128	1,842
AL-03BR	1,070	6,922	16,165	512
AL-03D	5,070	6,789	27,110	66
AL-03S	76,700	77,000	77,000	77,000
AL-04BR	8,720	2,931	24,472	19
AL-04BRL	0	874	13,220	2
AL-04D	2,570	2,931	24,472	19
BG-01BRA	0	0	0	0
BG-01D	0	0	0	0
BG-01S	0	0	0	0
BG-02BR	0	0	0	0
BG-02S	0	0	0	0
BG-03BR	0	0	0	0
BG-03D	0	0	0	0
BG-03S	0	0	0	0
GWA-01BR	0	103	201	1
GWA-01D	0	41	130	0
GWA-01S	0	0	10	0
GWA-02DA	40	19	29	1
GWA-02S	0	0	0	0

GWA-03D	0	0	0	0
GWA-03S	0	0	0	0
GWA-04D	43	0	0	0
GWA-04S	57	0	0	0
GWA-05D	0	0	0	0
GWA-06D	0	0	0	0
GWA-06S	0	0	0	0
GWA-07D	0	0	0	0
GWA-07S	31	0	0	0
GWA-08D	0	0	0	0
GWA-08S	0	0	0	0
GWA-09BR	0	0	0	0
GWA-10D	0	68	179	10
GWA-10S	89	20	34	1
GWA-11BR	0	1,943	2,274	787
GWA-11D	997	2,272	2,569	799
GWA-11S	2,740	2,623	2,783	391
GWA-12BR	0	0	0	0
GWA-12D	0	0	0	0
GWA-12S	0	0	0	0
GWA-13DA	0	0	0	0
GWA-13S	0	0	0	0
GWA-14D	0	0	0	0
GWA-14S	0	0	0	0
GWA-15S	1,640	2,399	2,662	130
MS-08	0	0	0	0
MS-10	0	0	0	0
MS-11	0	0	0	0
MS-13	0	0	0	0
MW-01	187	2,858	2,891	1,783
MW-02	2,900	2,311	9,259	217
MW-03	0	120	284	12
MW-04	0	0	0	0
MW-04D	0	0	0	0
MW-05	0	277	818	16
MW-06D	172	162	164	121
MW-06S	285	4	14	0
MW-07D	353	3,575	3,581	3,125
MW-07S	3,520	1,954	2,116	397
MW-08D	258	869	899	520
MW-08S	220	378	432	47
MW-09D	466	478	517	296
MW-09S	0	329	360	105
MW-10D	0	1,658	2,121	387
MW-10S	0	12	116	0

MW-11D	0	0	0	0
MW-11S	0	0	0	0
MW-12D	0	0	0	0
MW-12S	0	0	4	0
MW-13D	0	0	0	0
MW-13S	0	0	0	0
MW-14BR	126	853	1,388	161
MW-14D	2,030	765	1,622	53
MW-14S	2,430	839	1,969	22
OB-01 (Ash Basin)	0	0	1	0
CCR-01D	5	98	100	62
CCR-01S	3	99	99	99
CCR-02D	137	456	534	55
CCR-02S	168	901	930	618
CCR-03D	4	67	166	0
CCR-03S	5	3	13	0
CCR-04D	6	212	547	33
CCR-04S	279	42	137	0
CCR-05D	5	361	526	76
CCR-05S	168	214	337	16
CCR-09DA	21	1,363	1,365	1,189
CCR-09S	4,410	3,209	3,248	2,457
CCR-11D	2,800	2,225	2,232	1,928
CCR-11S	5,070	3,000	3,000	3,000
CCR-12D	12	1,720	2,114	514
CCR-12S	4,160	3,000	3,000	3,000
CCR-13D	190	1,518	1,570	778
CCR-13S	4,160	1,900	1,929	1,071
CCR-14D	2,300	2,046	2,051	1,961
CCR-14S	4,310	3,000	3,000	3,000
CCR-15D	3	36	150	5
CCR-15S	5	3	6	1
CCR-16D	4	1	14	0
CCR-16S	8	2	4	1

FIGURES

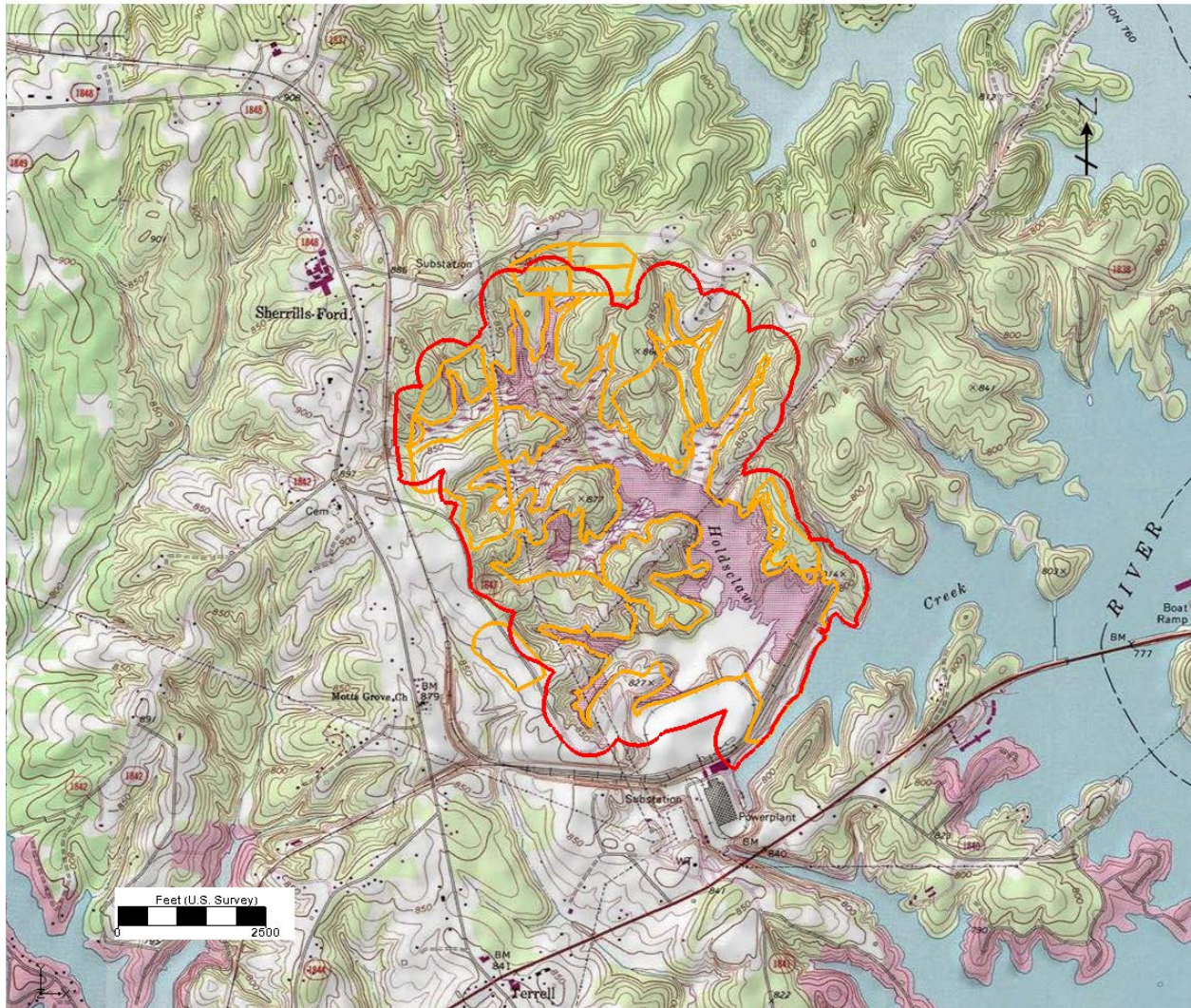


Figure 1-1. Site location map, Marshall Steam Station, Terrell, NC. The ash basin and landfill boundaries are outlined in orange. The ash basin compliance boundary is shown in red.

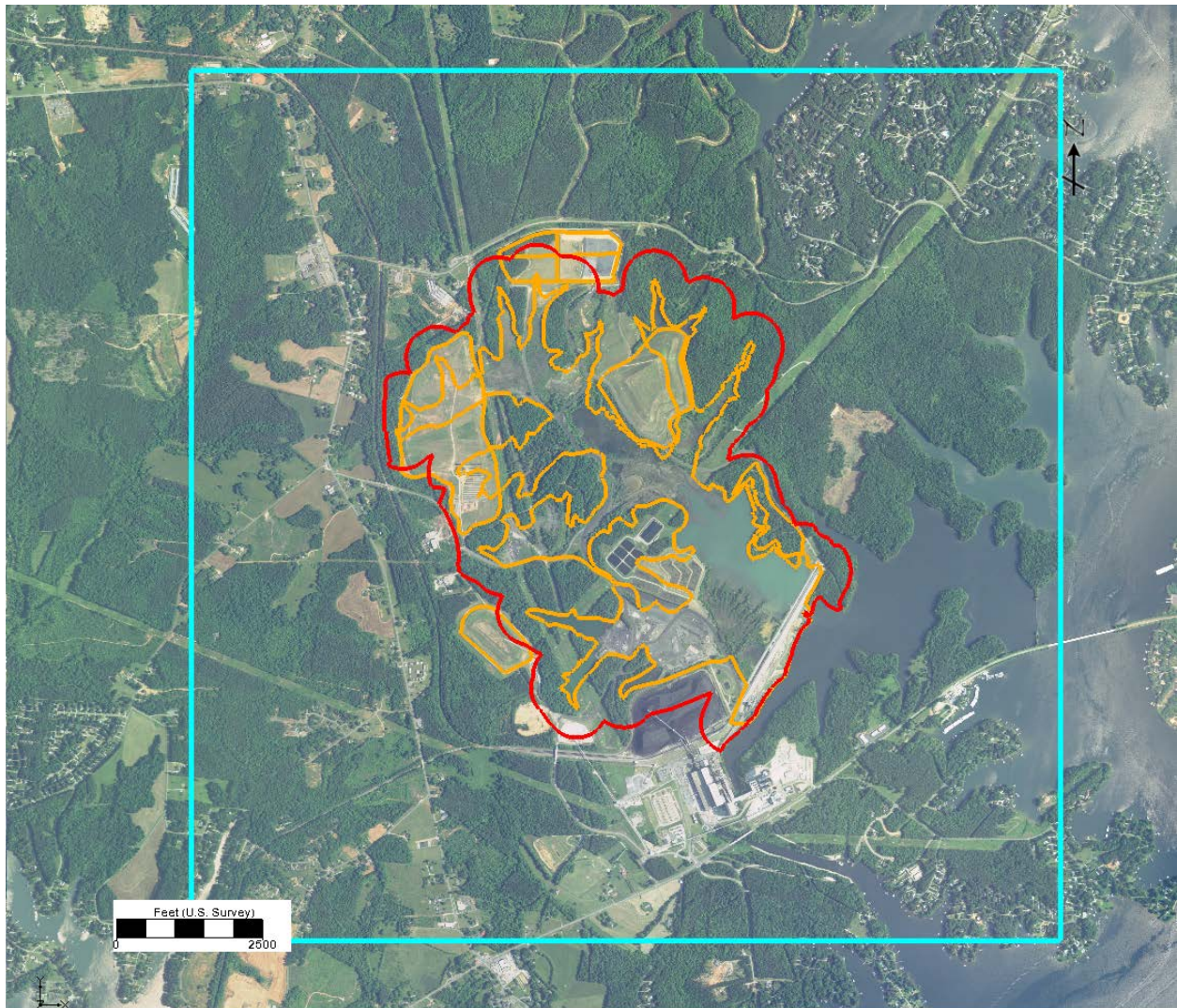


Figure 4-1. Numerical model domain. The model domain is shown in turquoise, the current compliance boundary is in red, and the waste boundary and landfill boundaries are in orange.

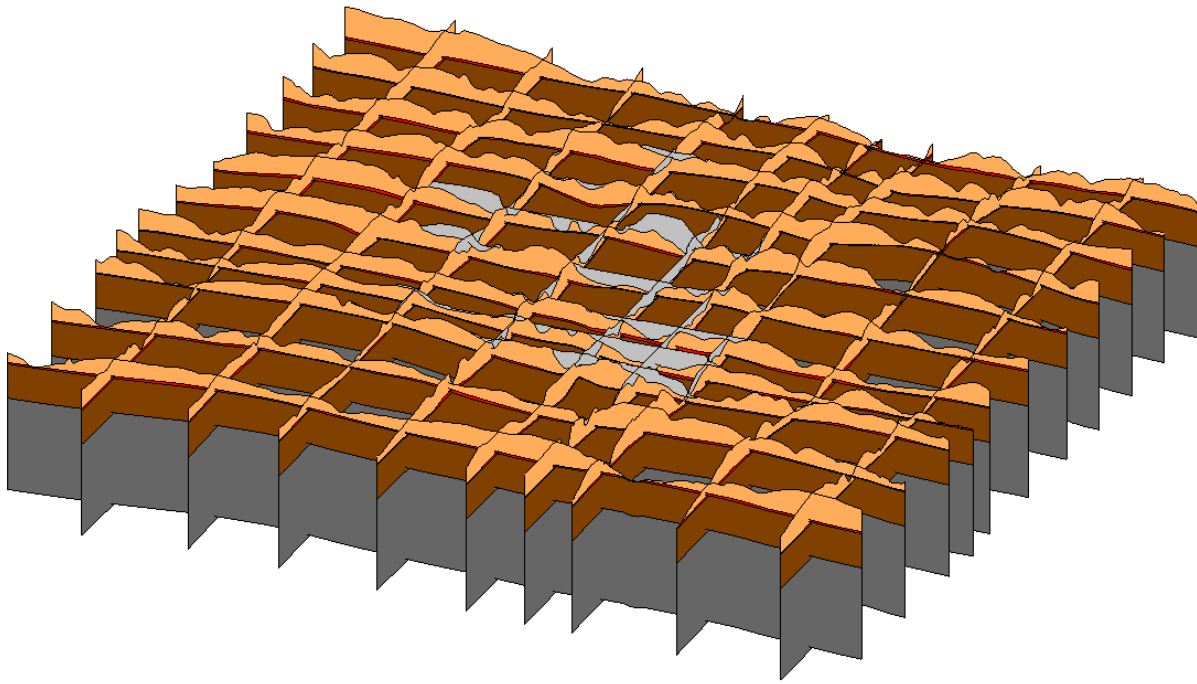


 Figure 4-2. Fence diagram of the 3D hydrostratigraphic model used to construct the model grid. The view is from the southeast, with 4x vertical exaggeration.

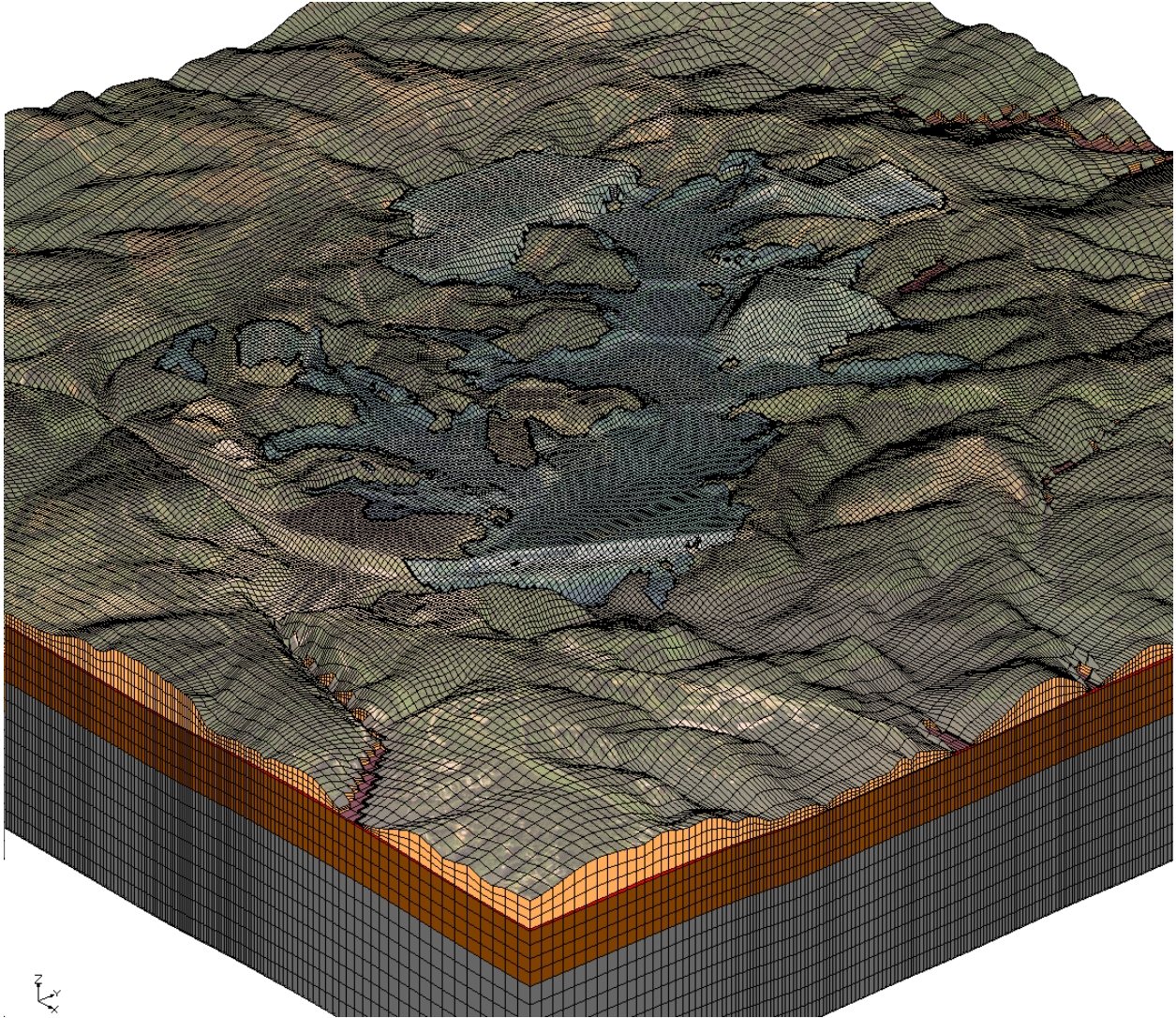


Figure 4-3. Numerical grid used for flow and transport modeling viewed from the southeast. Vertical exaggeration is 4x.

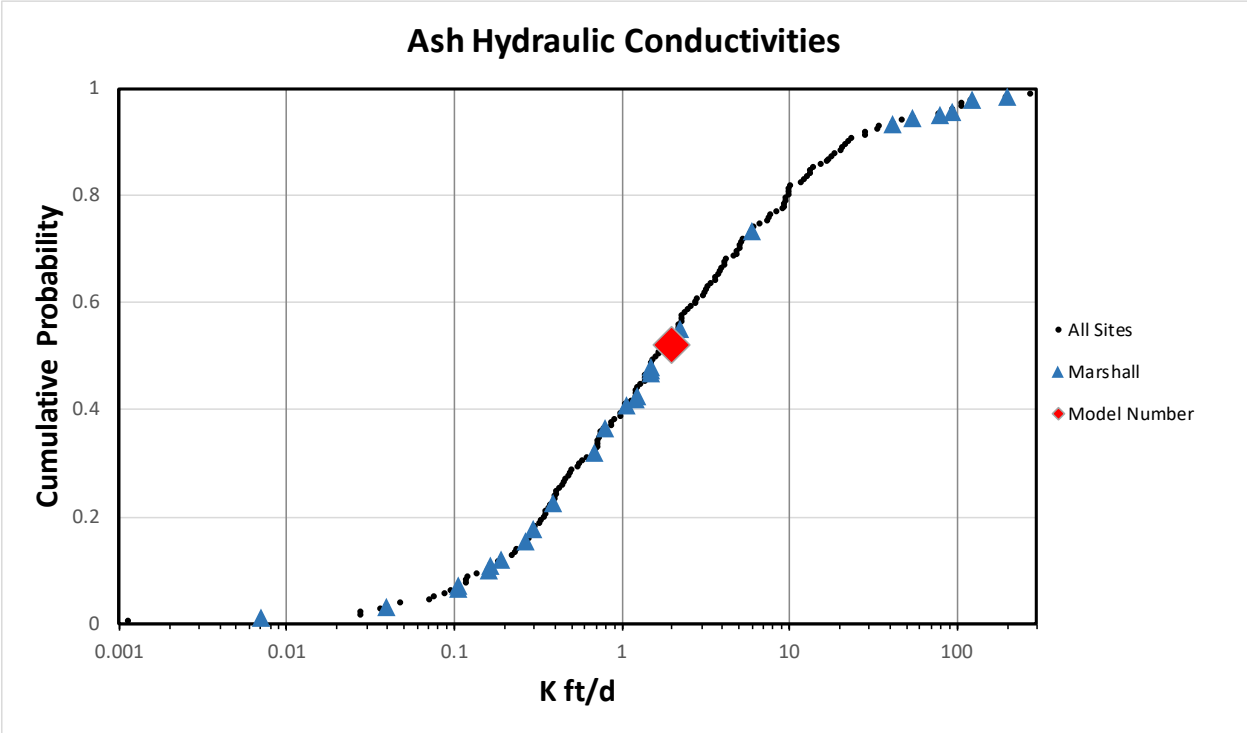


Figure 4-4. Hydraulic conductivity measured in slug tests performed in coal ash at 14 sites in North Carolina.

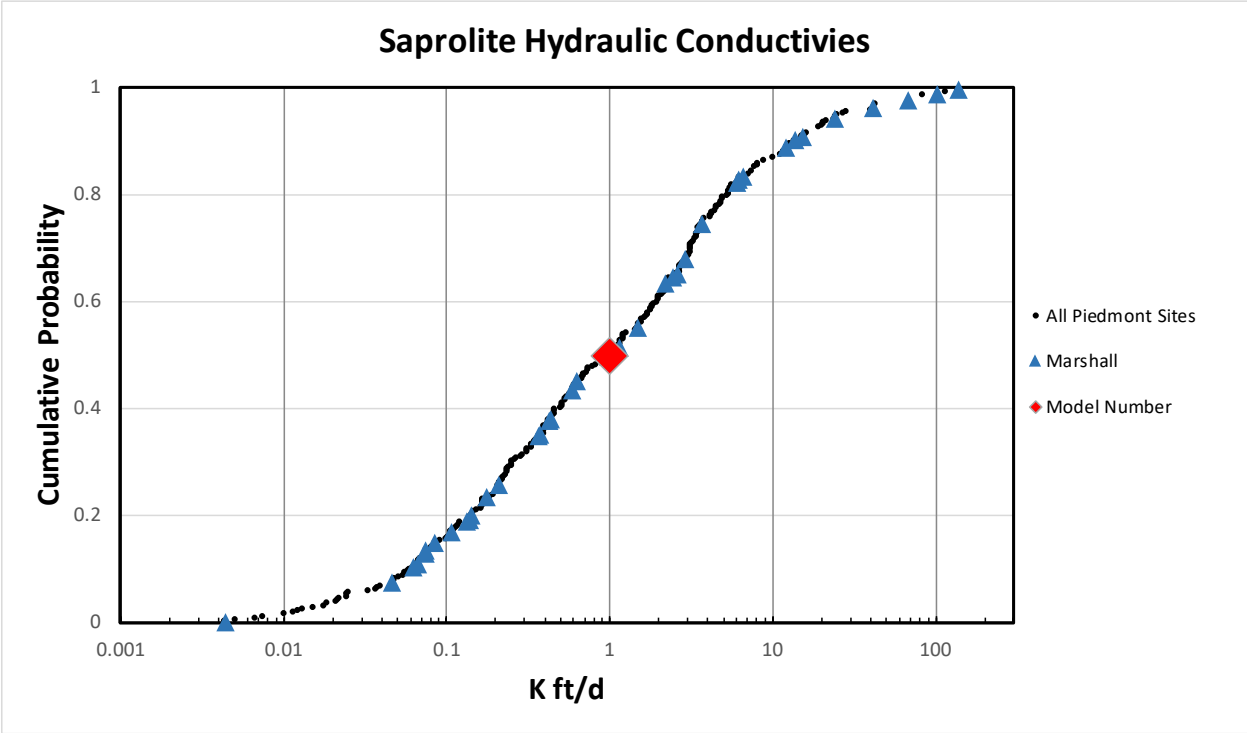


Figure 4-5. Hydraulic conductivity measured in slug tests performed in saprolite at 10 Piedmont sites in North Carolina.

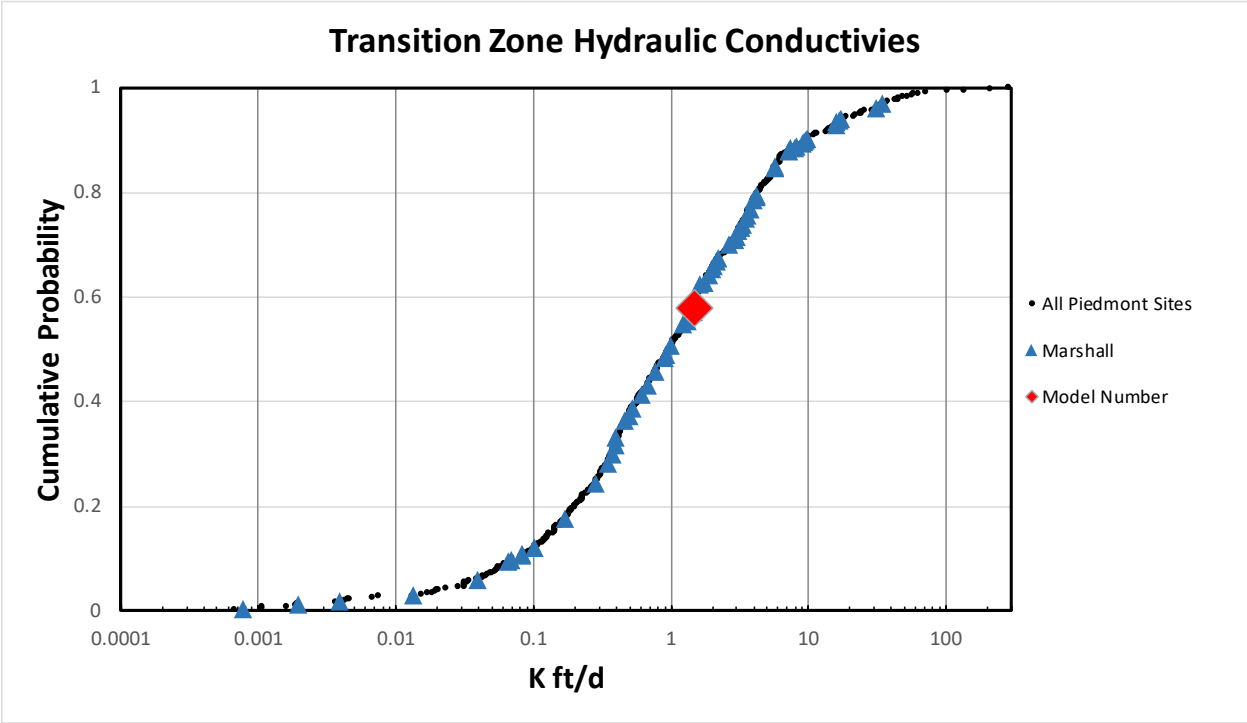


Figure 4-6. Hydraulic conductivity measured in slug tests performed in the transition zone at 10 Piedmont sites in North Carolina.

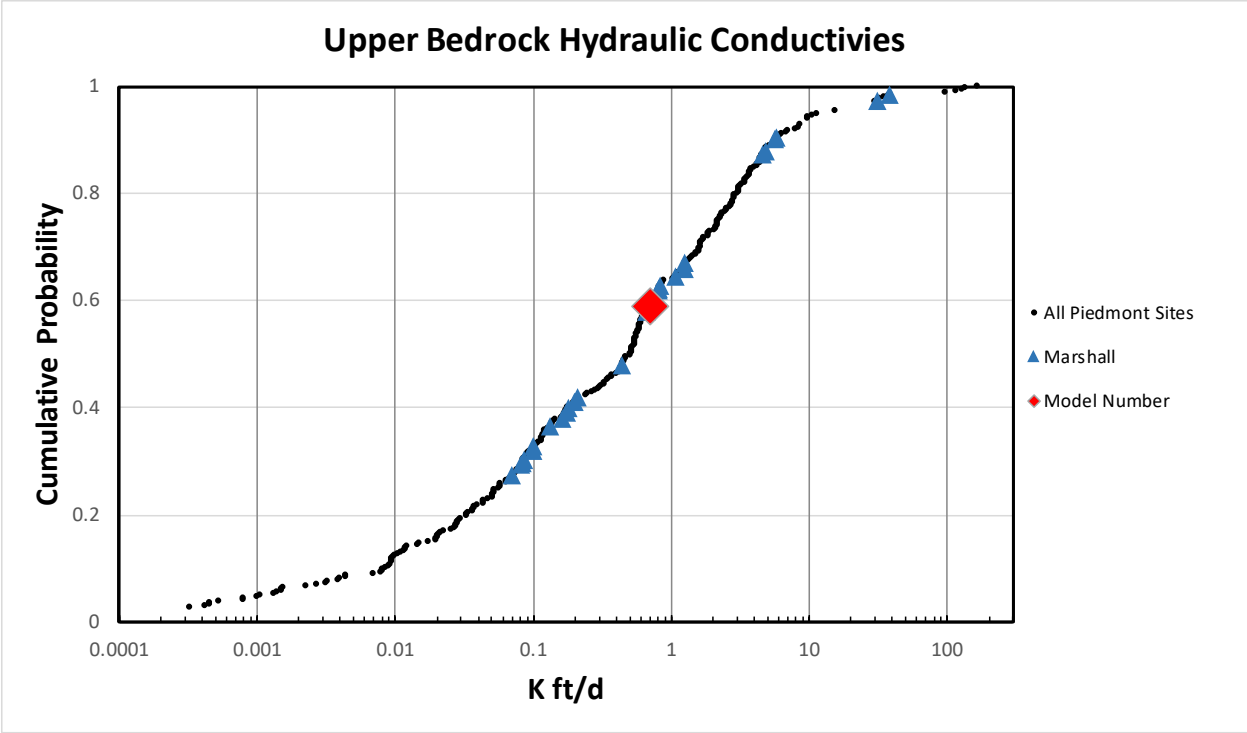


Figure 4-7. Hydraulic conductivity measured in slug tests performed in bedrock at 10 Piedmont sites in North Carolina.

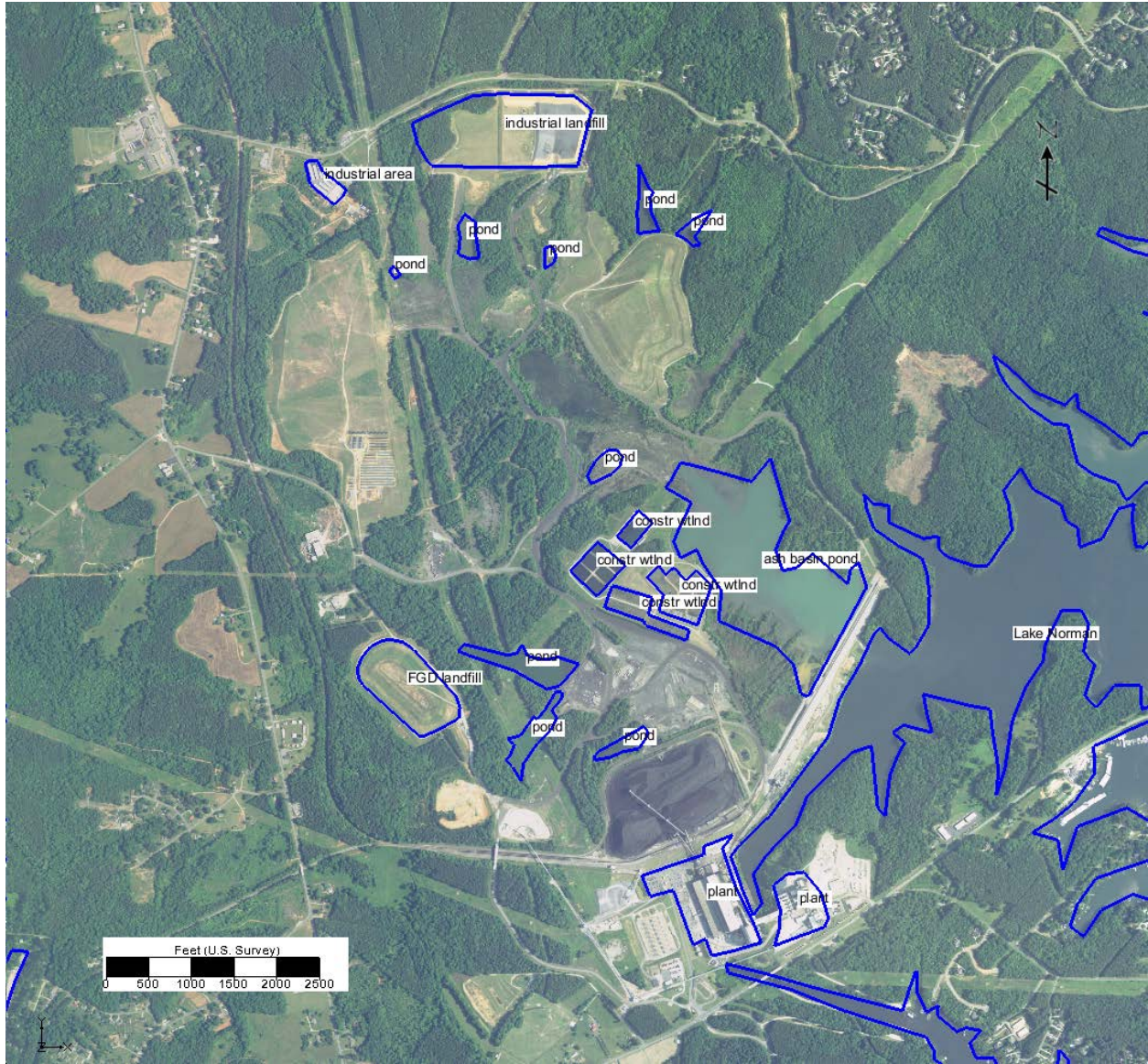


Figure 4-8. Distribution of recharge zones in the model. The background recharge rate is 8 inches/year.

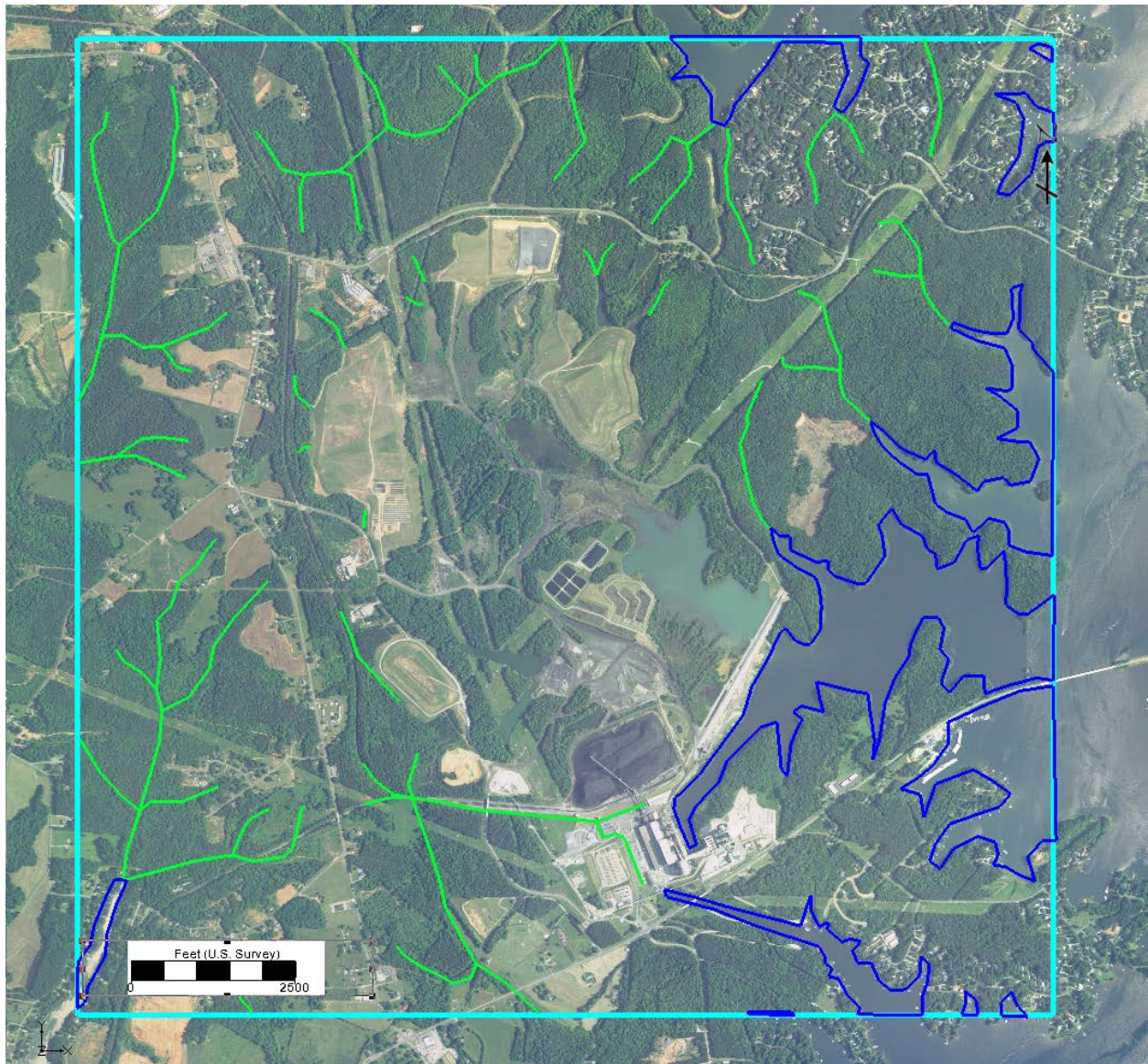


Figure 4-9. Surface water features included in the model outside of the ash basin area (the ash basin area is shown in Figure 4.10). The areas enclosed by dark blue lines are general head zones where the elevation is specified. The green lines represent drains, and the turquoise line represents the model domain.

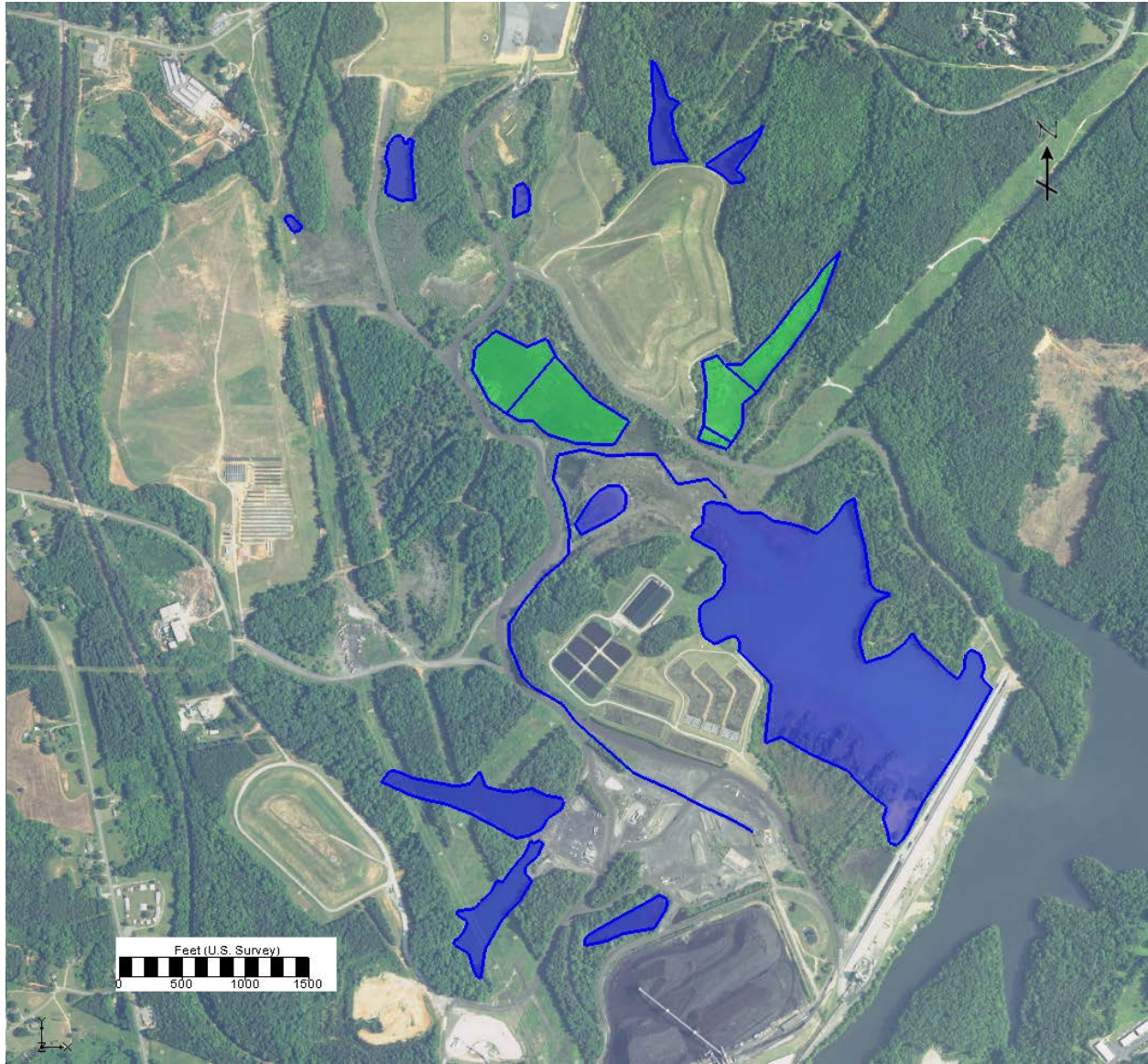


Figure 4-10. Surface water features included in the model in the ash basin area. The blue areas are simulated as general head boundaries with a specified elevation and a large conductance. The green areas represent drains that are set to the approximate ground or water surface elevation.

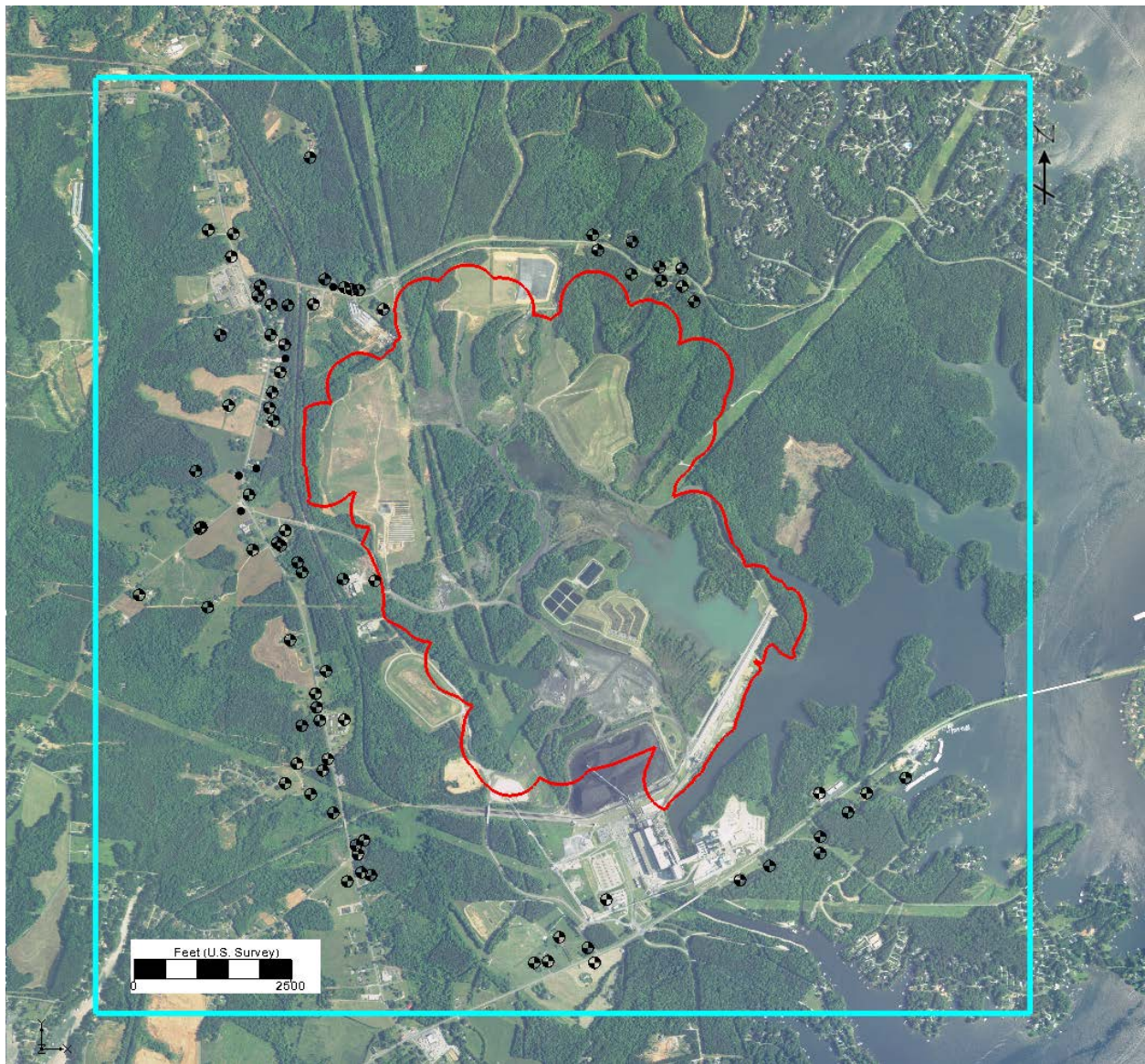


Figure 4-11. Location of water supply wells in the model area. The black dots represent the private and public supply wells, the turquoise line represents the model domain, and the red line represents the current compliance boundary.

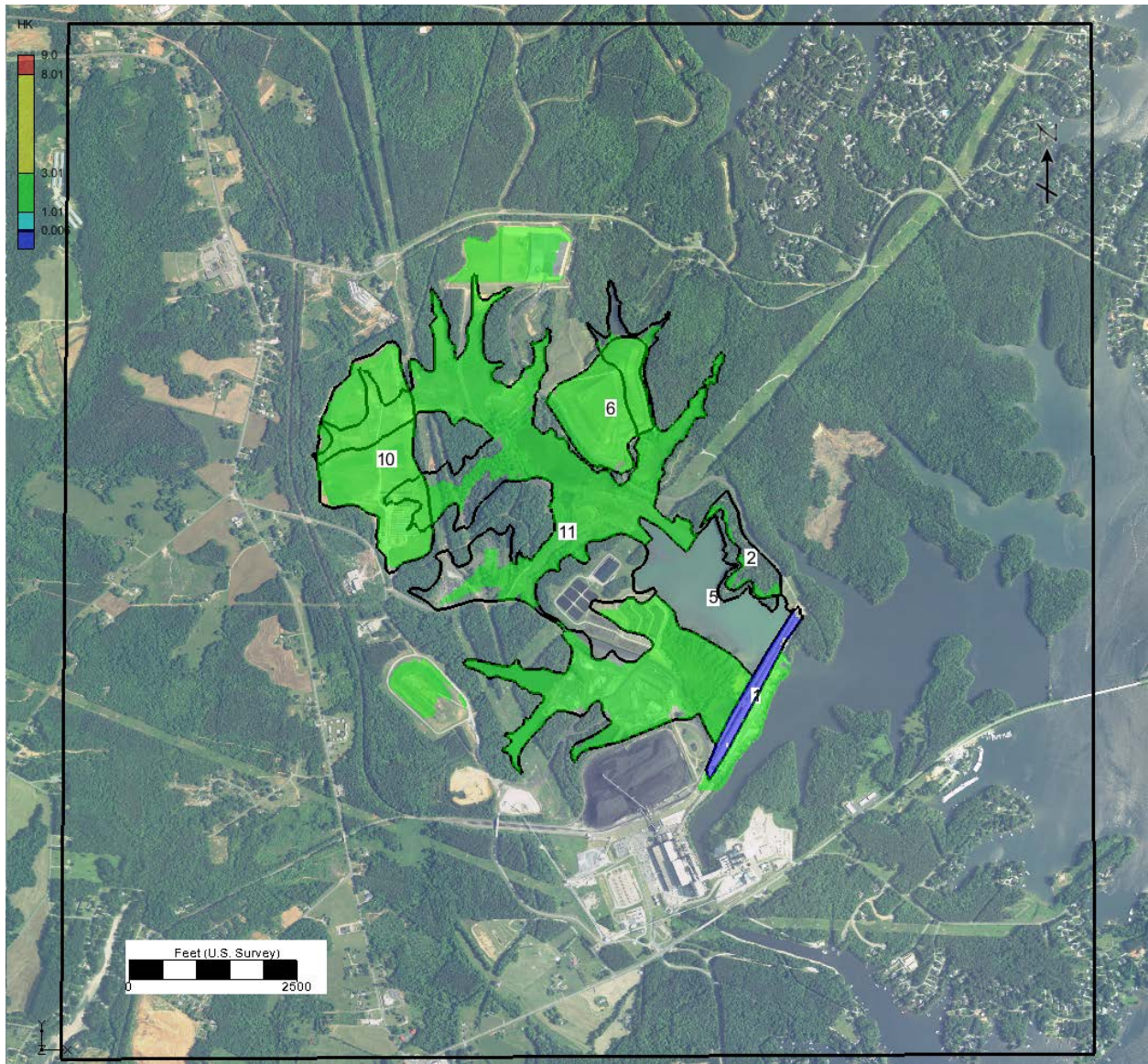


Figure 5-1. Zones used to define horizontal hydraulic conductivity and horizontal to vertical anisotropy in the ash (model layer 2 shown). Zone 5 (not shaded) represents an area of open water with $K=100$ ft/d.

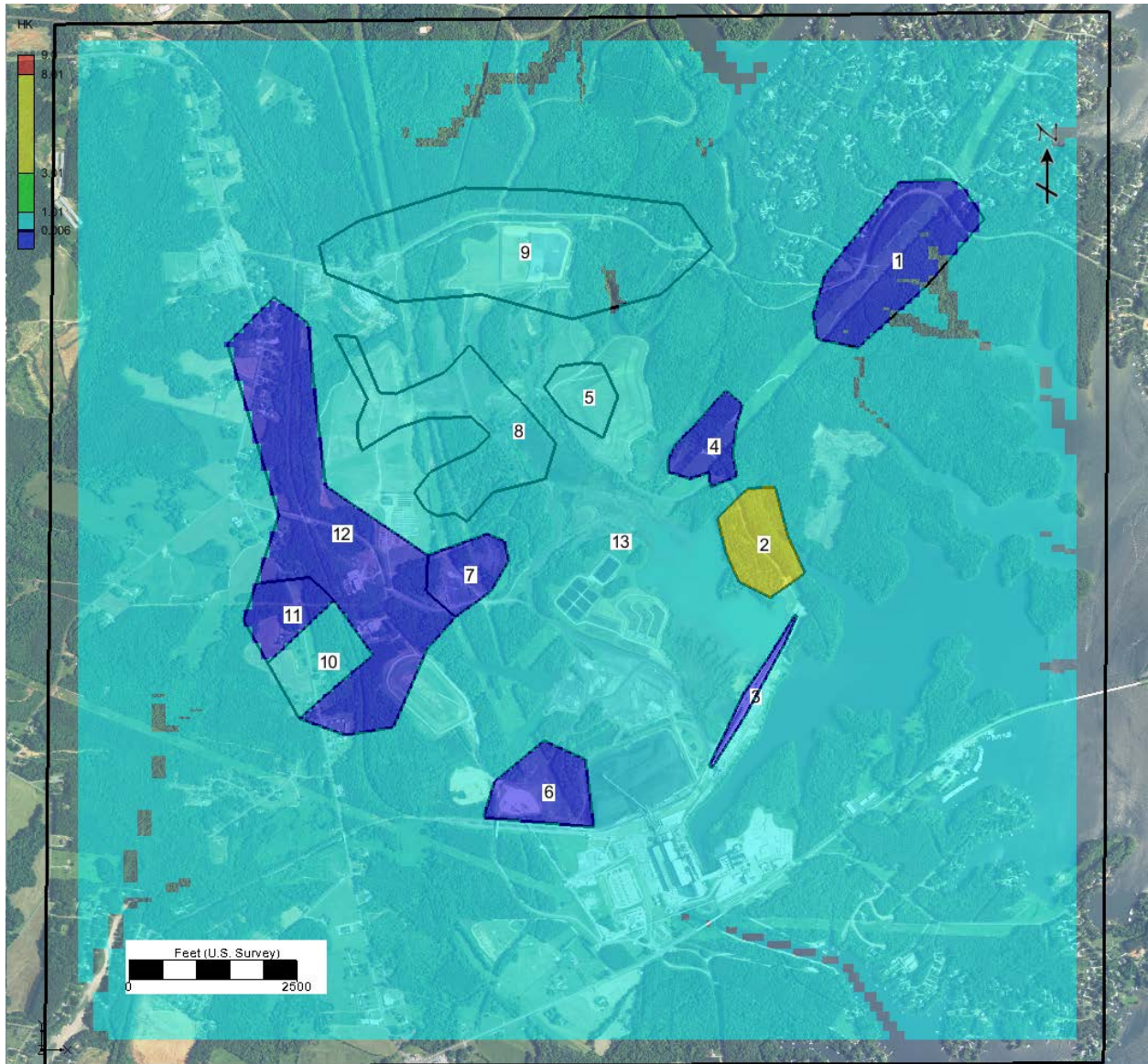


Figure 5-2. Zones used to define horizontal hydraulic conductivity and horizontal to vertical anisotropy in the saprolite, model layers 5-7.

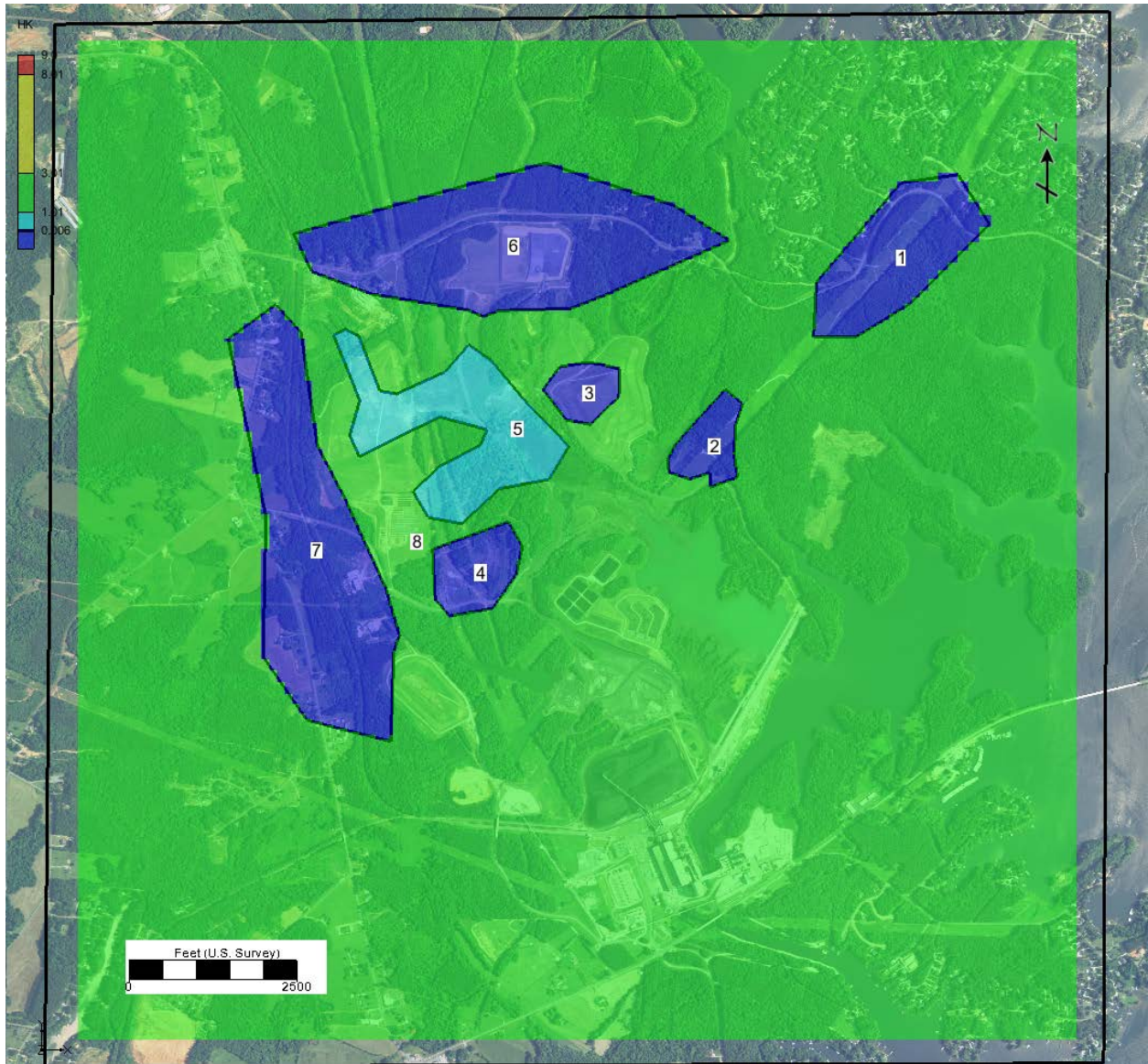


Figure 5-3. Zones used to define horizontal hydraulic conductivity and horizontal to vertical anisotropy in the transition zone, model layer 8.



Figure 5-4. Zones used to define horizontal hydraulic conductivity and horizontal to vertical anisotropy in the upper bedrock, model layer 9.

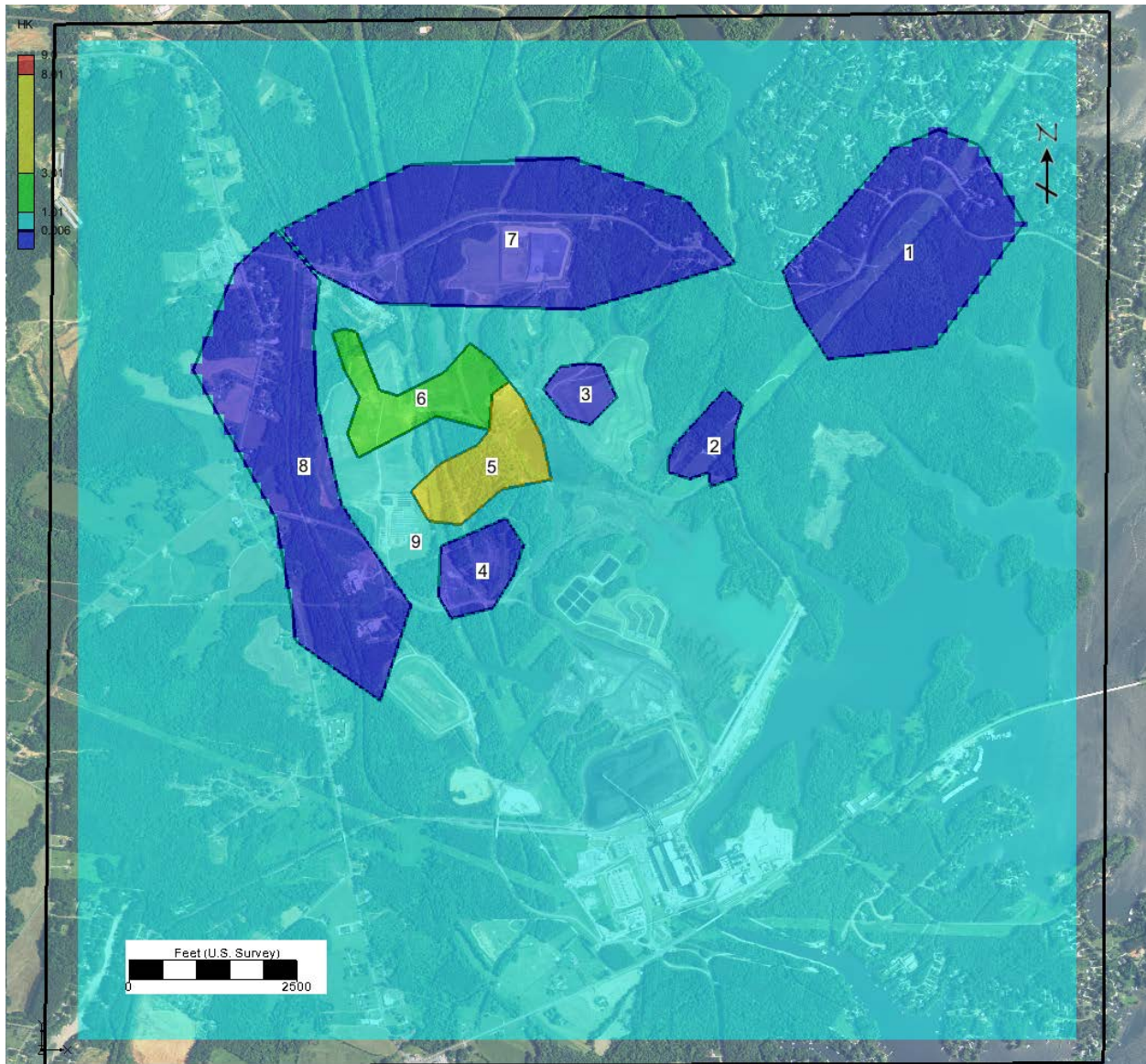


Figure 5-5. Zones used to define horizontal hydraulic conductivity and horizontal to vertical anisotropy in the upper bedrock, model layer 10.

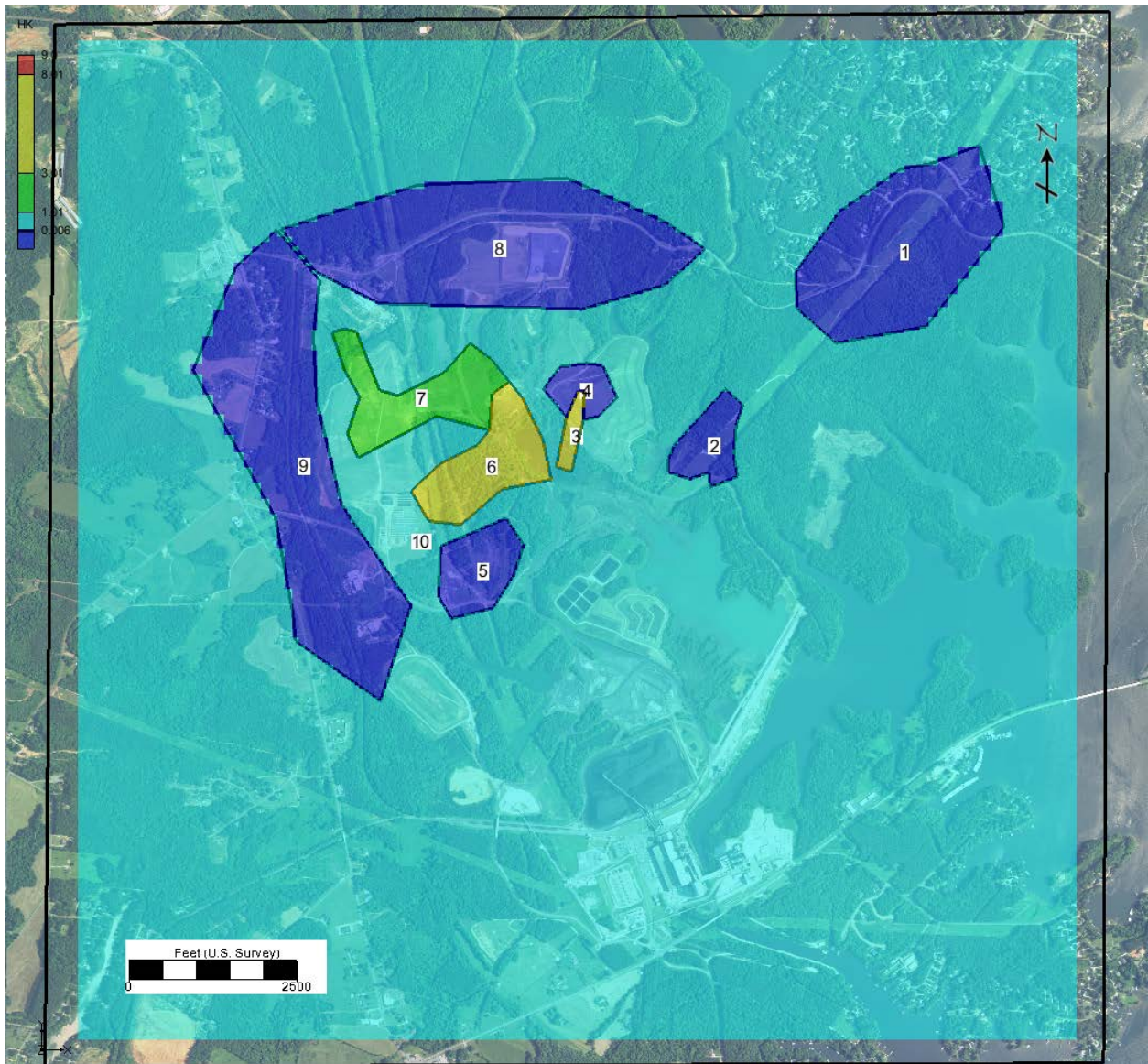


Figure 5-6. Zones used to define horizontal hydraulic conductivity and horizontal to vertical anisotropy in the upper bedrock, model layer 11.

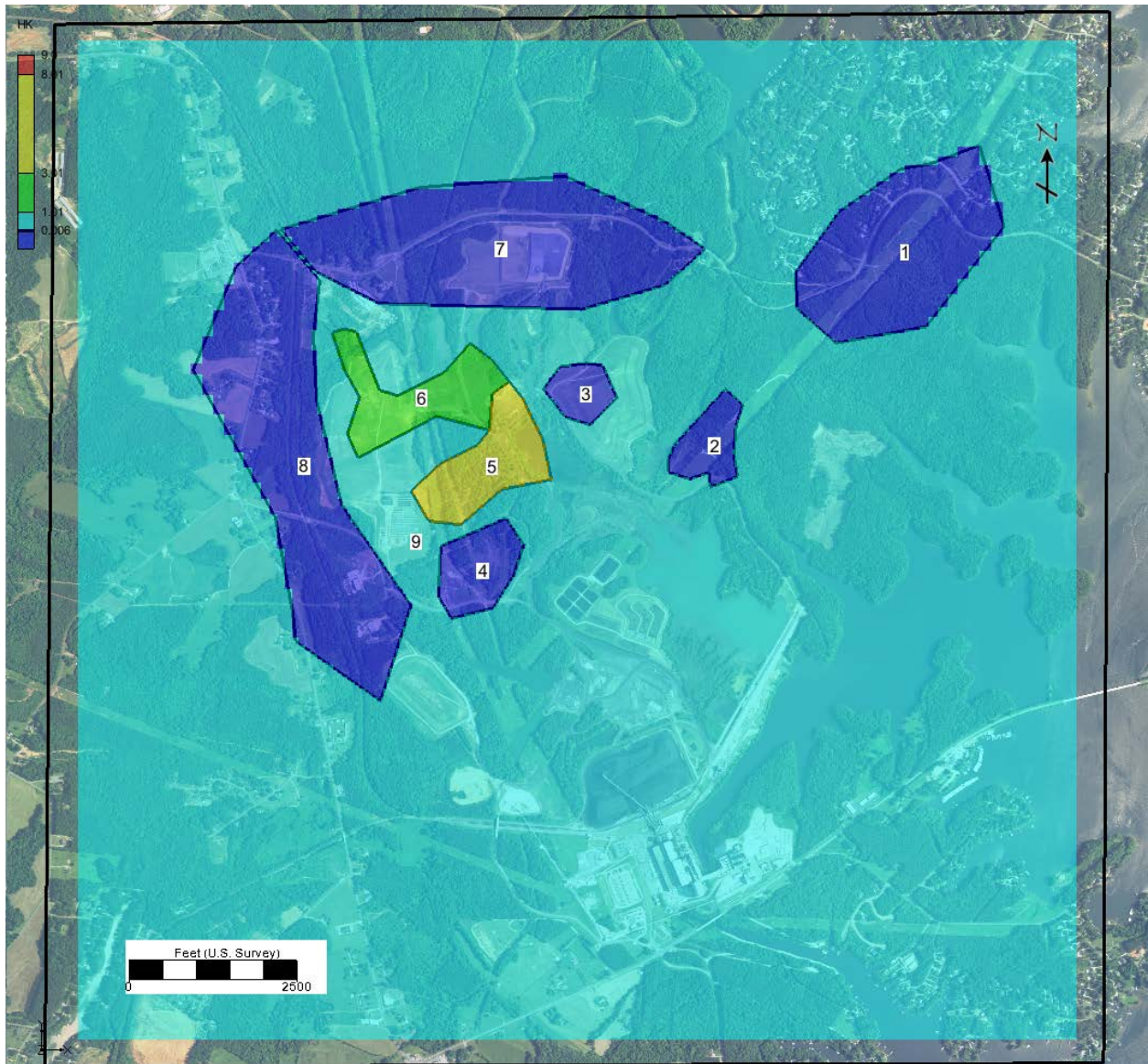


Figure 5-7. Zones used to define horizontal hydraulic conductivity and horizontal to vertical anisotropy in the upper bedrock, model layer 12.

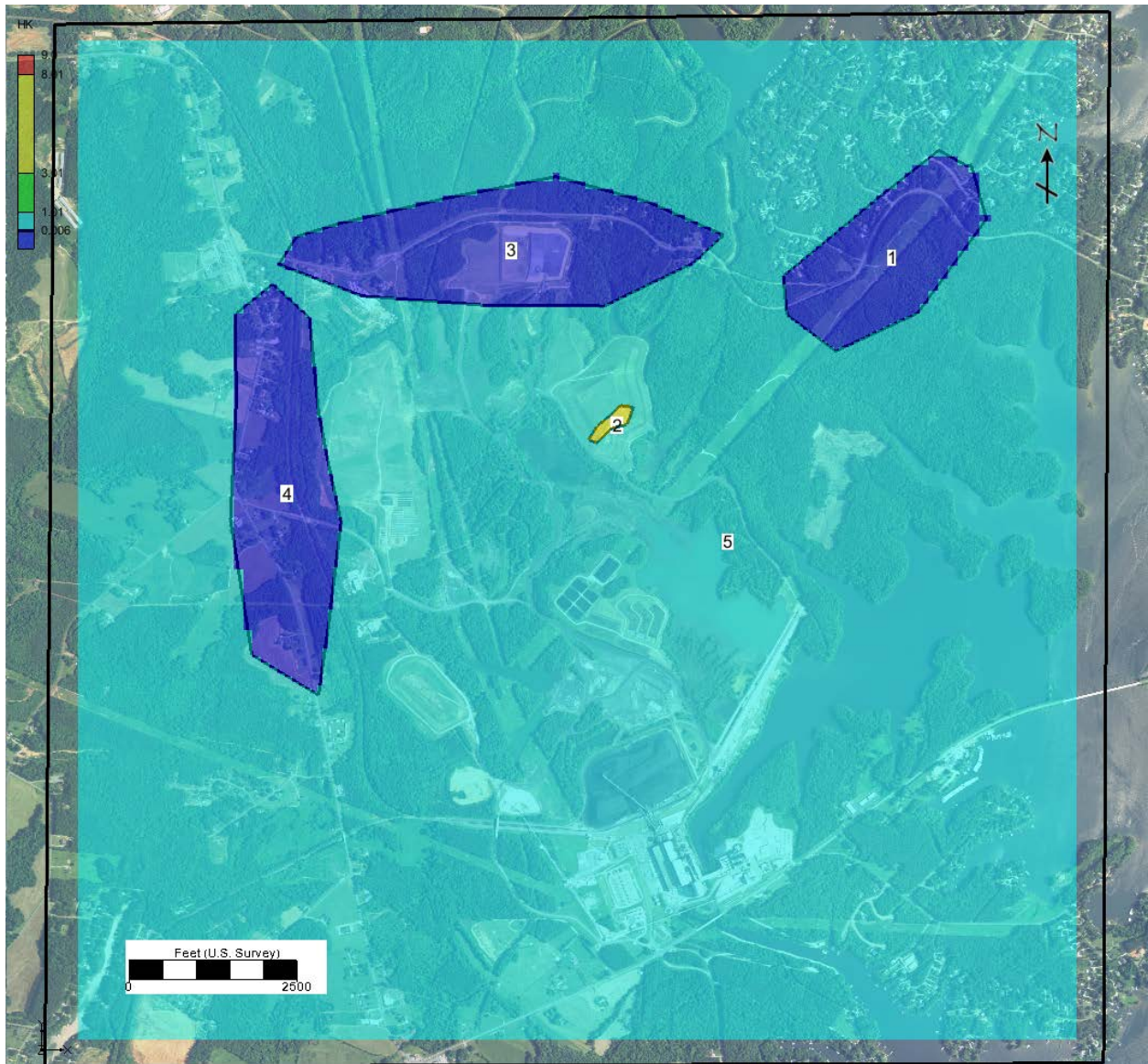


Figure 5-8. Zones used to define horizontal hydraulic conductivity and horizontal to vertical anisotropy in the mid-depth bedrock, model layers 13-15.



Figure 5-9. Zones used to define horizontal hydraulic conductivity and horizontal to vertical anisotropy in the lower bedrock, model layers 16-20.

Computed vs. Observed Values

Head

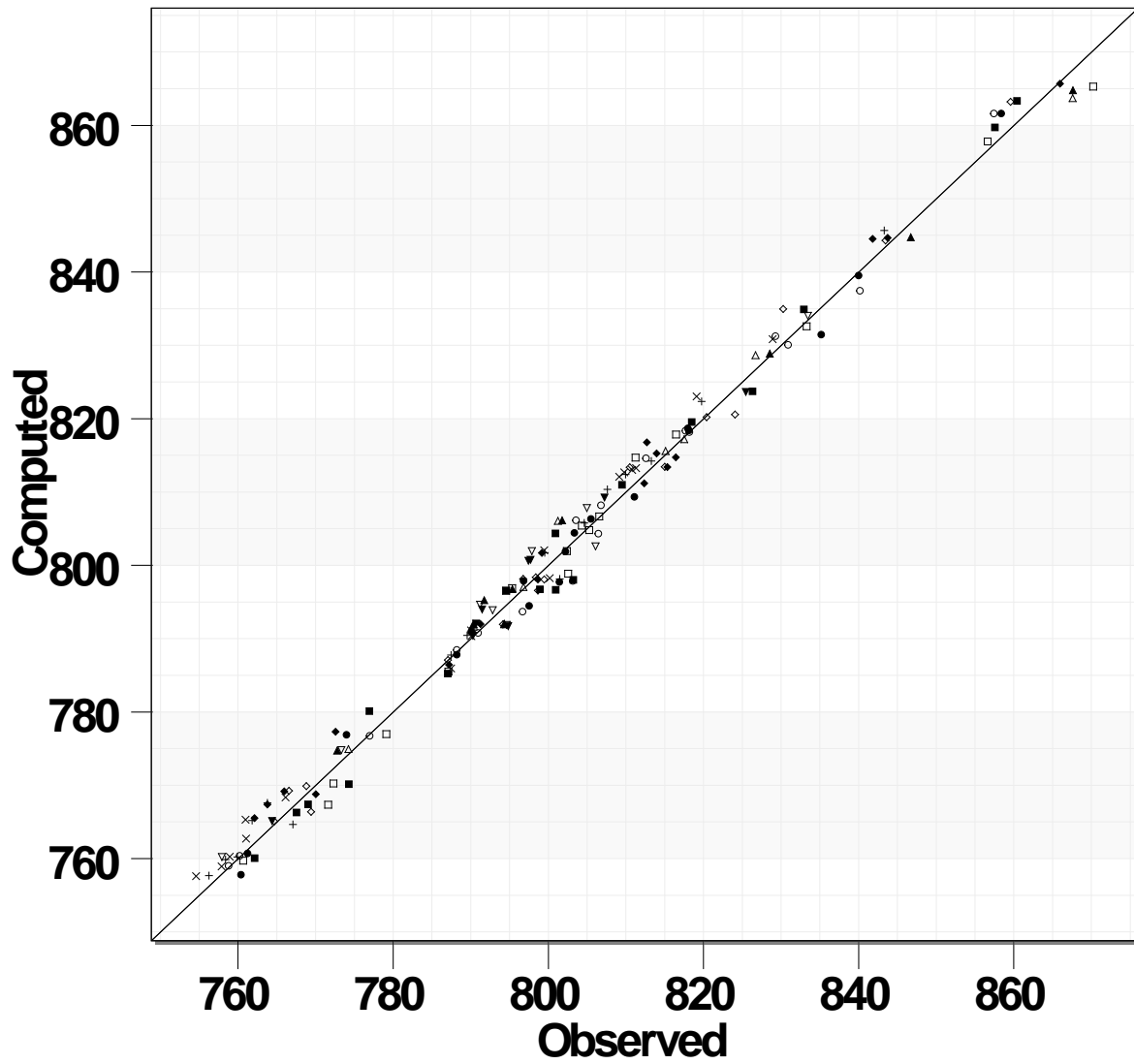


Figure 5-10. Comparison of observed and computed heads from the calibrated steady state flow model.

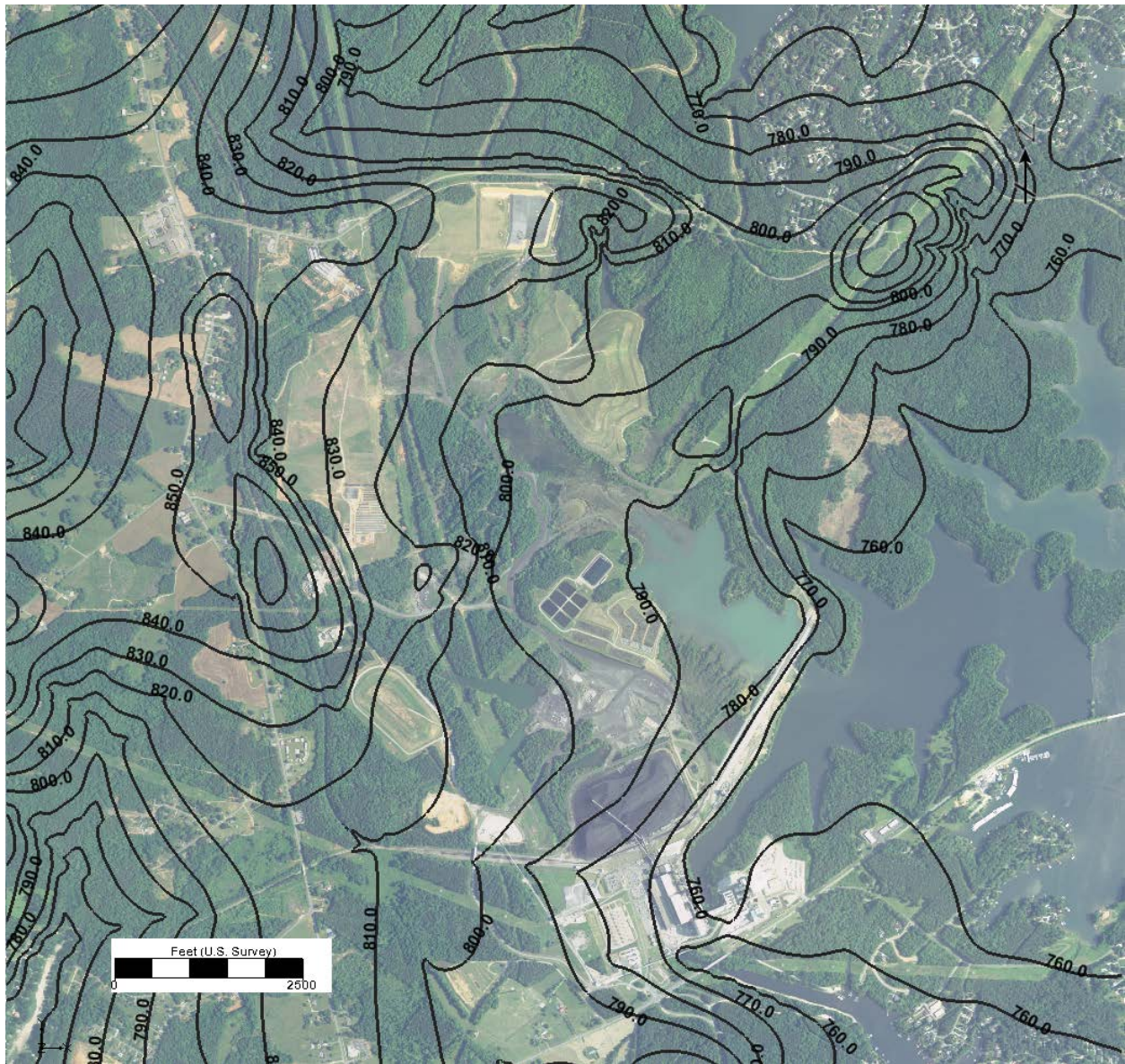


Figure 5-11. Simulated heads in the transition zone (model layer 8).

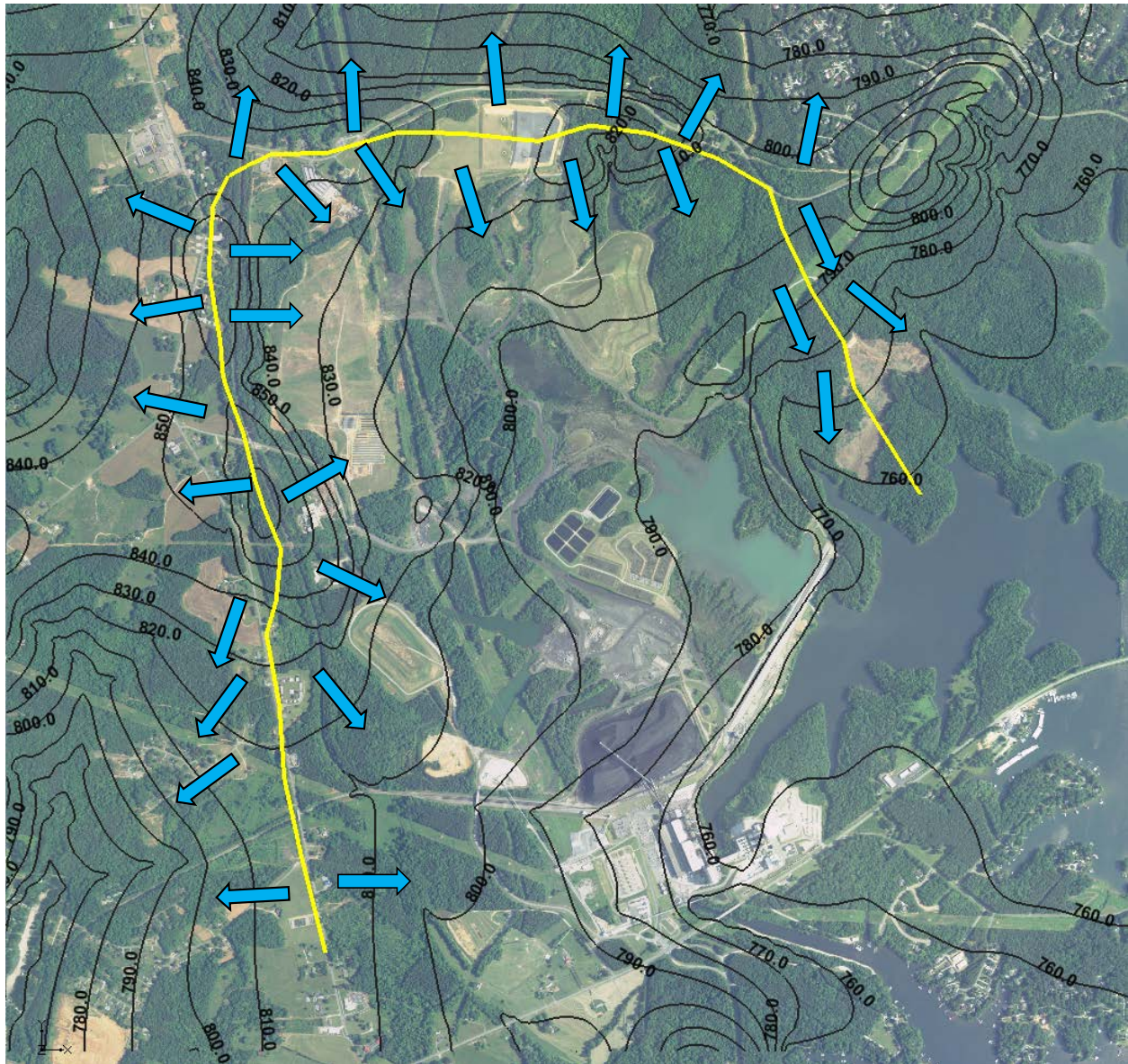


Figure 5-13. Groundwater divide and flow directions at the MSS. The approximate groundwater divide is shown as the yellow line, and the blue arrows indicate groundwater flow directions.

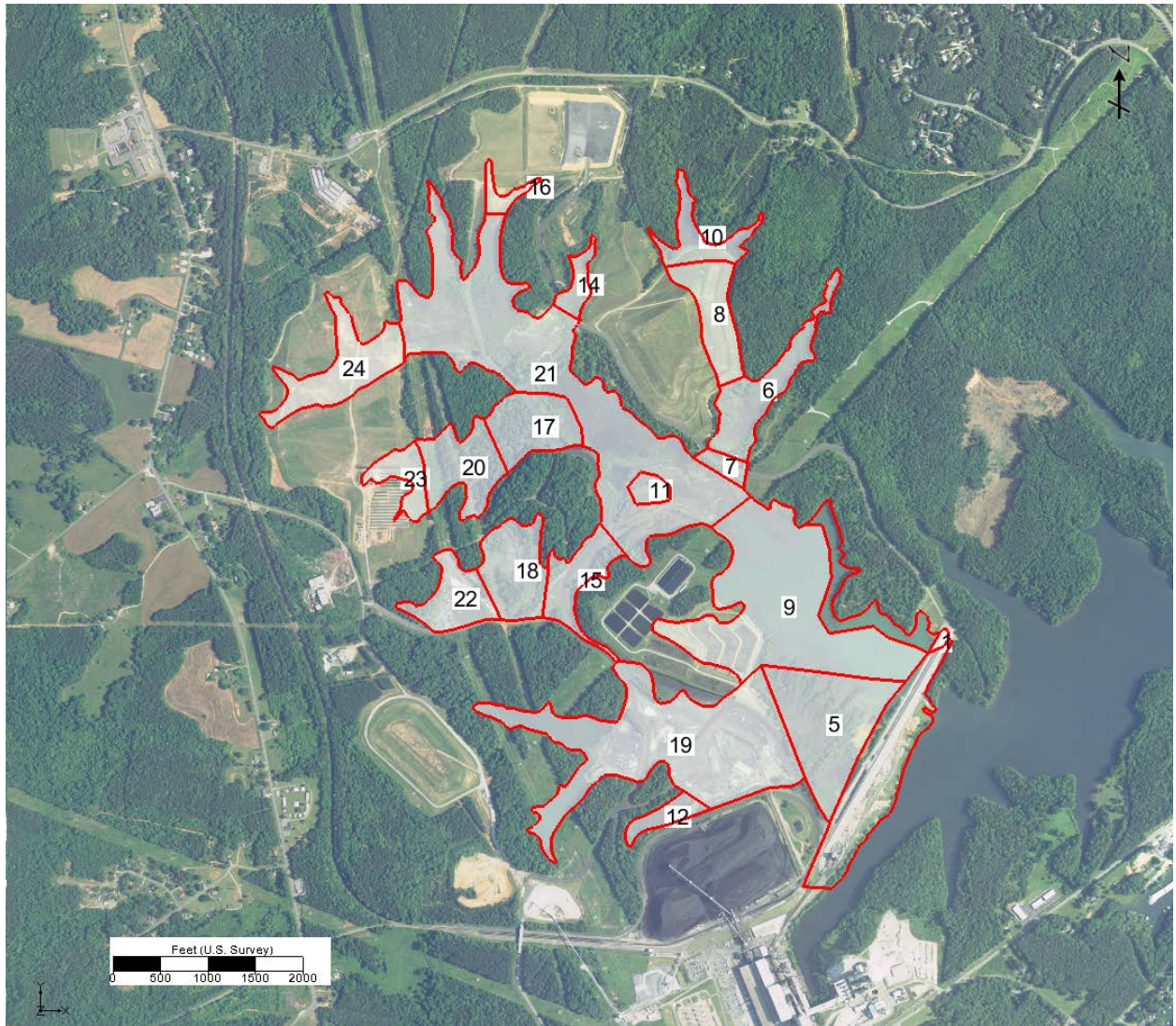


Figure 5-14. COI source zones in the ash basin for the historical transport model.

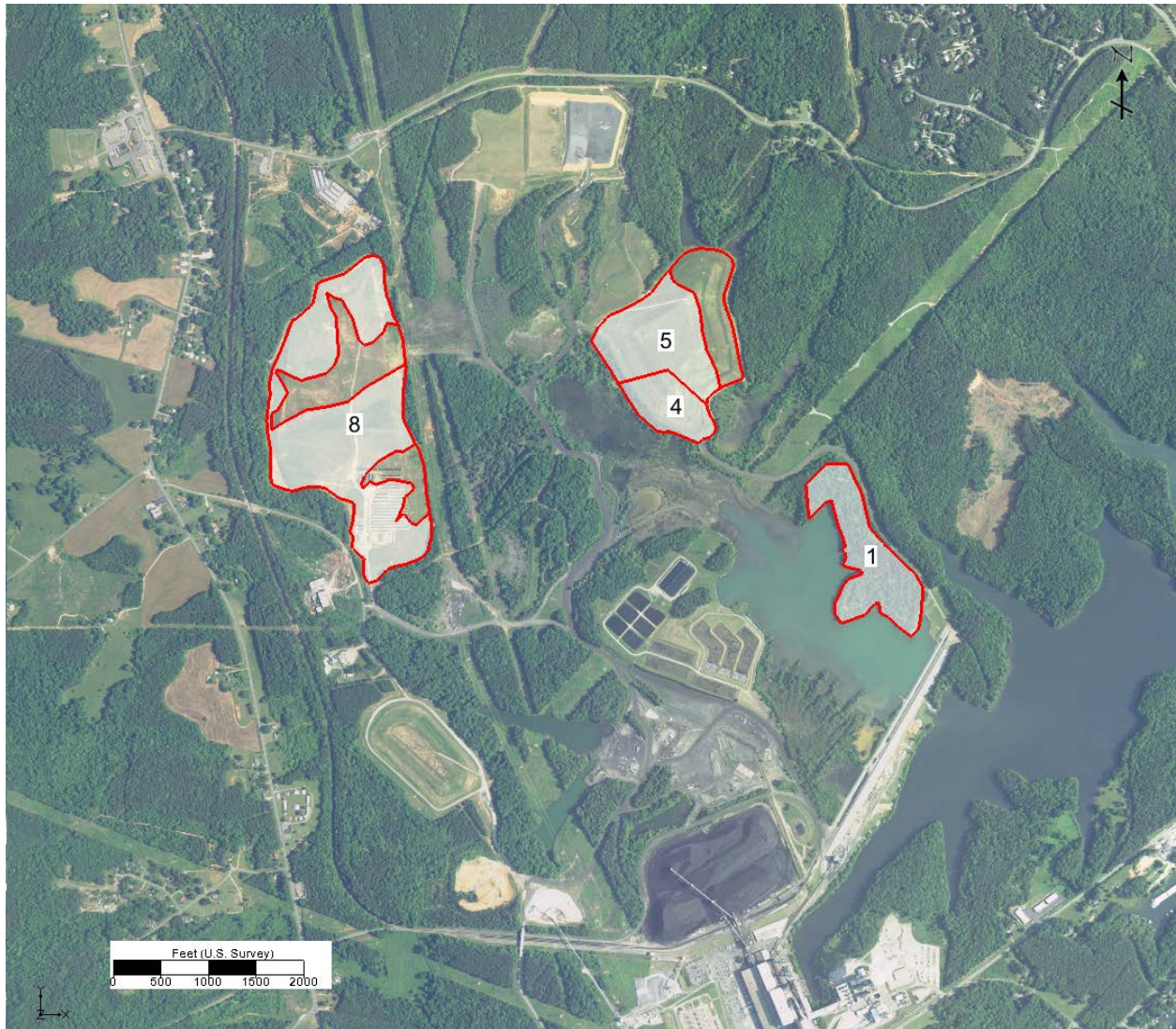


Figure 5-15. COI source zones in the ash landfills and structural fill for the historical transport model.

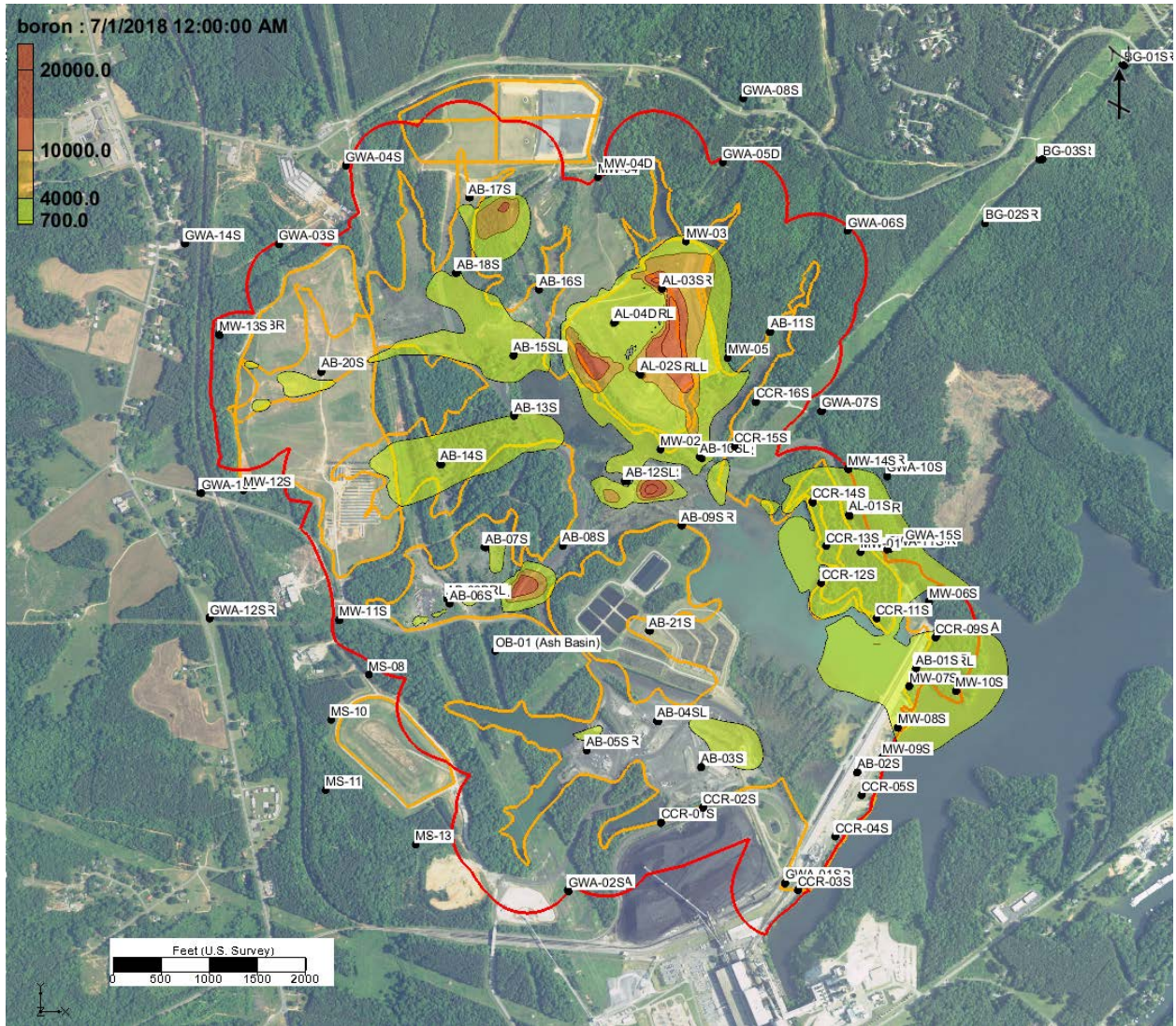


Figure 5-16b. Simulated July 2018 boron concentrations (ug/L) in the upper bedrock (layer 9). The red line is the current compliance boundary and orange lines are waste boundaries and landfill boundaries.

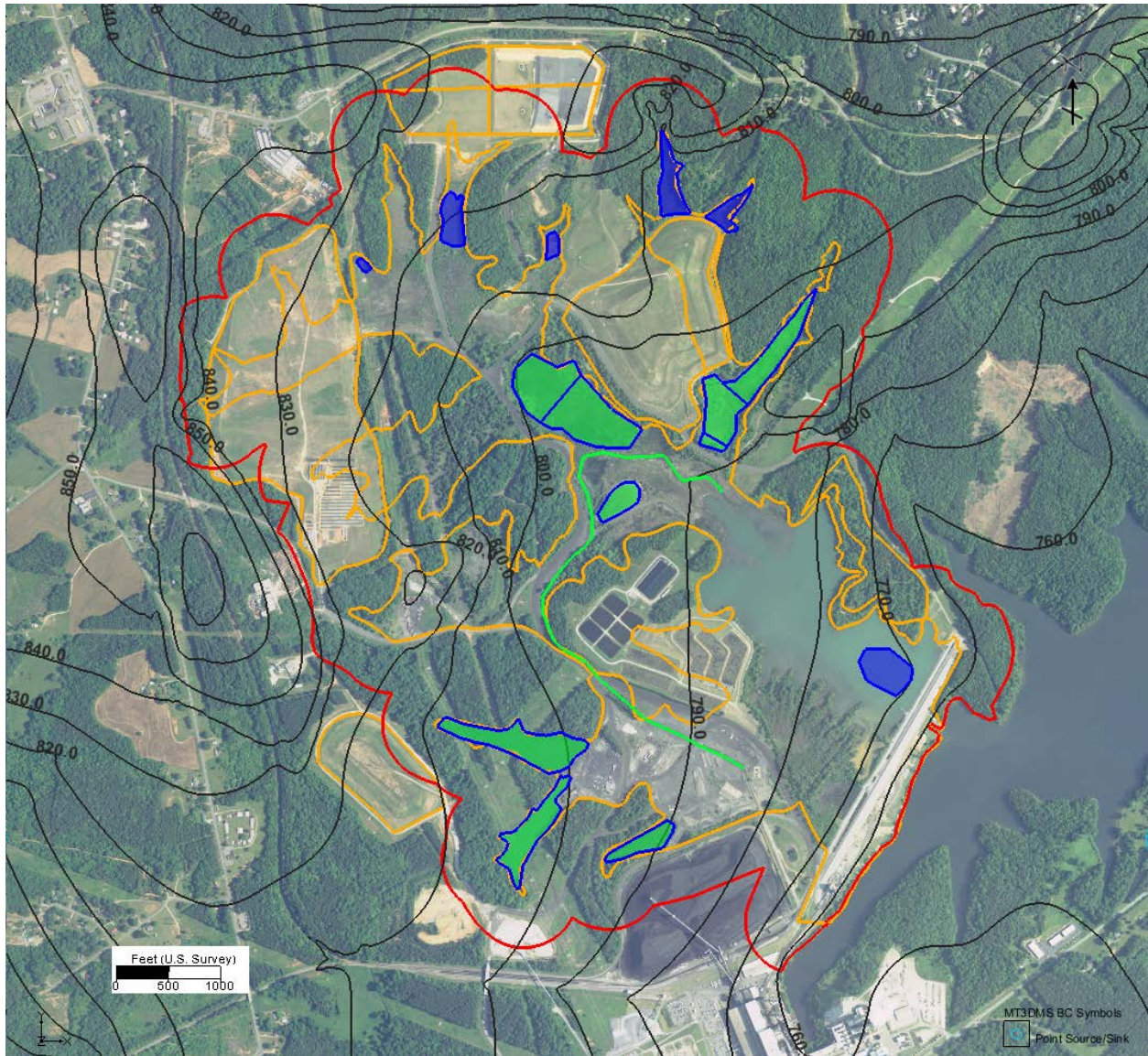


Figure 6-1. Simulated hydraulic heads in the transition zone after ash basin pond decanting. The blue polygons have specified general head conditions and the green polygons are simulated as drains. The red line is the current compliance boundary and orange lines are waste boundaries and landfill boundaries.

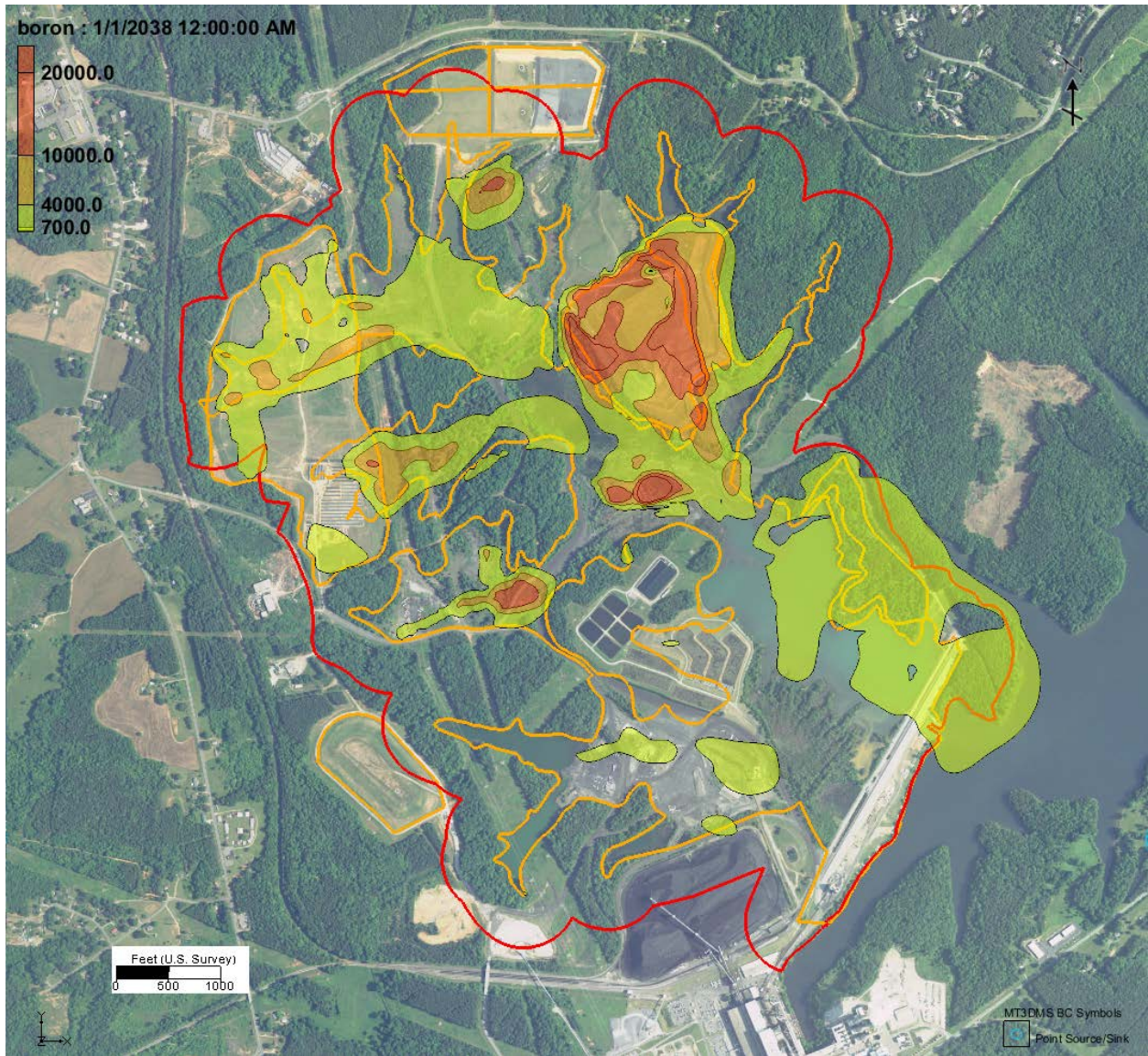


Figure 6-2. Simulated boron concentrations in the transition zone in 2038 for a simulation where the ash basin lake has been decanted. The red line is the current compliance boundary and orange lines are waste boundaries and landfill boundaries.

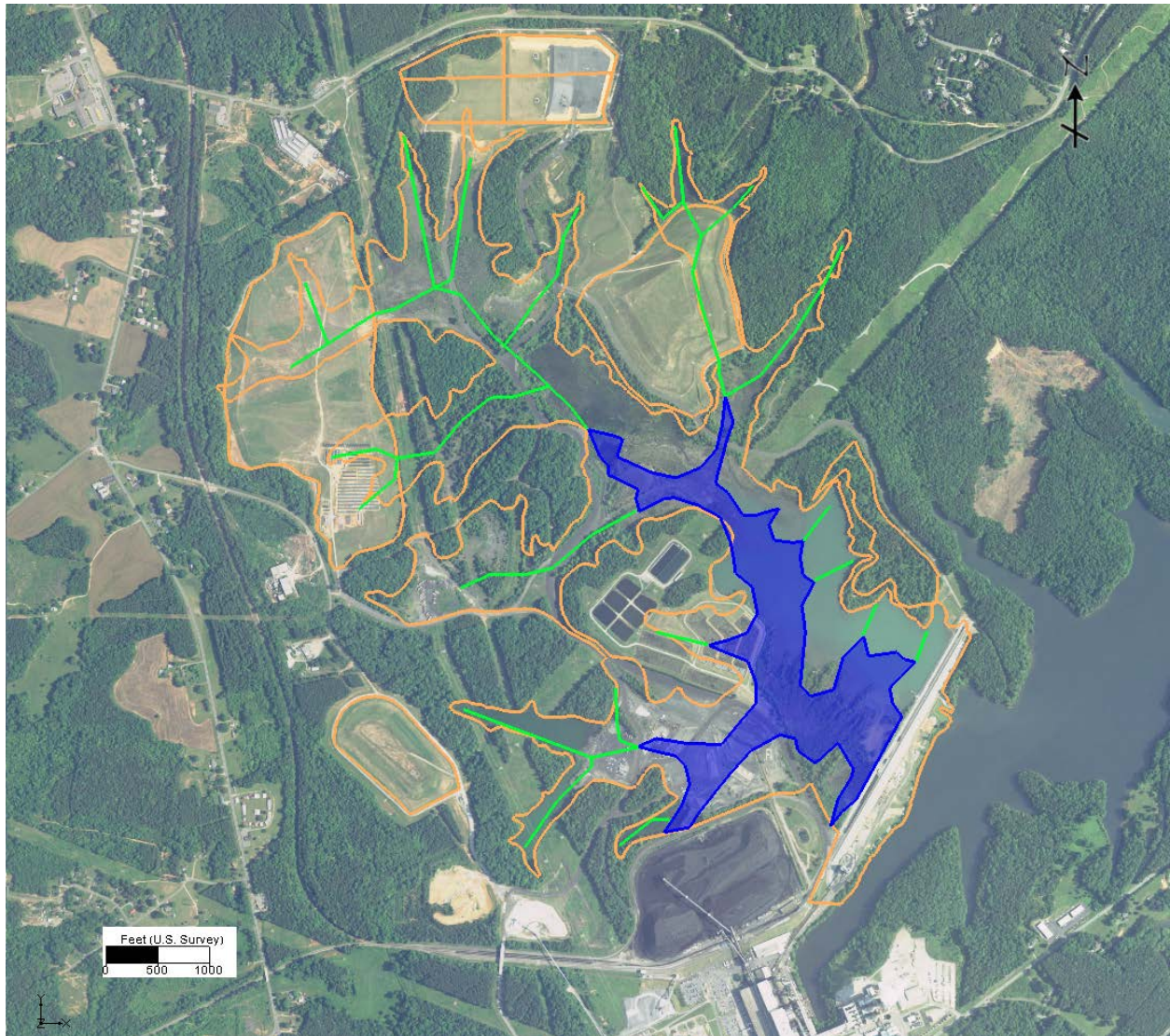


Figure 6-3. Drain network used in excavation simulations to represent springs and streams that may form. The elevations are set to the top of the saprolite surface, which approximately corresponds to the original ground surface. The blue area is a stormwater pond which will be present in the excavated area and was simulated with a specified general head condition. This pond has the approximate water level of Lake Norman. The green lines represent drains and orange lines are waste boundaries and landfill boundaries.

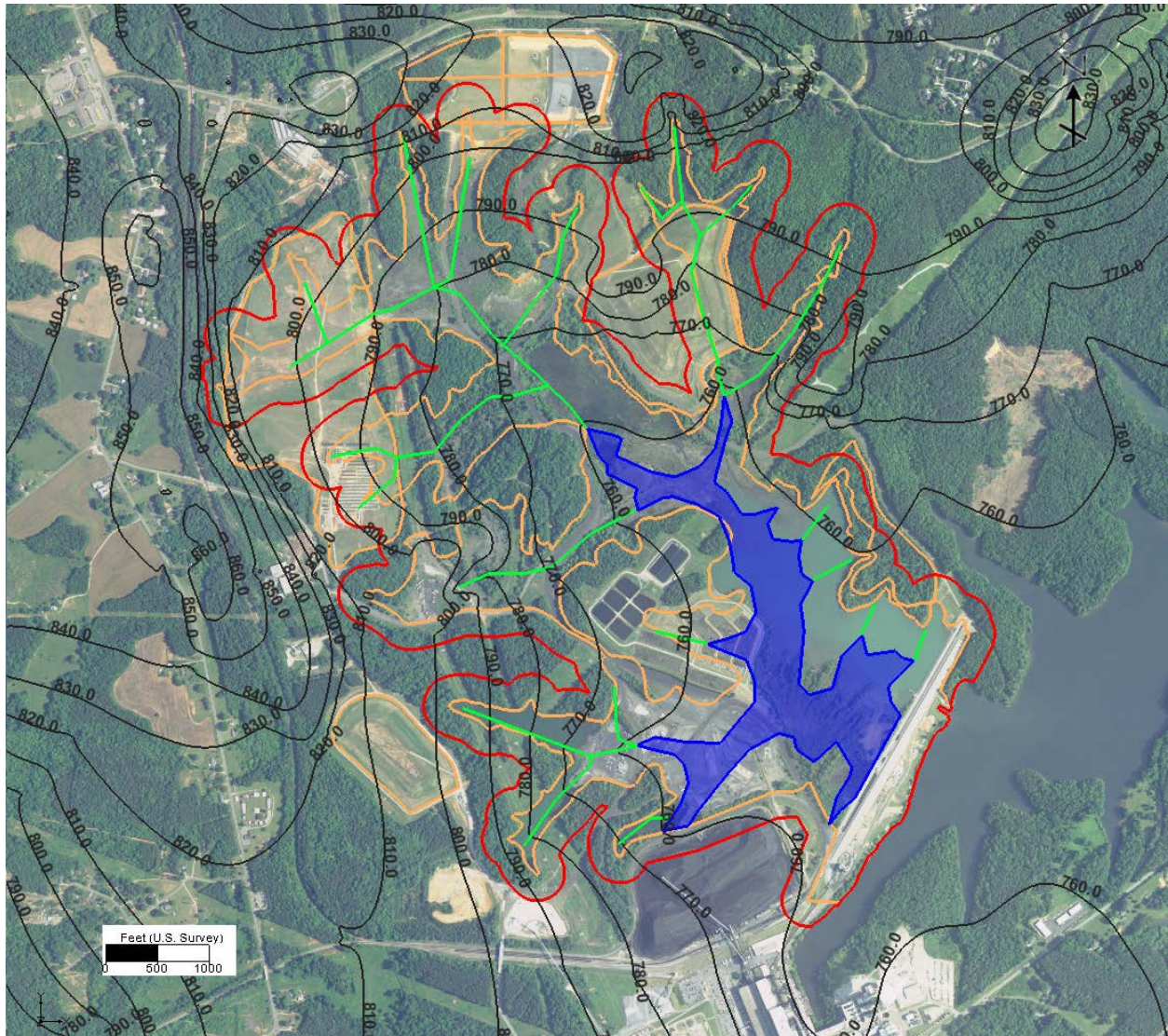


Figure 6-4. Simulated hydraulic heads for excavation case. The green lines represent drains and the blue polygon represents the stormwater pond which is simulated as general head condition. The red line is the potential compliance boundary and orange lines are waste boundaries and landfill boundaries.

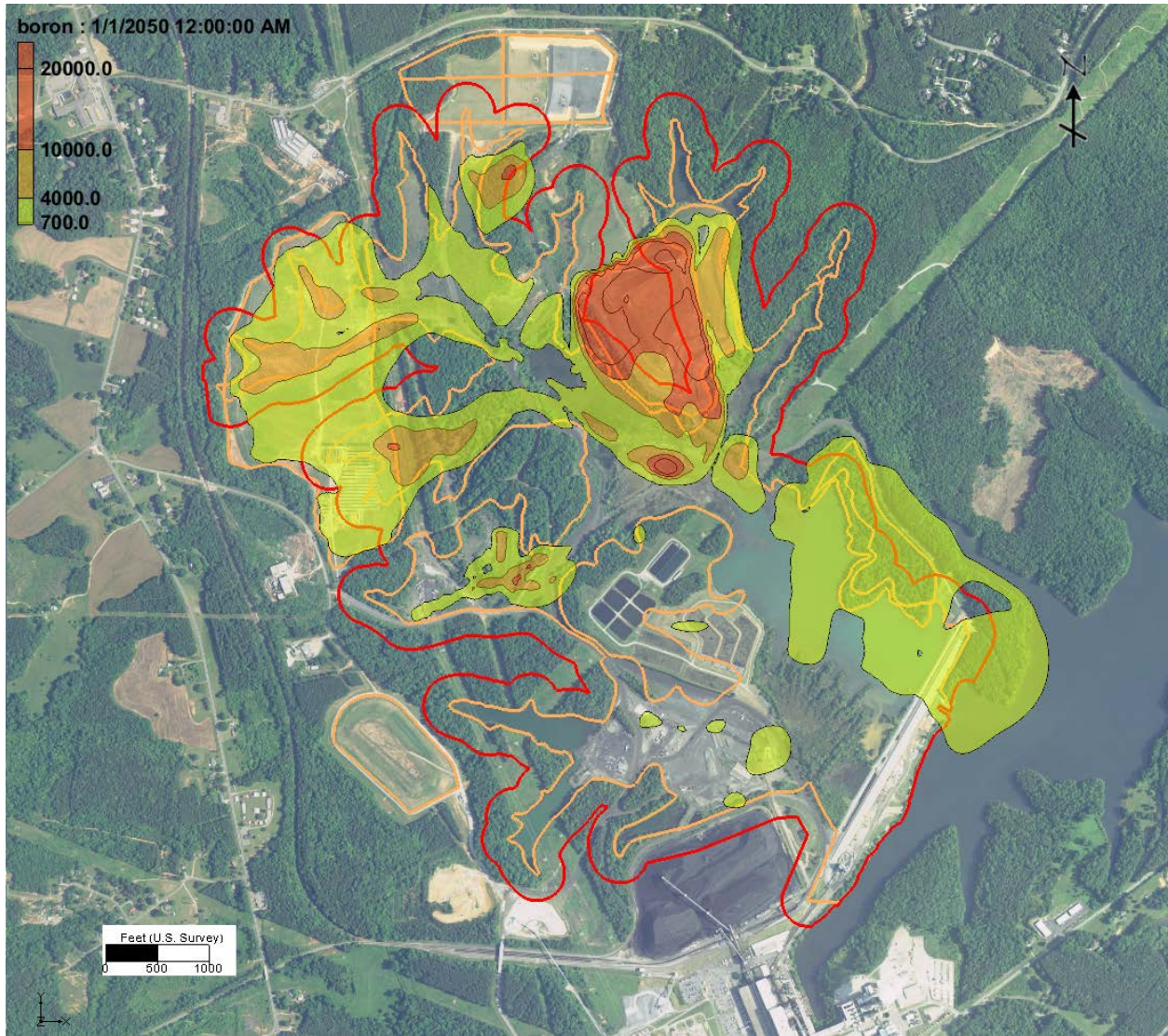


Figure 6-5a. Simulated boron concentrations in the transition zone (layer 8) in 2050 for the excavation case. The red line is the potential compliance boundary and orange lines are waste boundaries and landfill boundaries.

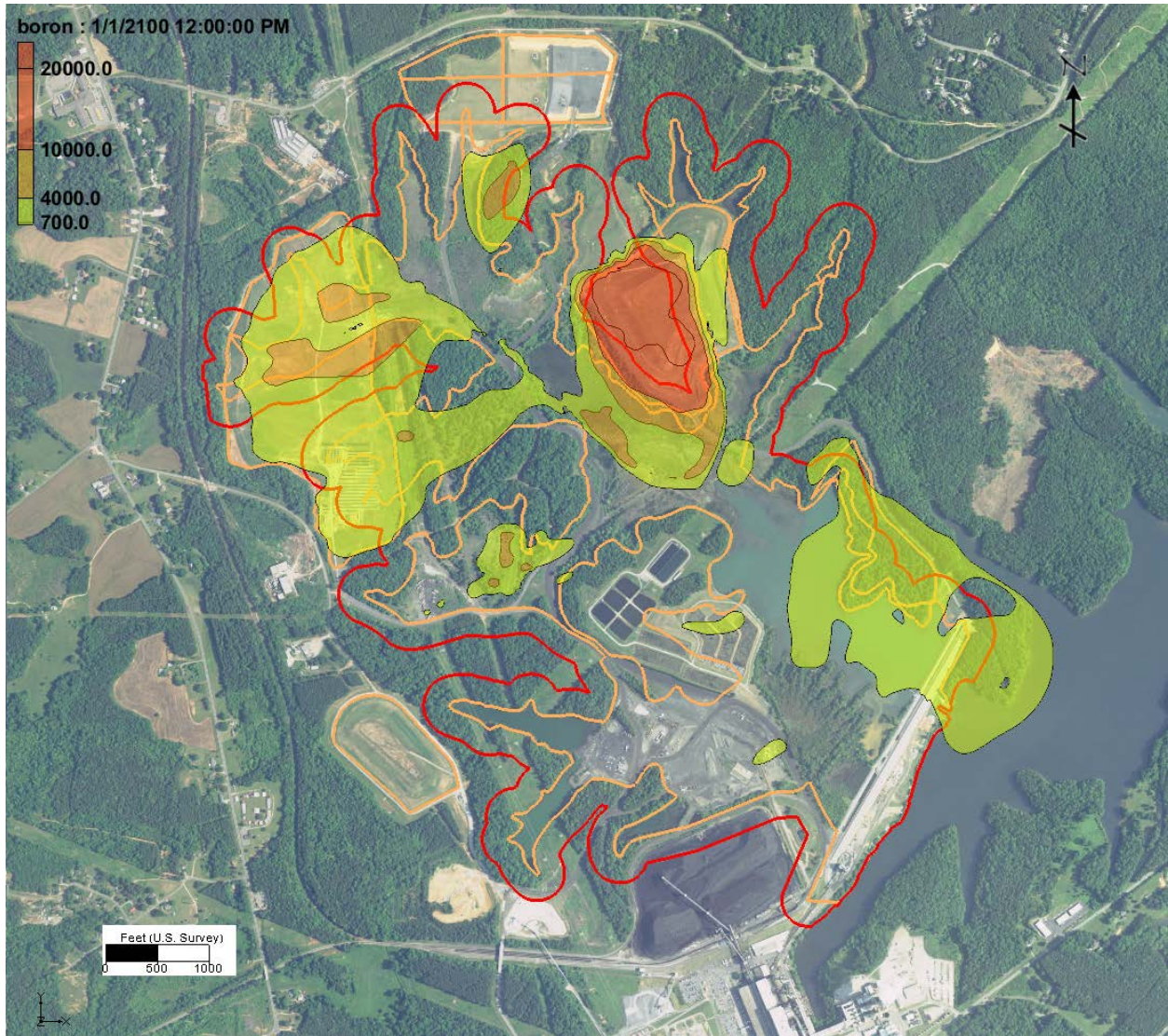


Figure 6-5b. Simulated boron concentrations in the transition zone (layer 8) in 2100 for the excavation case. The red line is the potential compliance boundary and orange lines are waste boundaries and landfill boundaries.

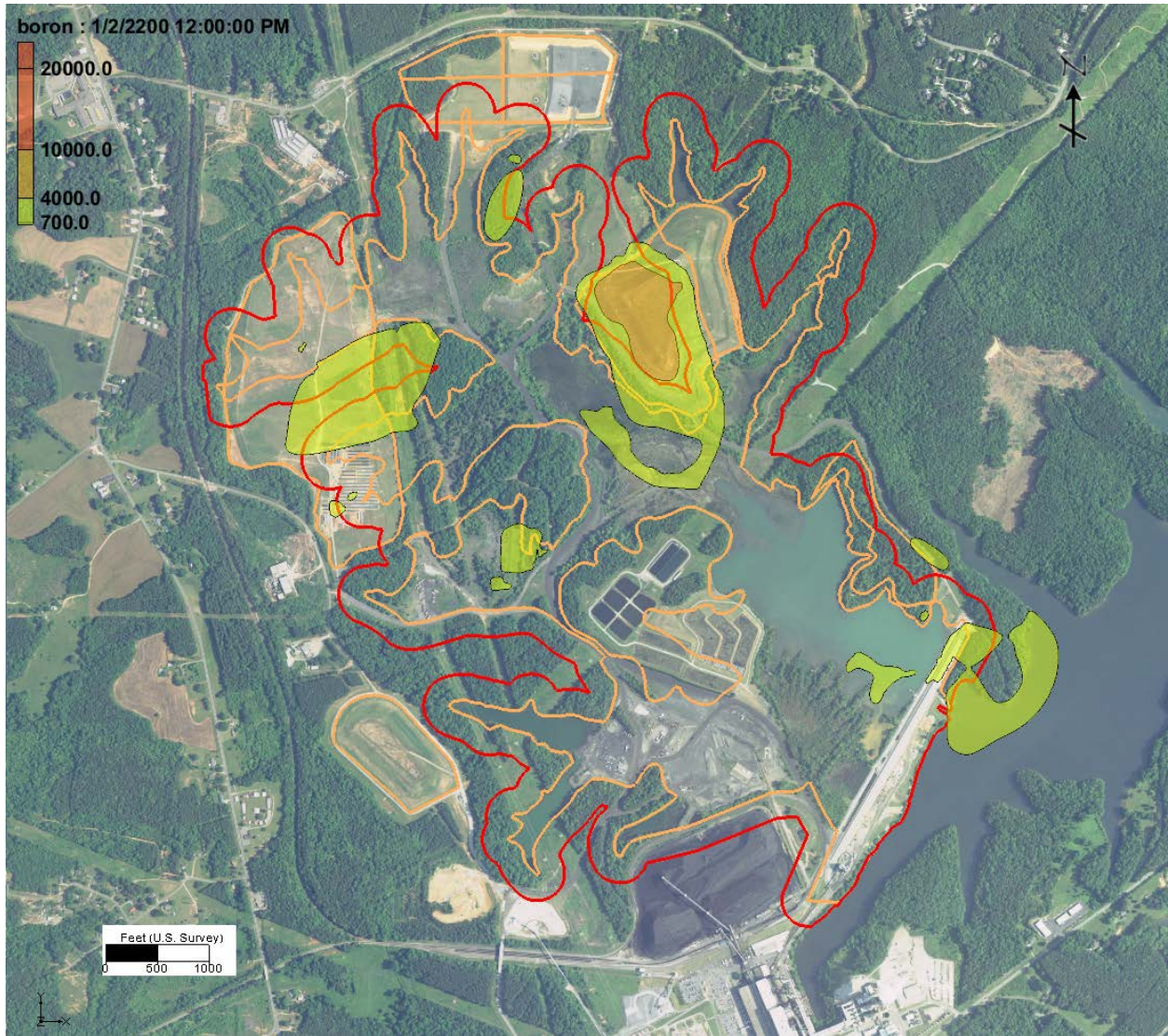


Figure 6-5c. Simulated boron concentrations in the transition zone (layer 8) in 2200 for the excavation case. The red line is the potential compliance boundary and orange lines are waste boundaries and landfill boundaries.

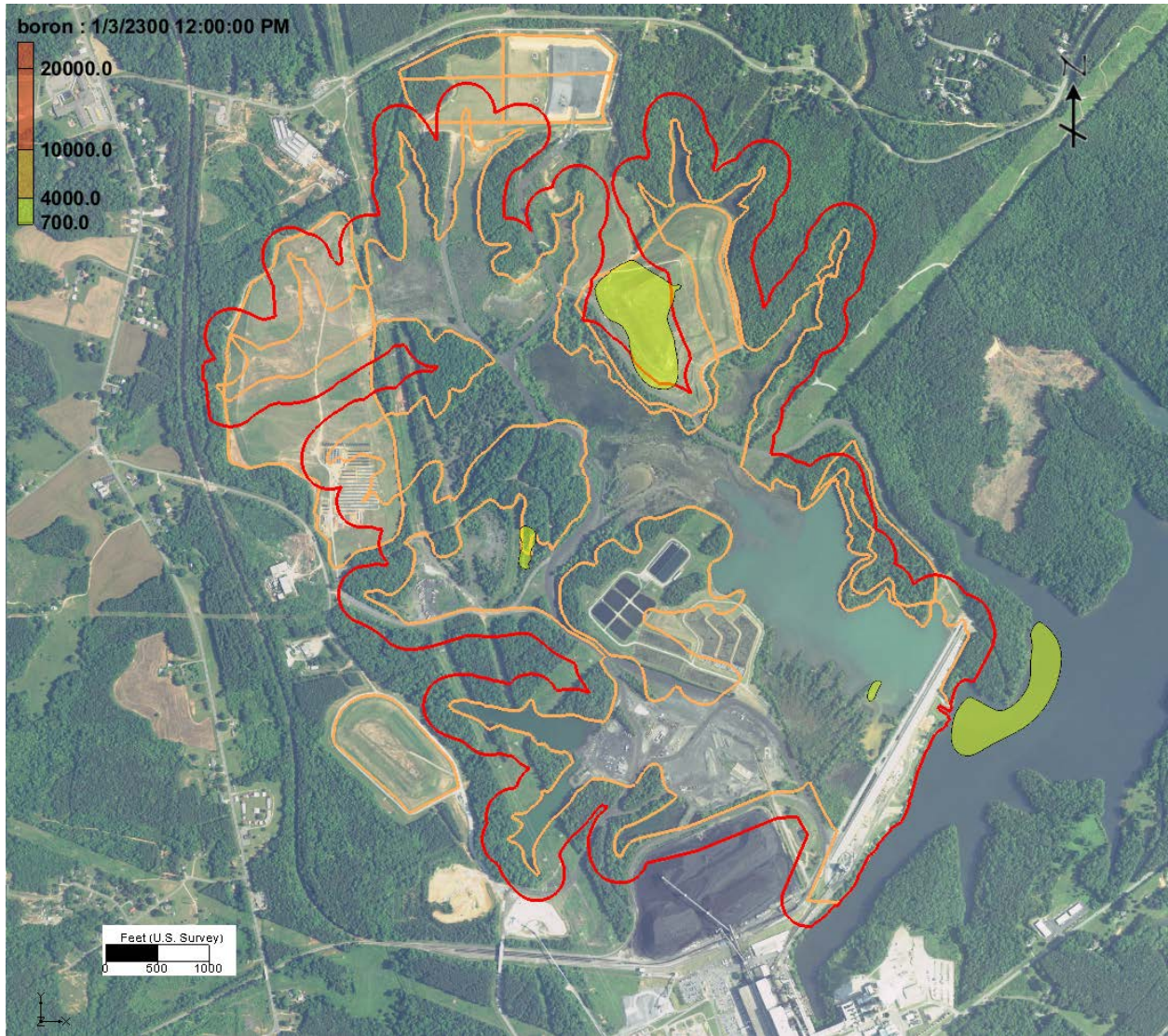


Figure 6-5d. Simulated boron concentrations in the transition zone (layer 8) in 2300 for the excavation case. The red line is the potential compliance boundary and orange lines are waste boundaries and landfill boundaries.

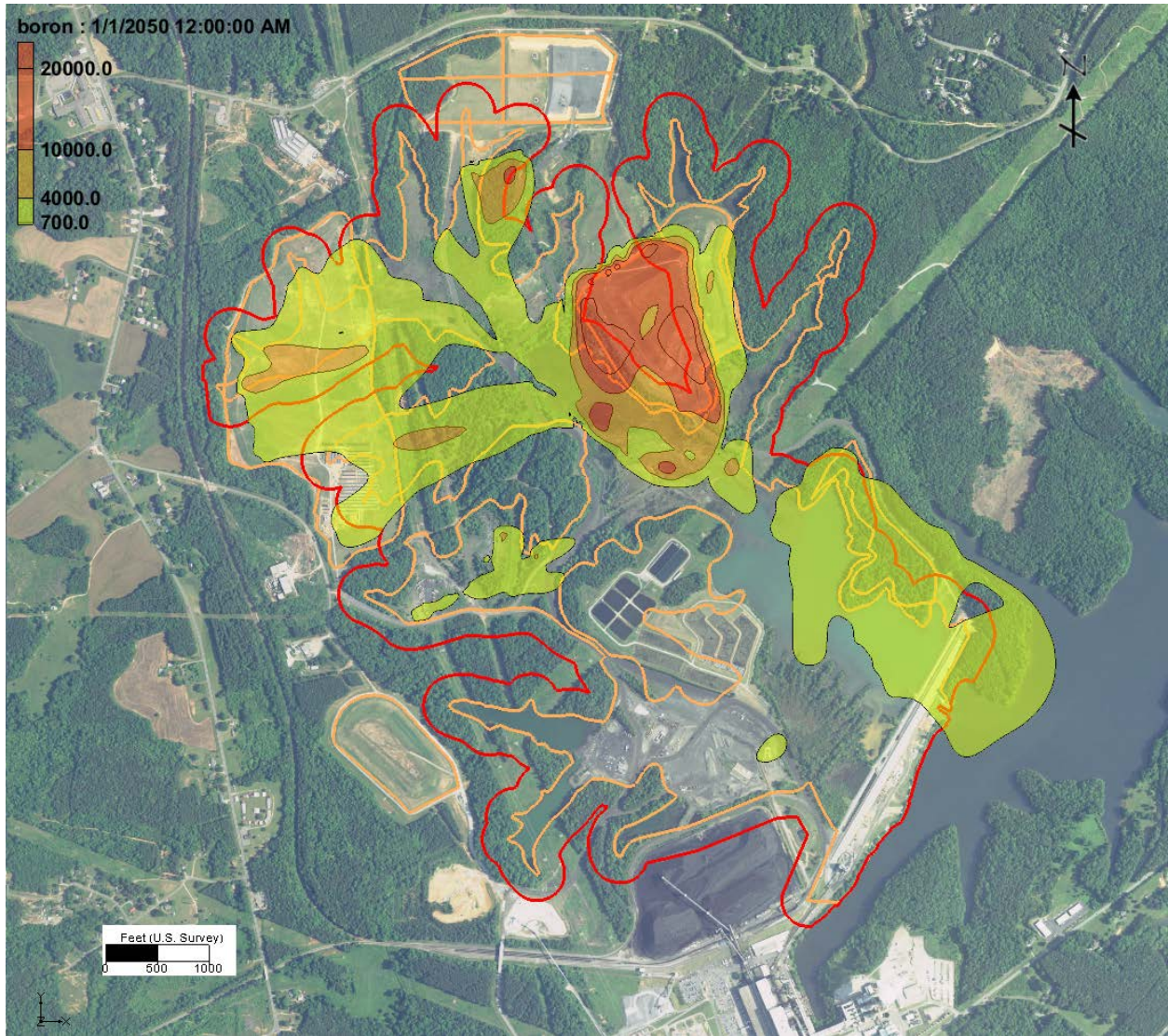


Figure 6-6a. Simulated boron concentrations in the upper bedrock (layer 9) in 2050 for the excavation case. The red line is the potential compliance boundary and orange lines are waste boundaries and landfill boundaries.

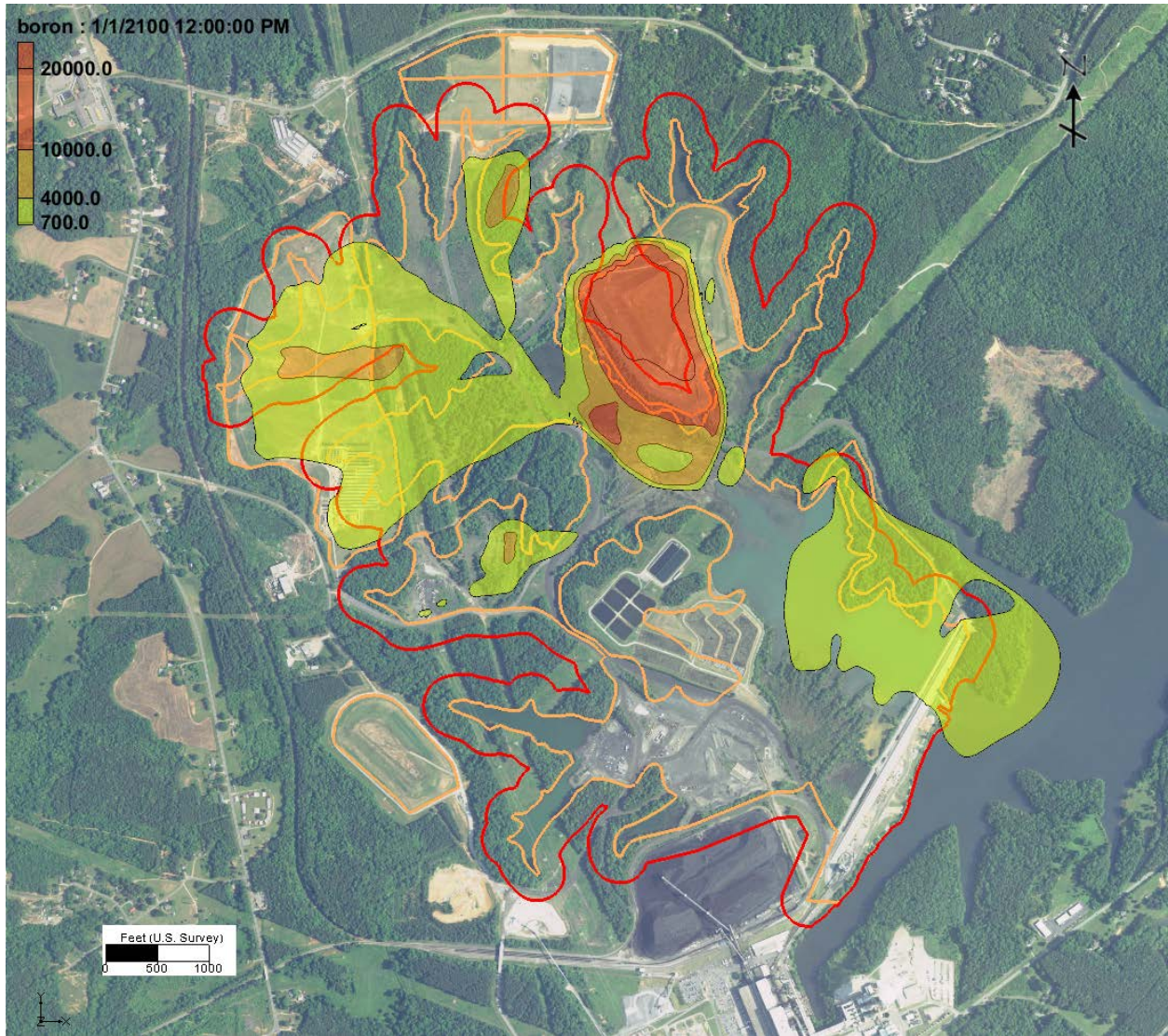


Figure 6-6b. Simulated boron concentrations in the upper bedrock (layer 9) in 2100 for the excavation case. The red line is the potential compliance boundary and orange lines are waste boundaries and landfill boundaries.

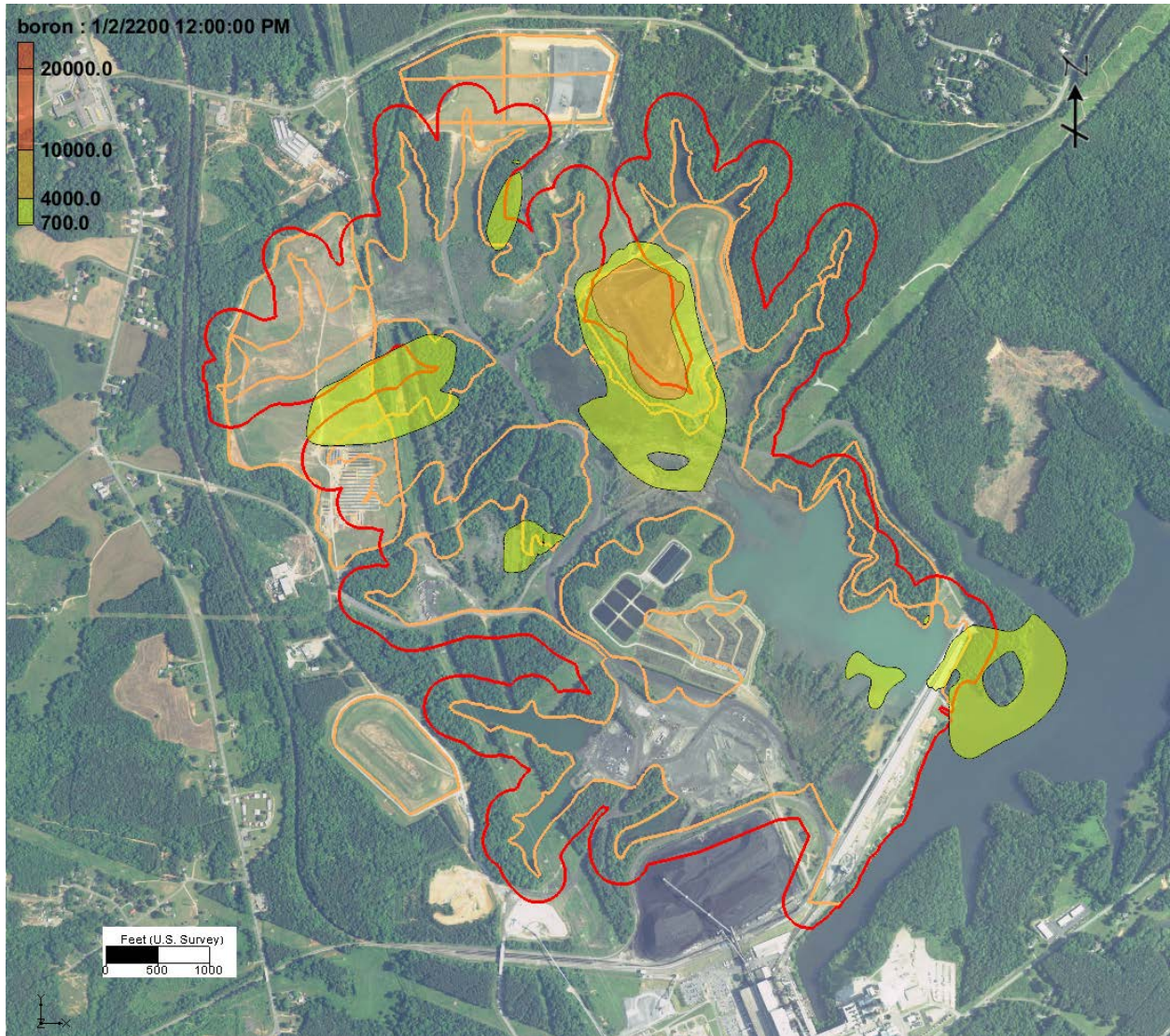


Figure 6-6c. Simulated boron concentrations in the upper bedrock (layer 9) in 2200 for the excavation case. The red line is the potential compliance boundary and orange lines are waste boundaries and landfill boundaries.

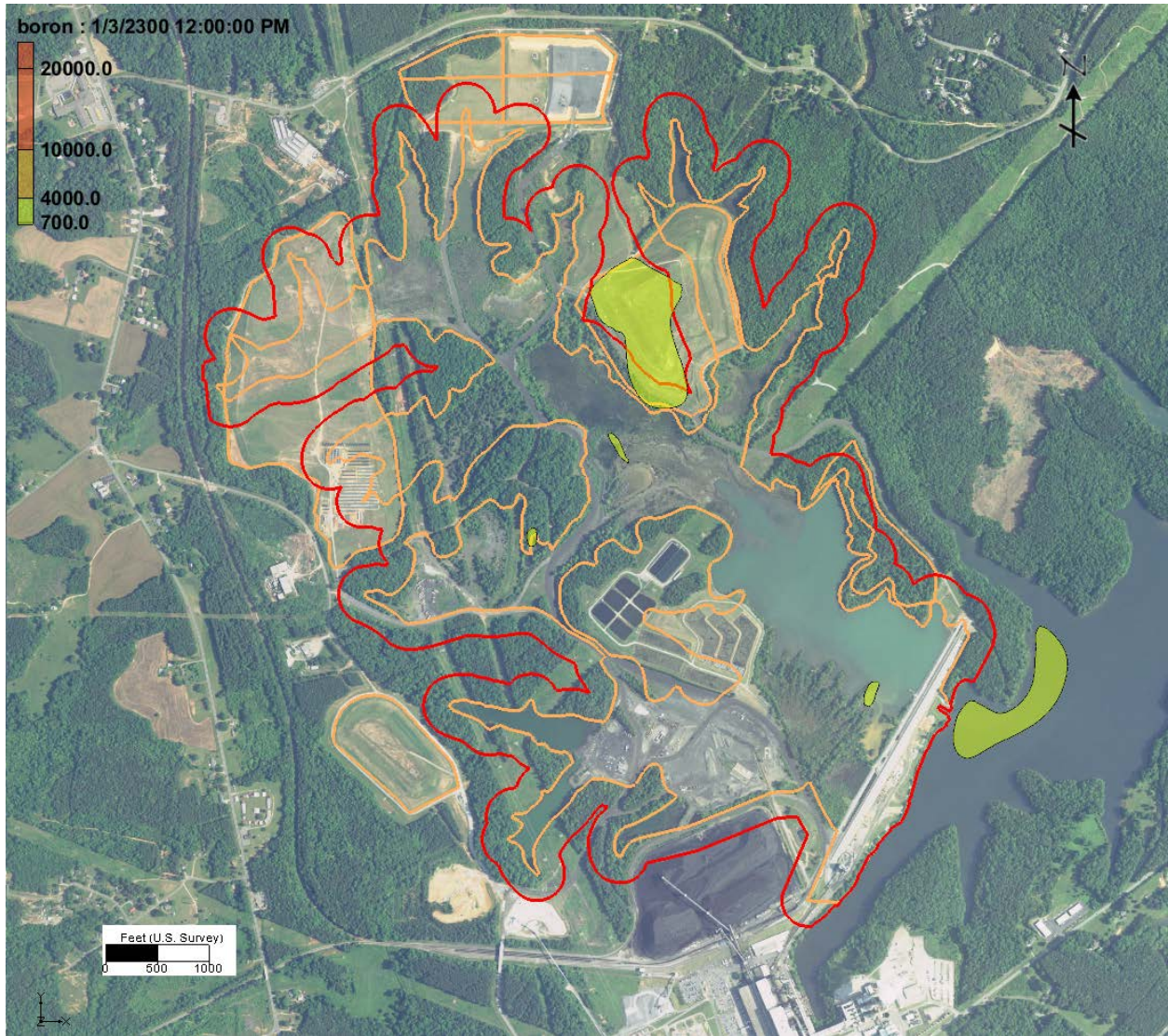


Figure 6-6d. Simulated boron concentrations in the upper bedrock (layer 9) in 2300 for the excavation case. The red line is the potential compliance boundary and orange lines are waste boundaries and landfill boundaries.



Figure 6-7. Locations for boron time-series plots (point 1 and point 2). The red line is the current compliance boundary and orange lines are waste boundaries and landfill boundaries.

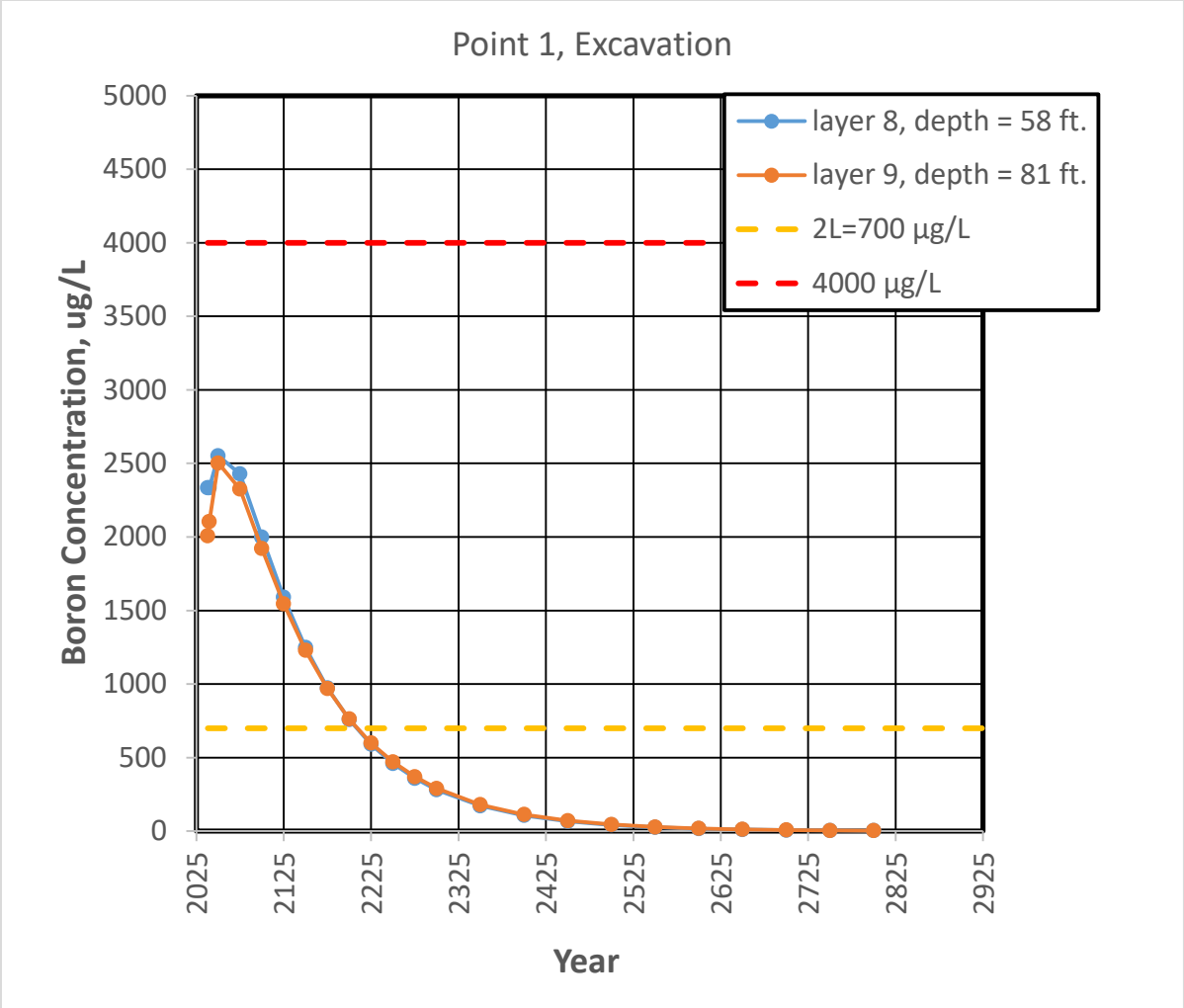


Figure 6-8. Predicted boron concentrations at point 1 near Lake Norman for the excavation case.

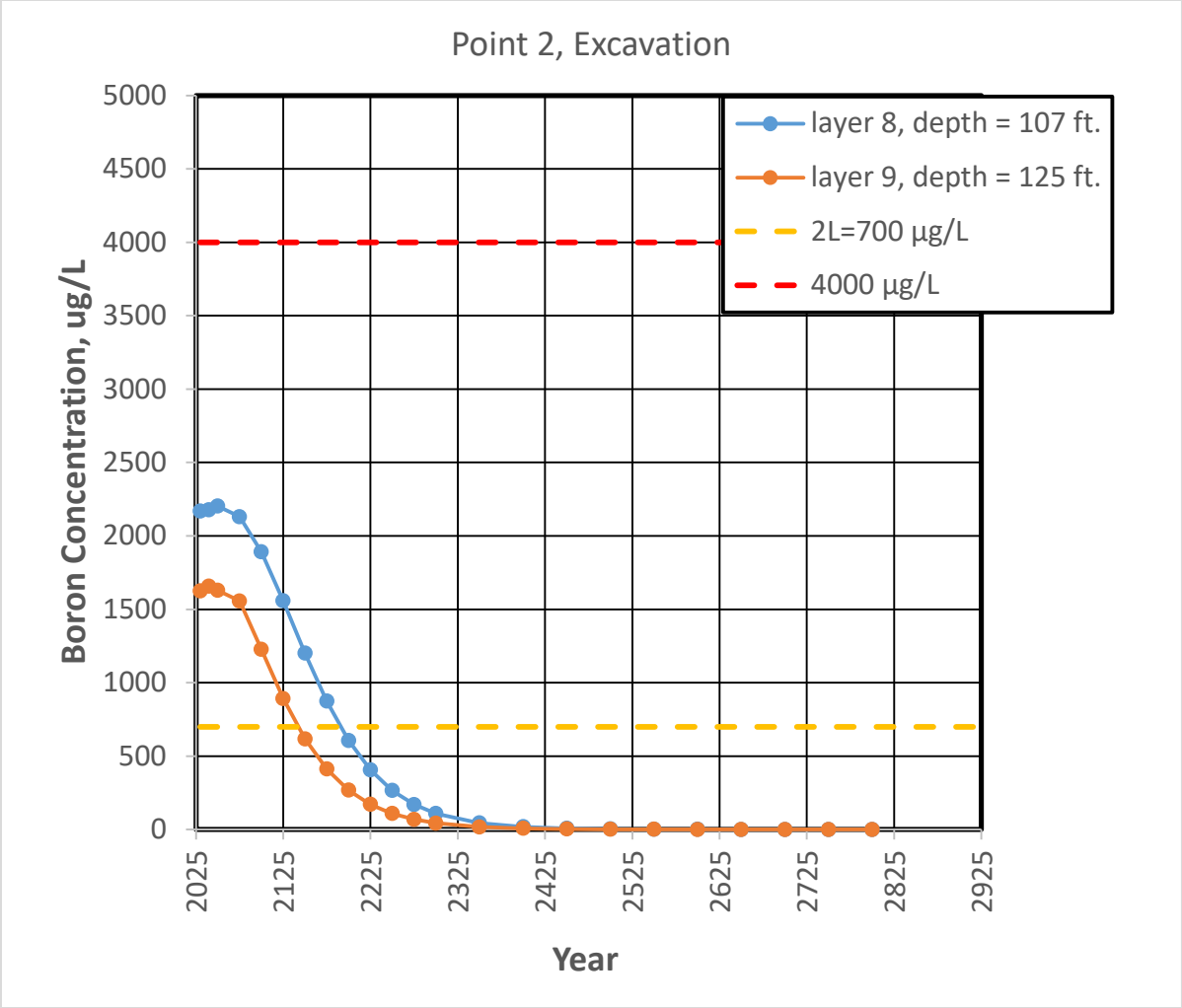


Figure 6-9. Predicted boron concentrations at point 2 east of the Phase I ash landfill for the excavation case.

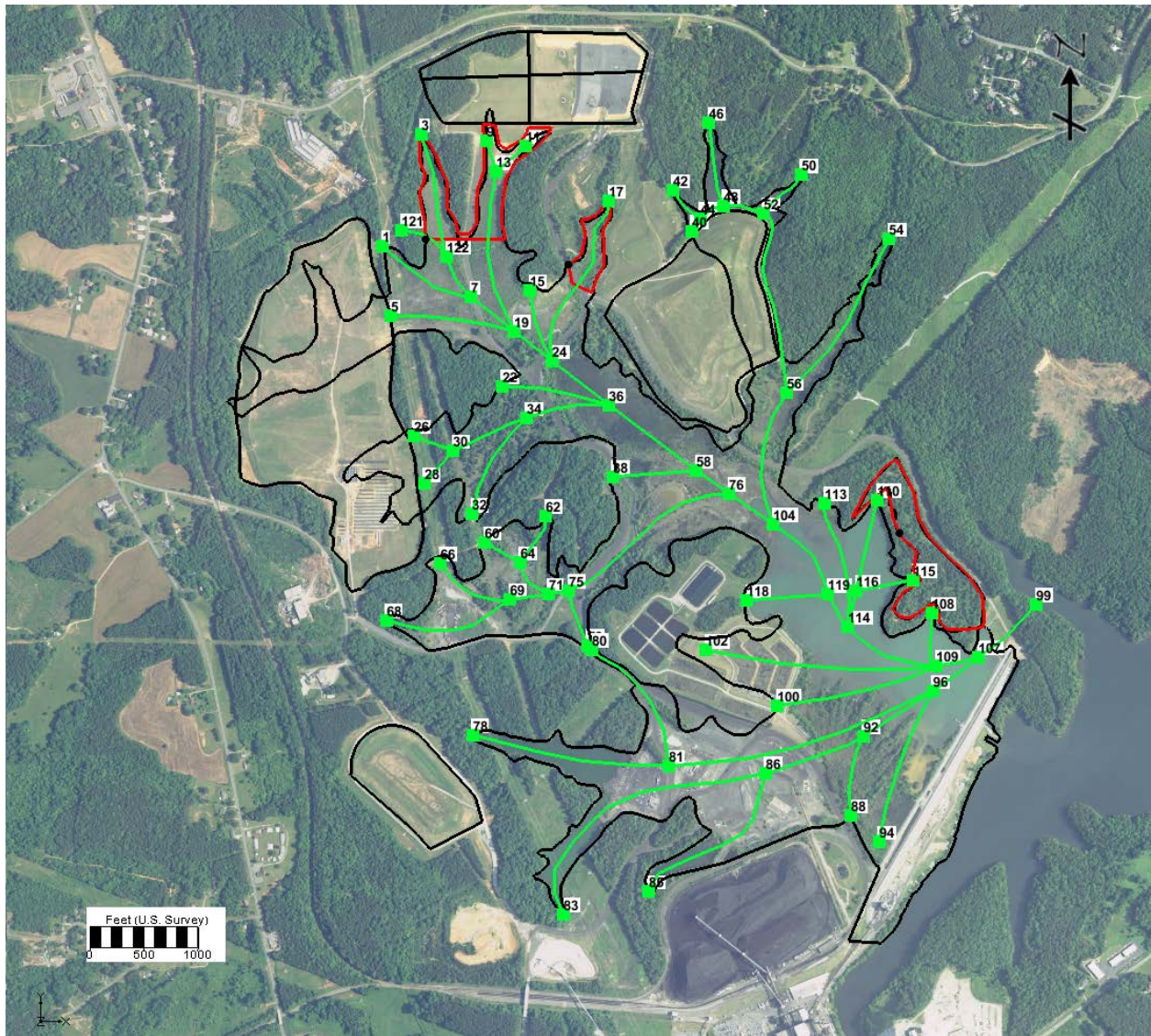


Figure 6-10. Proposed ash basin underdrain system for the final cover simulations. The numbered locations are nodes where the drain elevation was specified based on the draft design from AECOM (2018). The areas outlined in red will be excavated and the Phase II ash landfill and the PV structural fill will be capped in addition to the ash basin.

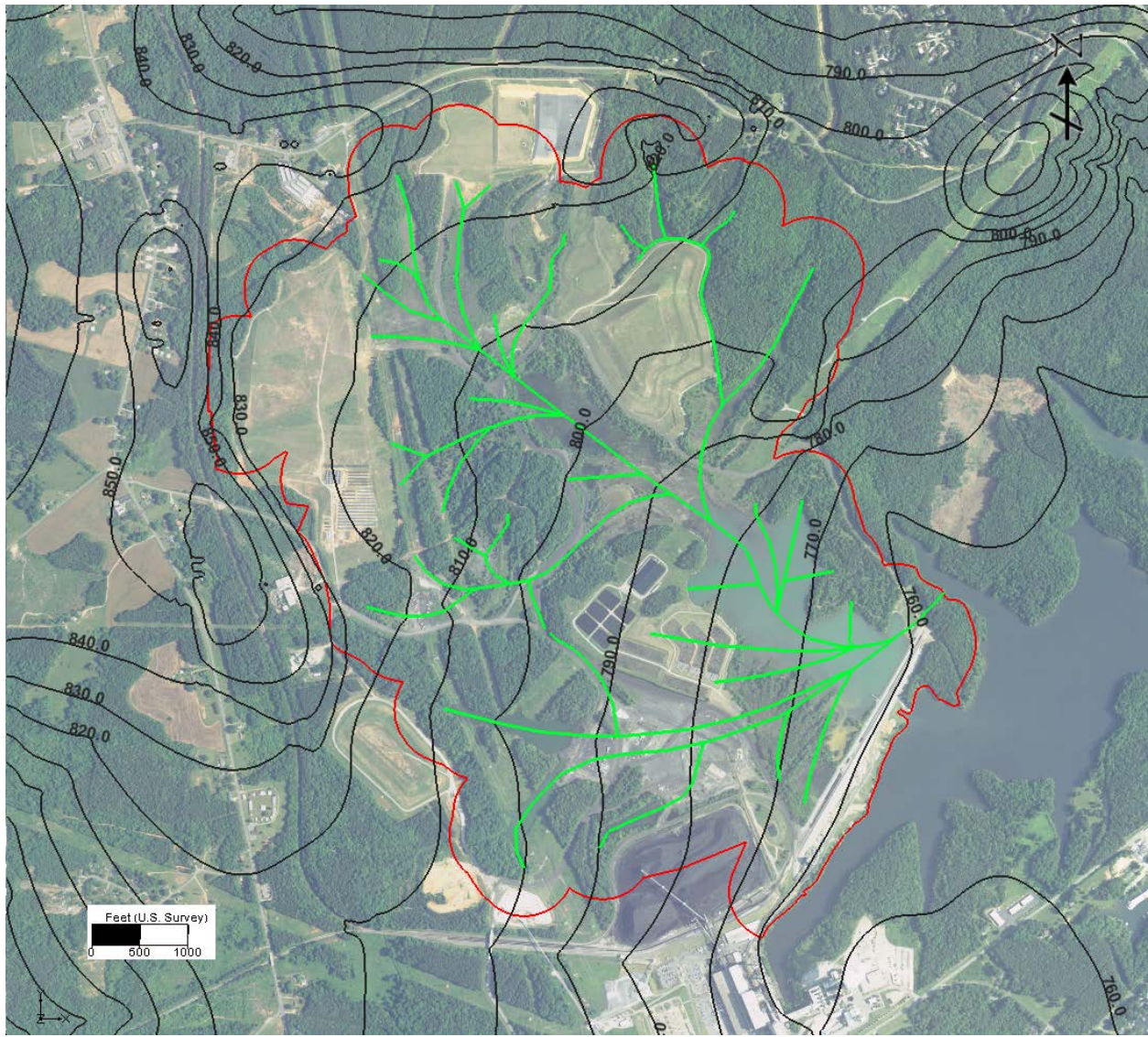


Figure 6-11. Simulated hydraulic heads for the final cover case. The red line is the current compliance boundary.

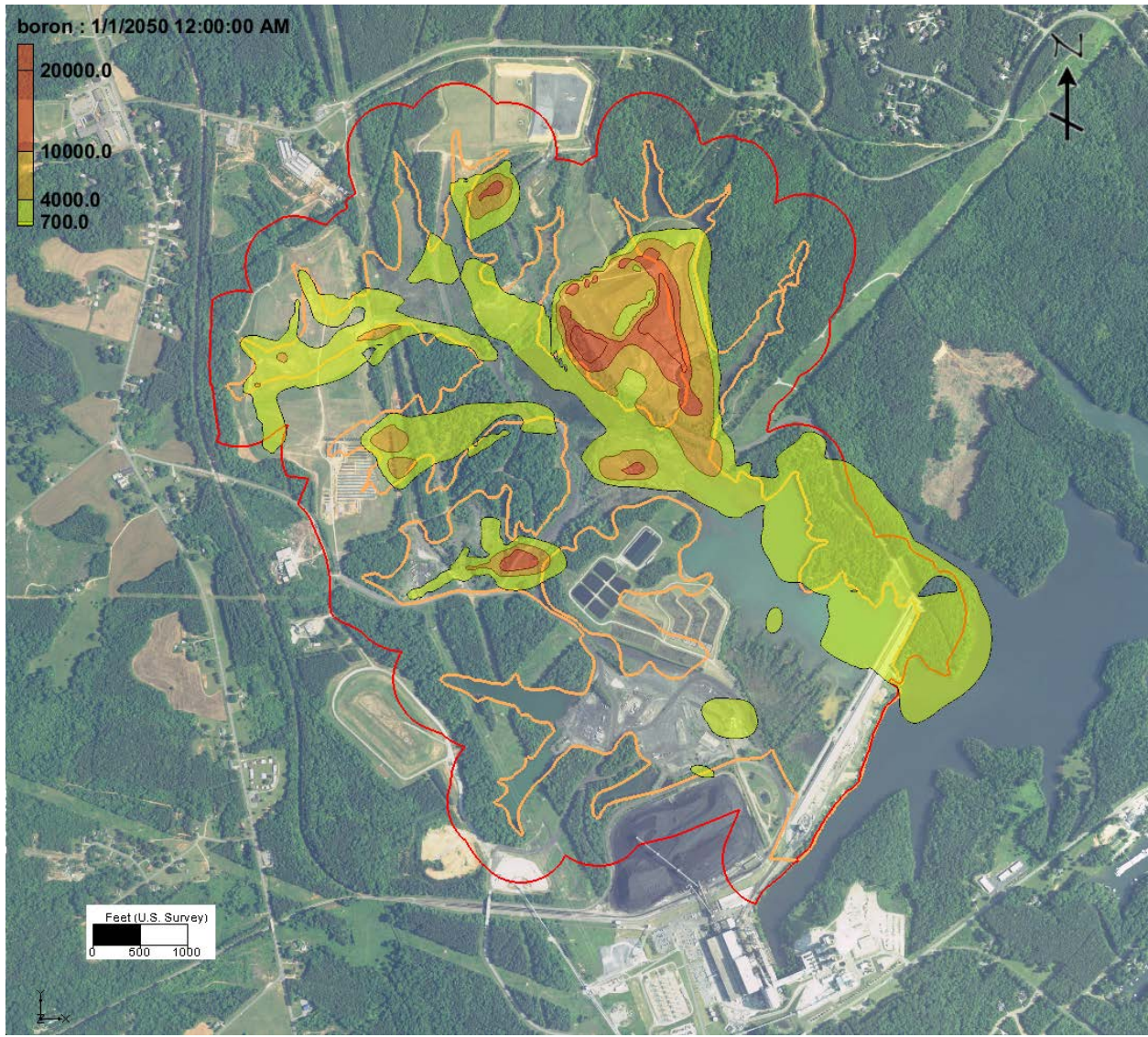


Figure 6-12a. Simulated boron concentrations in the transition zone (layer 8) in 2050 for the final cover case. The red line is the current compliance boundary and orange lines are waste boundaries and landfill boundaries.

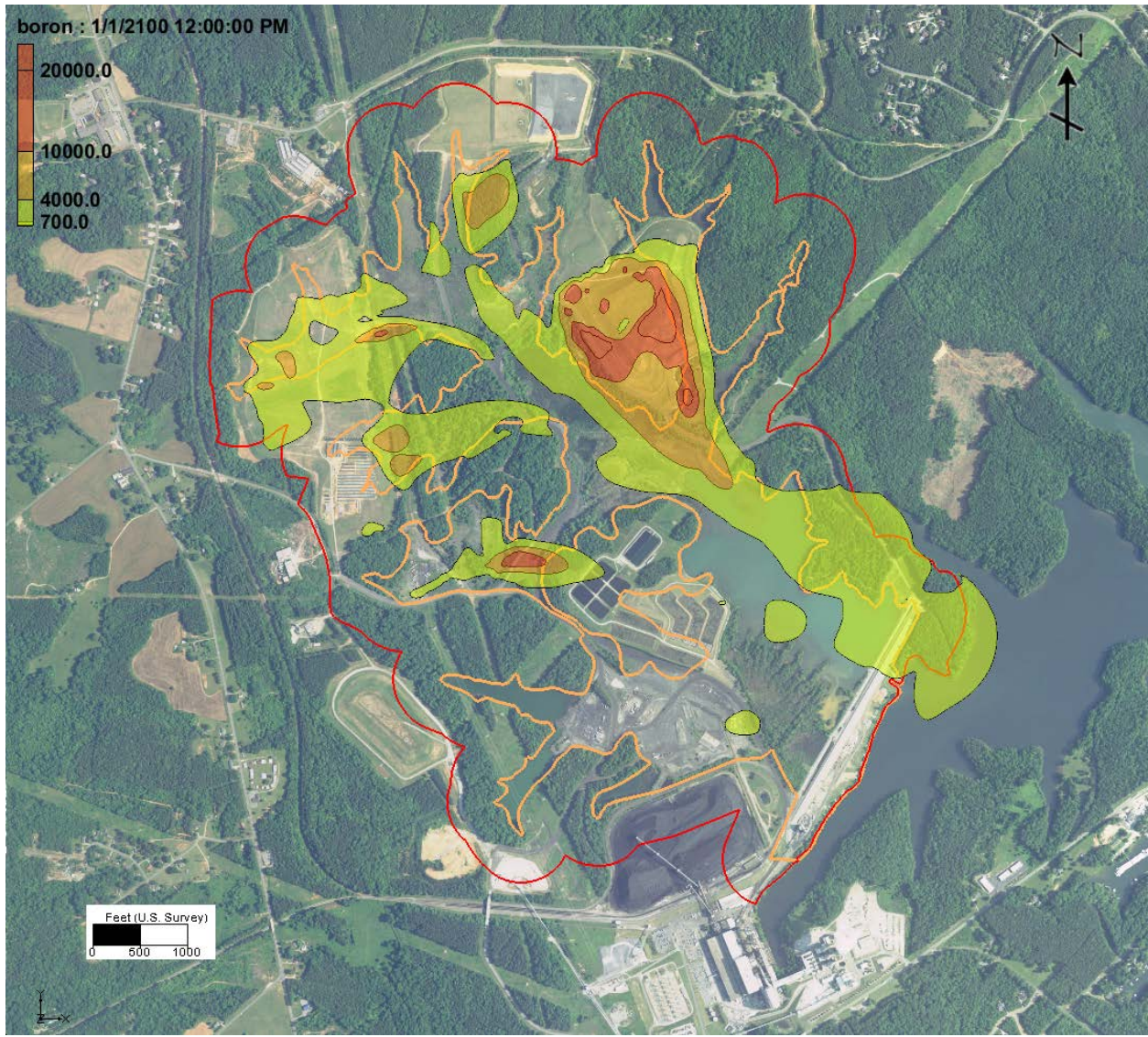


Figure 6-12b. Simulated boron concentrations in the transition zone (layer 8) in 2100 for the final cover case. The red line is the current compliance boundary and orange lines are waste boundaries and landfill boundaries.

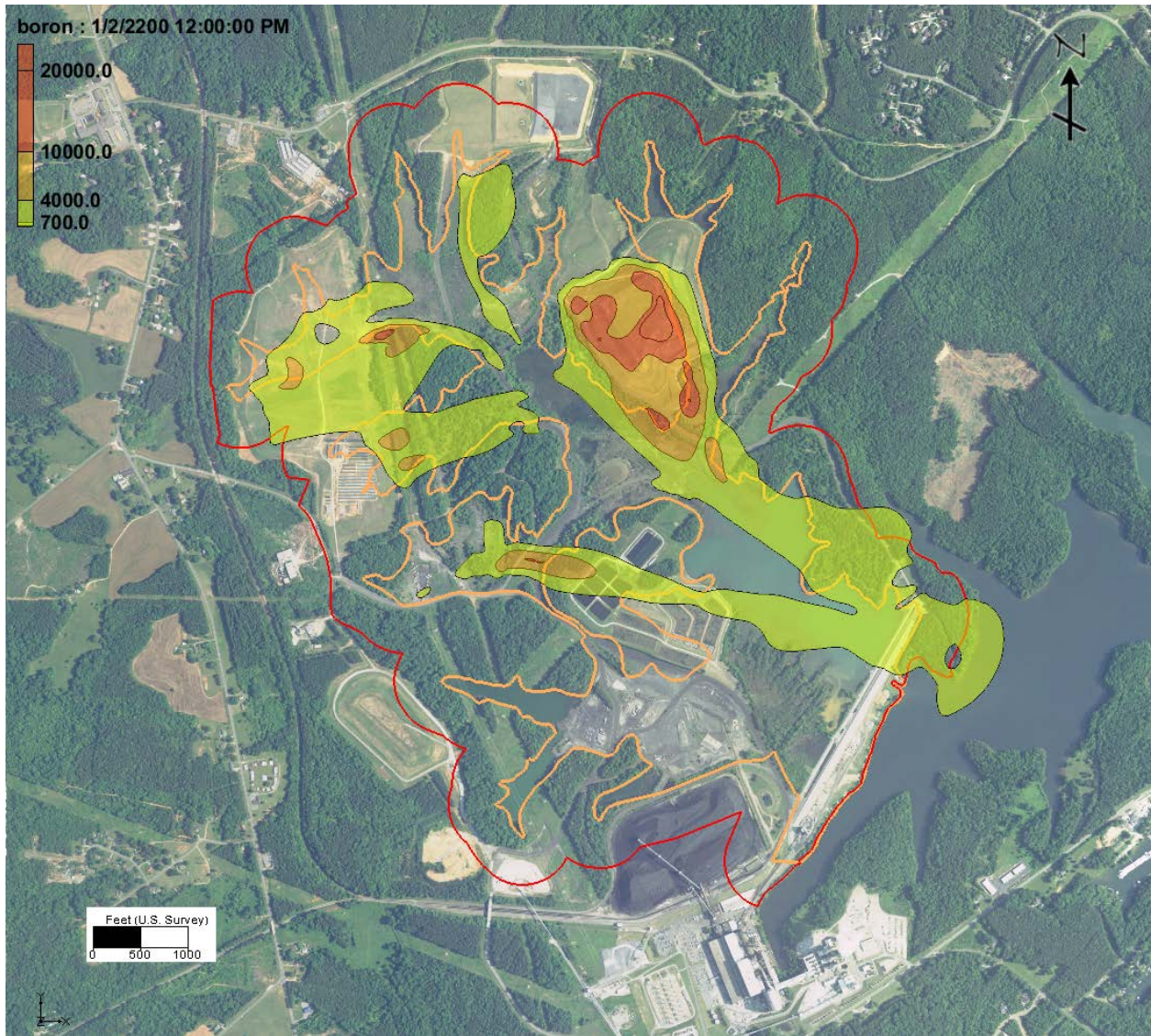


Figure 6-12c. Simulated boron concentrations in the transition zone (layer 8) in 2200 for the final cover case. The red line is the current compliance boundary and orange lines are waste boundaries and landfill boundaries.

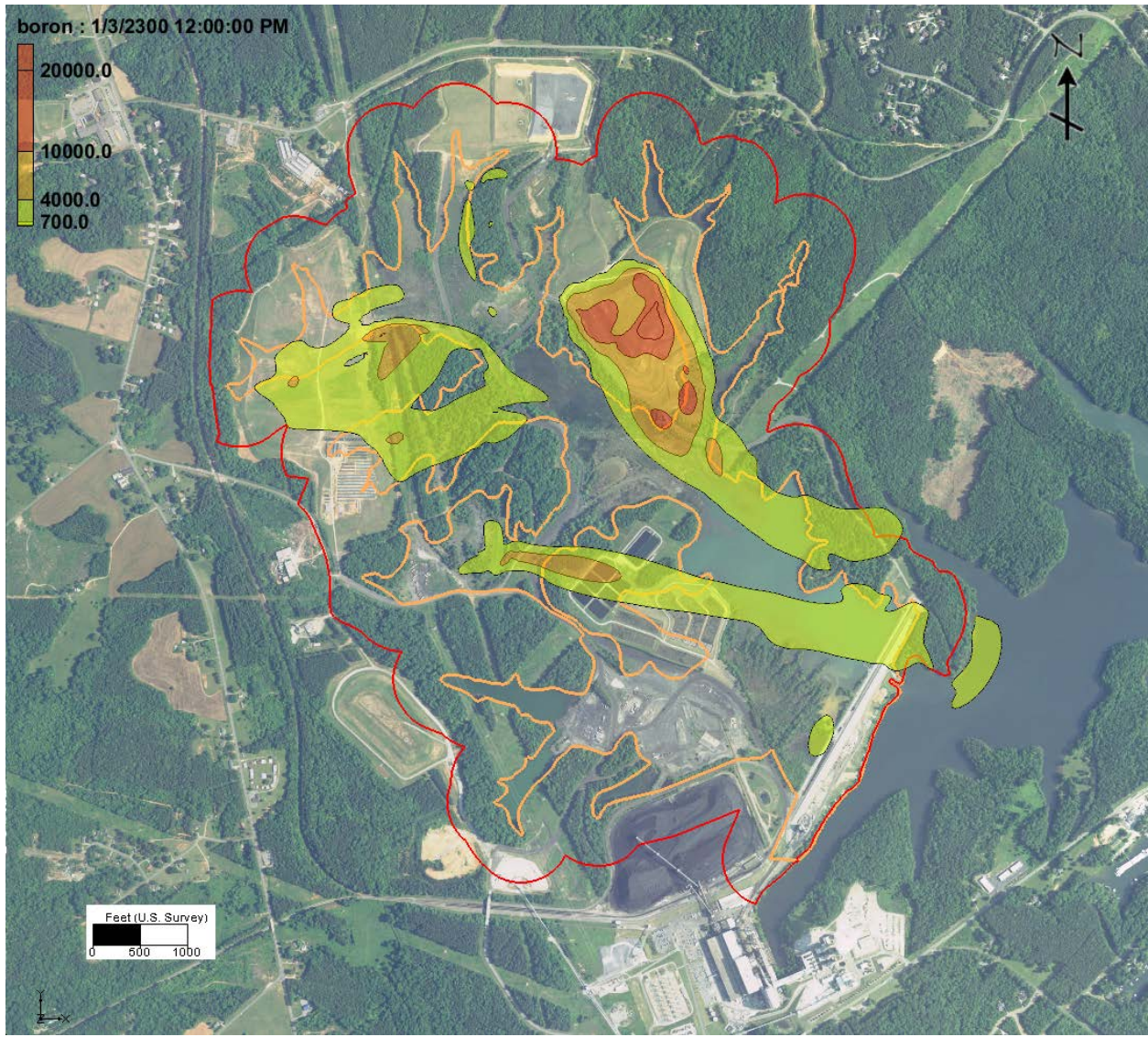


Figure 6-12d. Simulated boron concentrations in the transition zone (layer 8) in 2300 for the final cover case. The red line is the current compliance boundary and orange lines are waste boundaries and landfill boundaries.

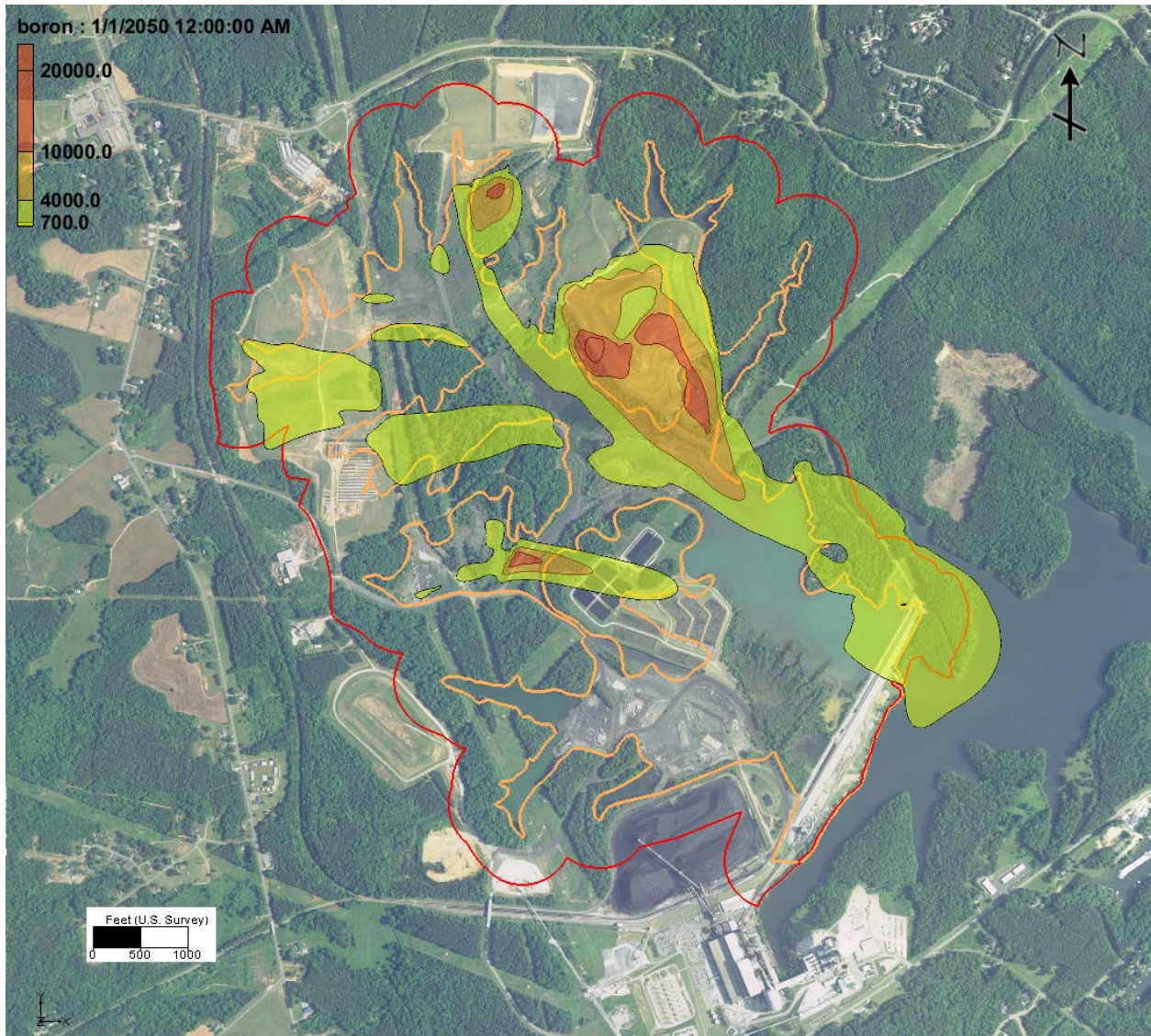


Figure 6-13a. Simulated boron concentrations in the upper bedrock (layer 9) in 2050 for the final cover case. The red line is the current compliance boundary and orange lines are waste boundaries and landfill boundaries.

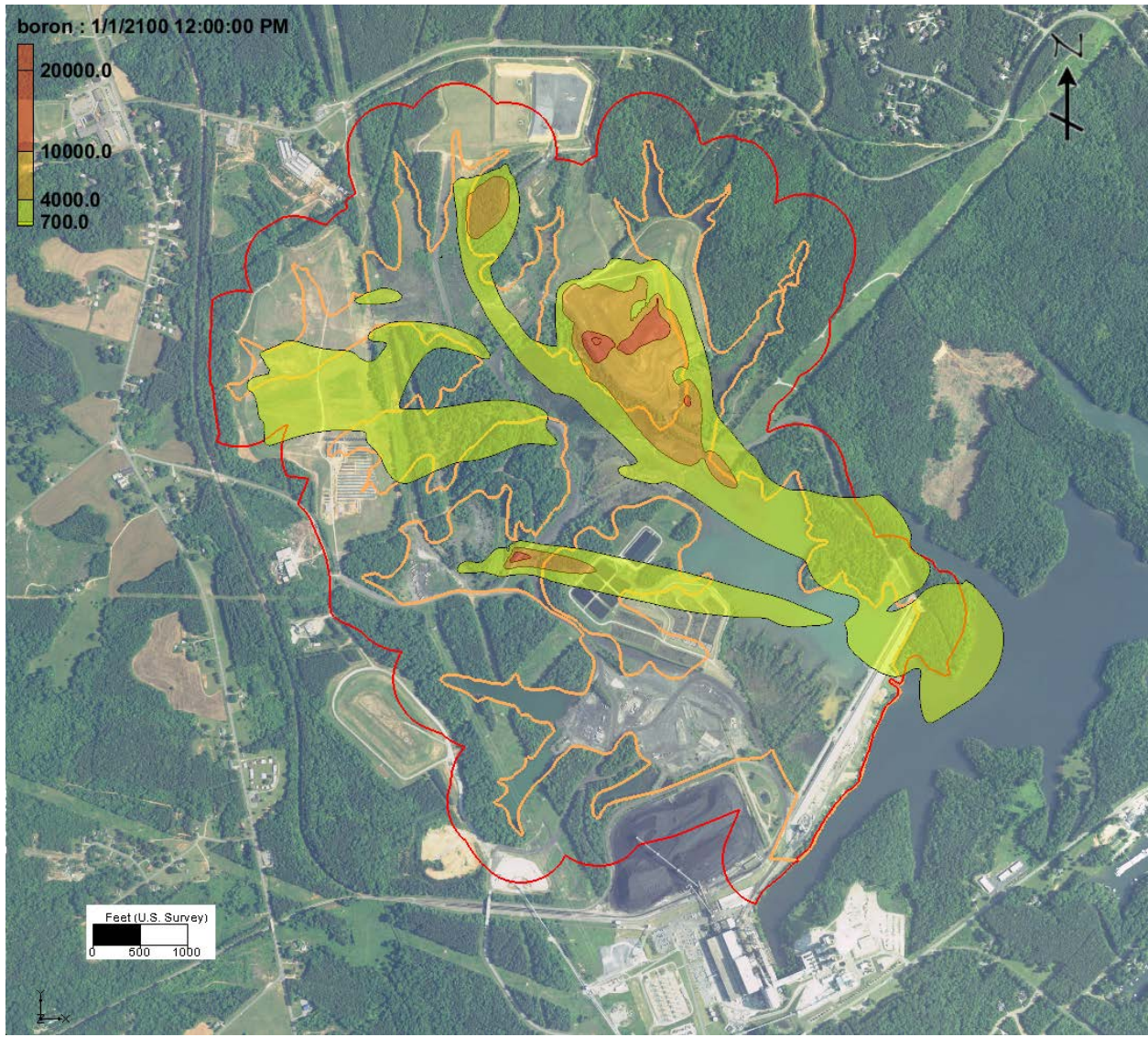


Figure 6-13b. Simulated boron concentrations in the upper bedrock (layer 9) in 2100 for the final cover case. The red line is the current compliance boundary and orange lines are waste boundaries and landfill boundaries.

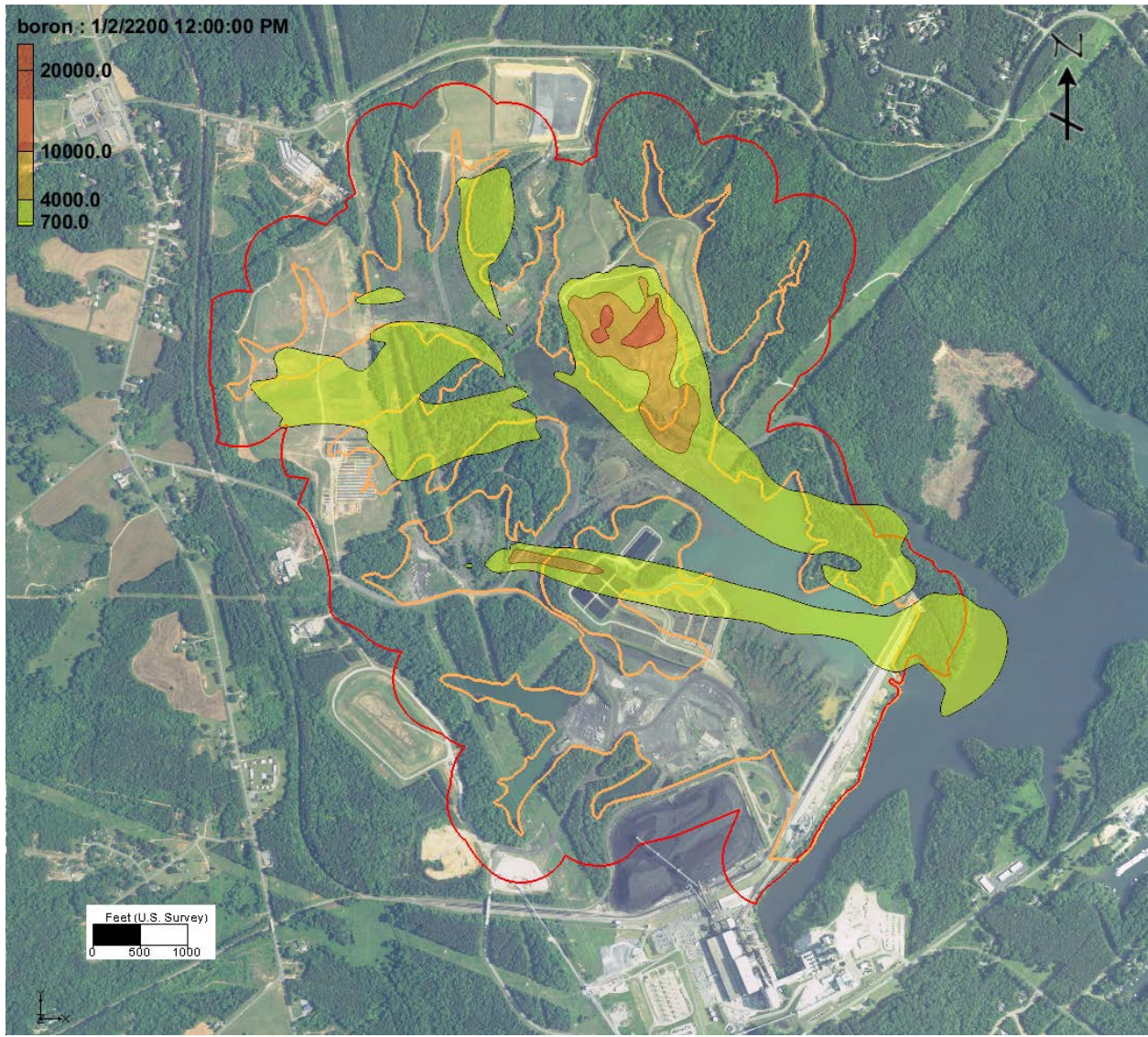


Figure 6-13c. Simulated boron concentrations in the upper bedrock (layer 9) in 2200 for the final cover case. The red line is the current compliance boundary and orange lines are waste boundaries and landfill boundaries.

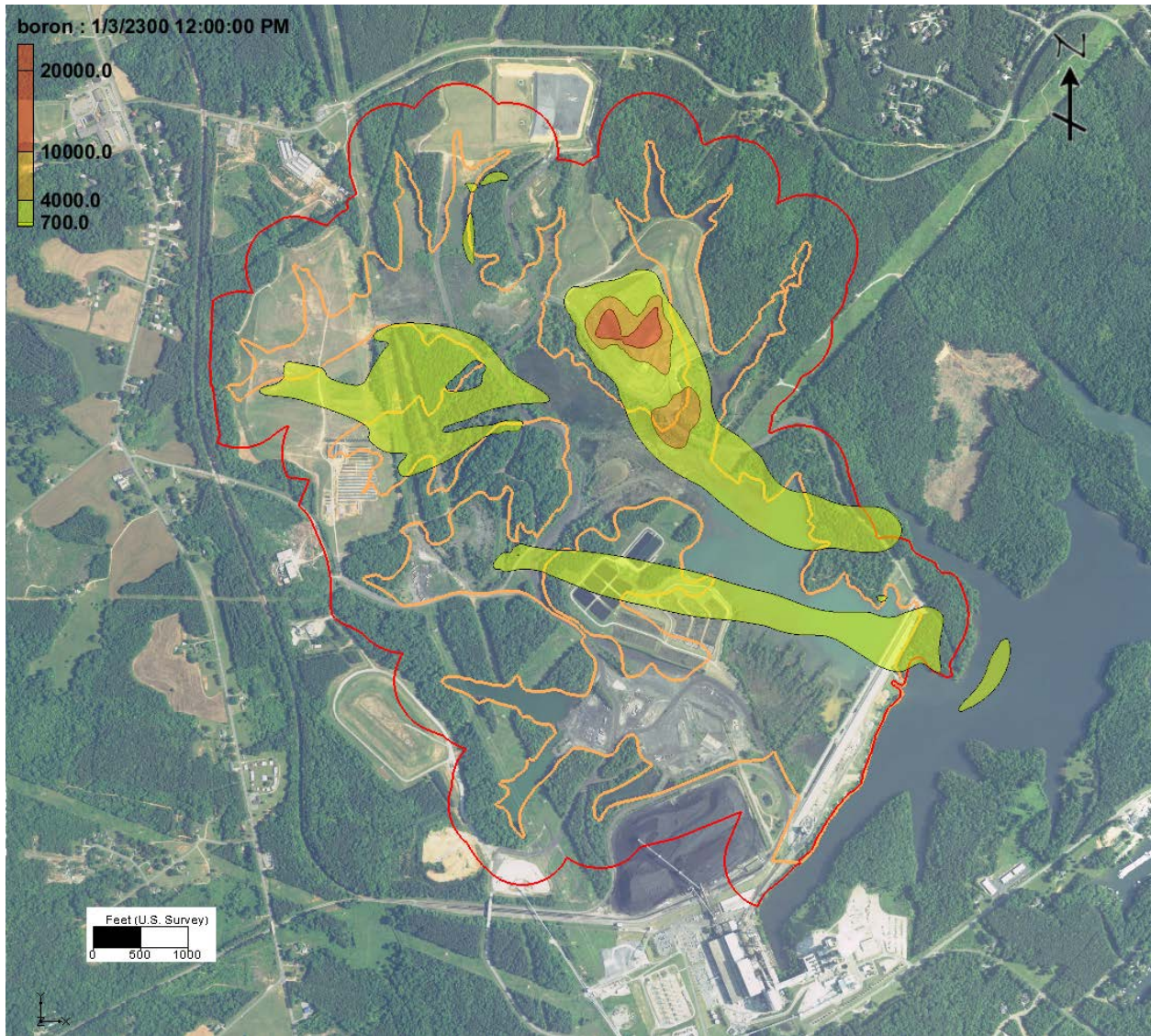


Figure 6-13d. Simulated boron concentrations in the upper bedrock (layer 9) in 2300 for the final cover case. The red line is the current compliance boundary and orange lines are waste boundaries and landfill boundaries.

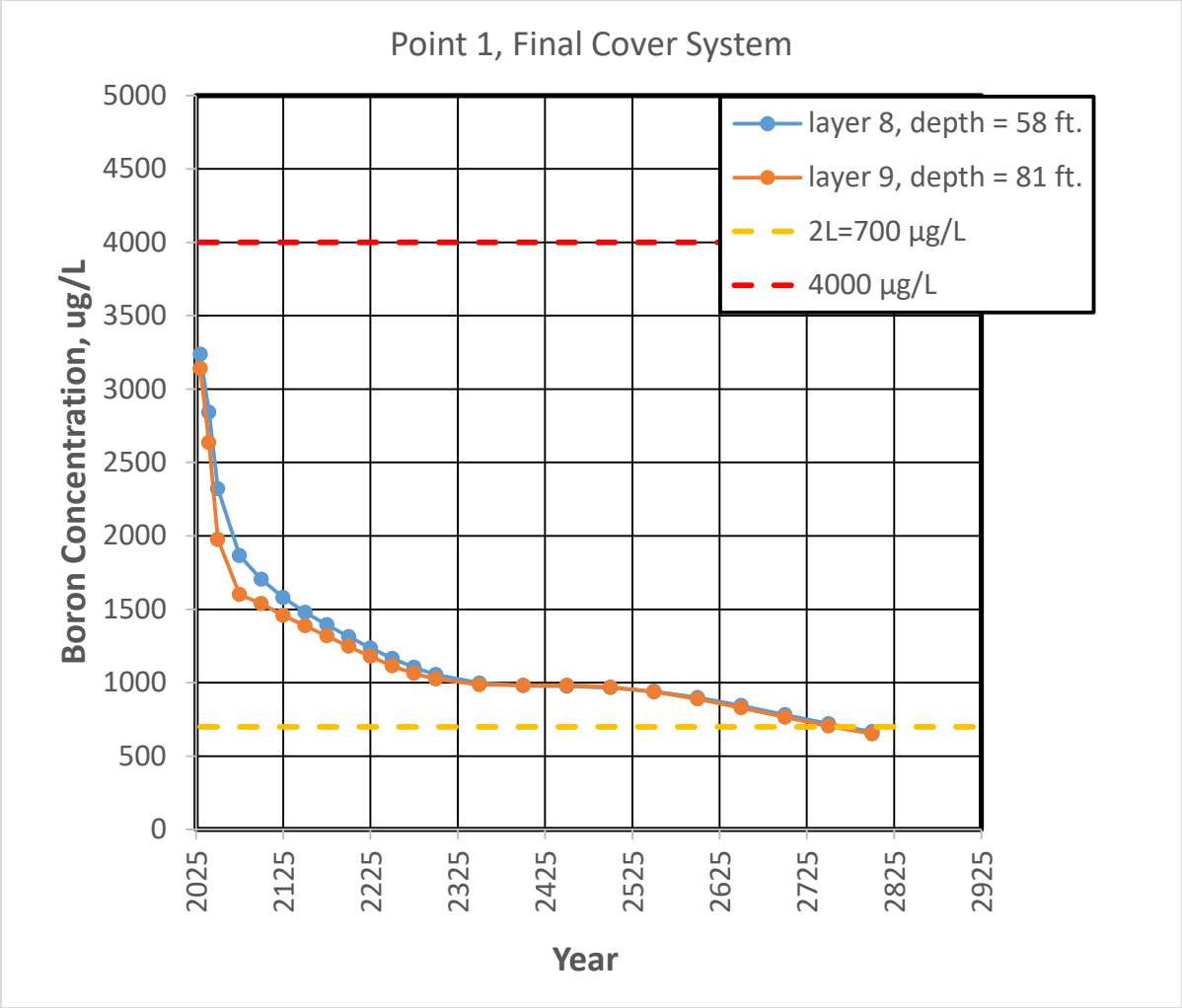


Figure 6-14. Predicted boron concentrations at point 1 near Lake Norman for the final cover case.

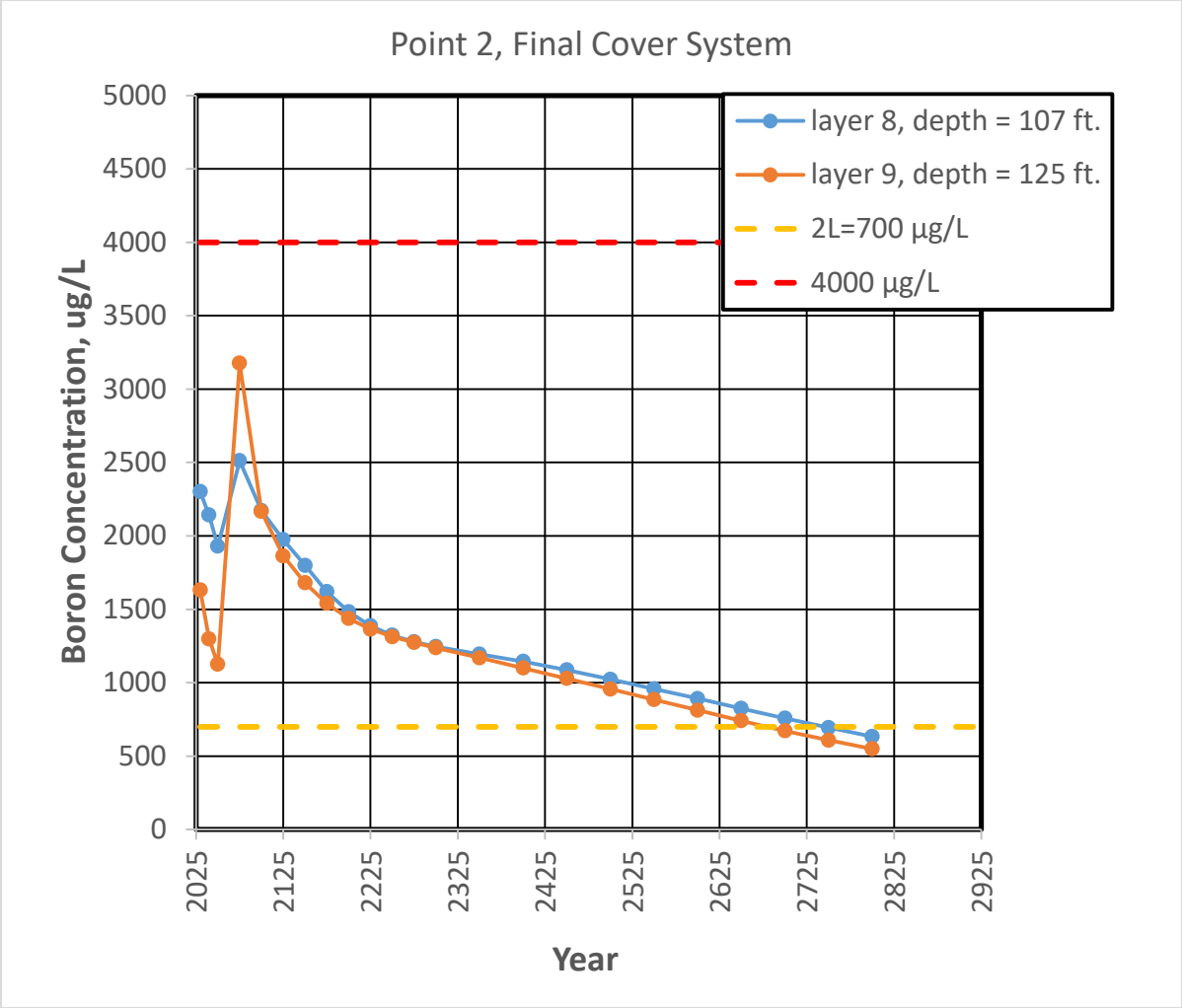


Figure 6-15. Predicted boron concentrations at point 2 east of the Phase I ash landfill for the final cover case.

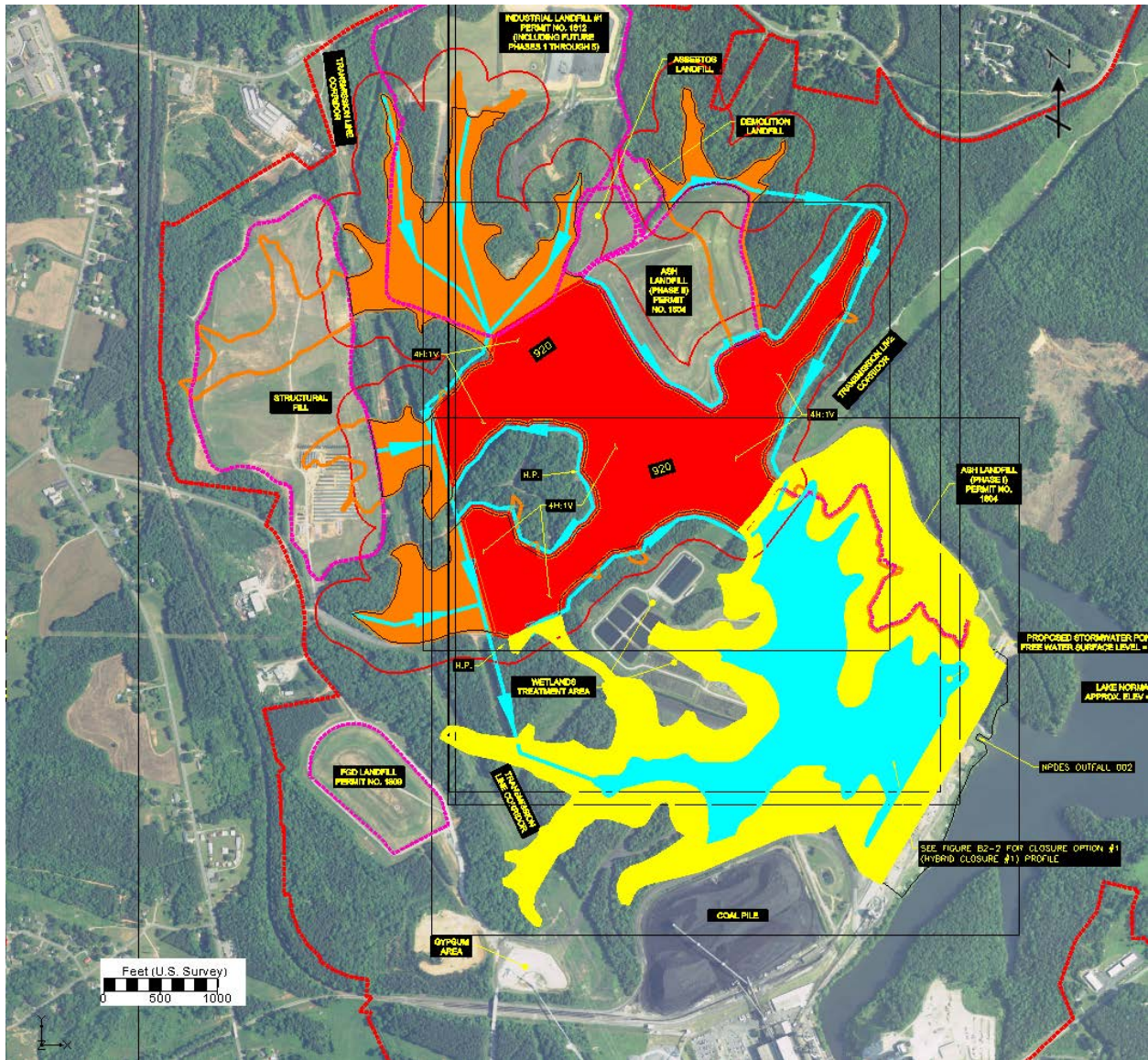


Figure 6-16. Hybrid closure design used in simulations (from AECOM, 2015). The yellow area is excavated forming a stormwater pond (blue) that has a water surface elevation similar to Lake Norman. The excavated ash is stacked in the red area to a maximum height of 920 ft. The orange areas are capped and the Phase II ash landfill and the PV structural fill will be capped in addition to the ash basin. The Phase I ash landfill is excavated. The blue arrows show the surface water drainage pattern.

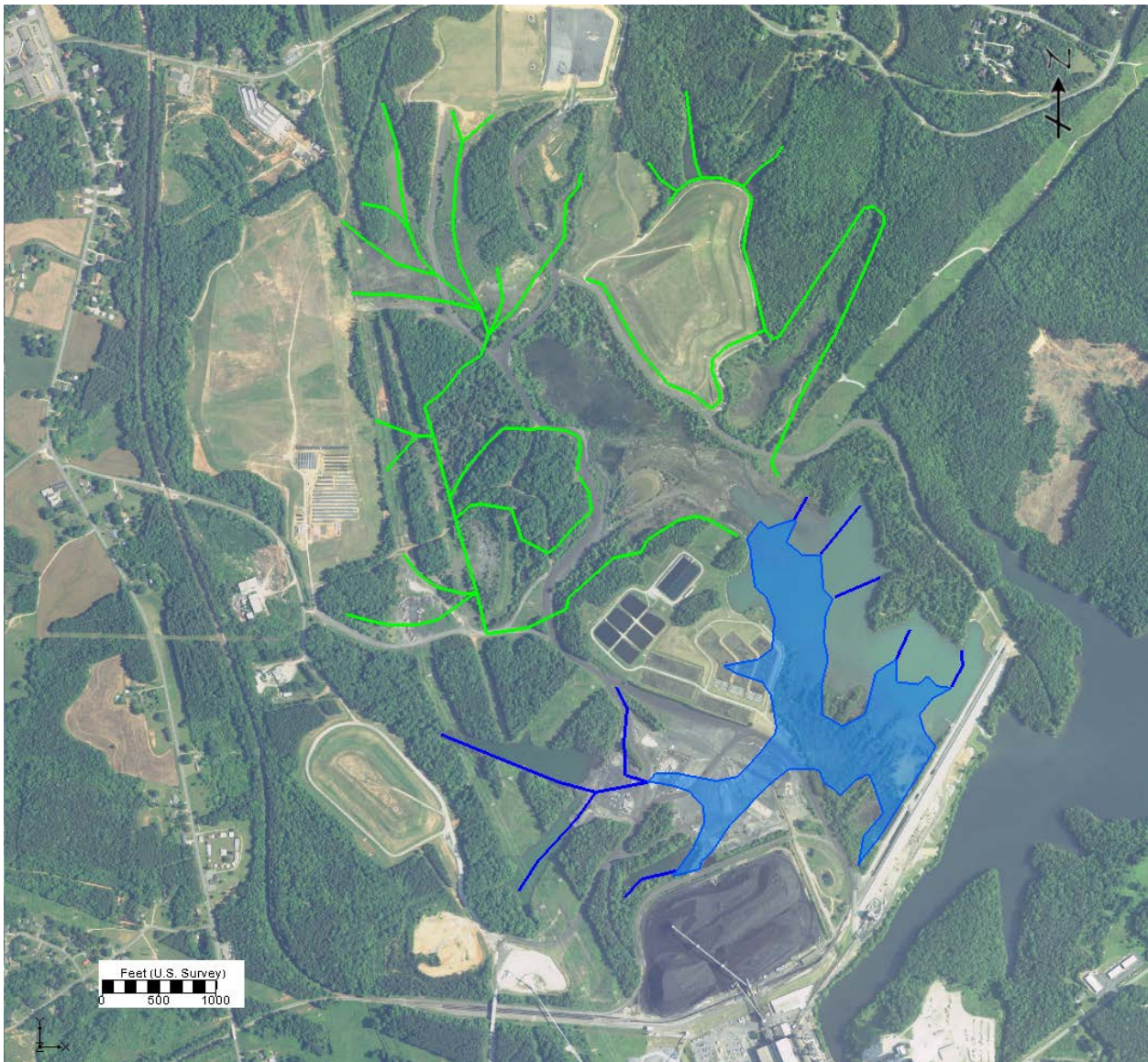


Figure 6-17. Drains used in the hybrid design simulation. Proposed ash basin underdrains (green lines) are present five feet beneath the cover system in the northern part of the basin. A drain network (blue lines) is used in the excavated (southern) part of the basin to represent springs and streams that may form. The elevations are set to the top of the saprolite surface, which approximately corresponds to the original ground surface in this part of the basin. The stormwater pond is shown as the blue polygon.

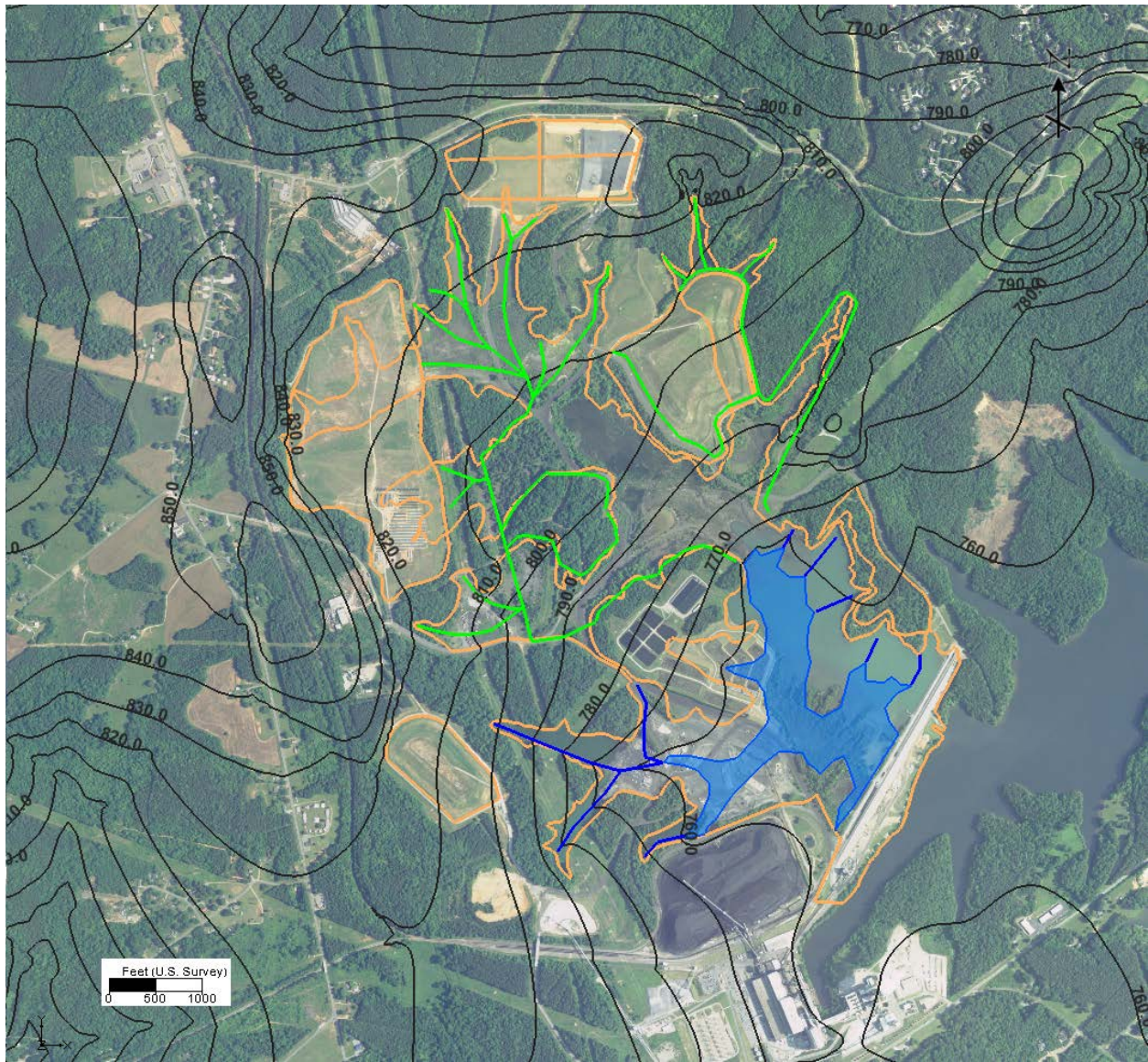


Figure 6-18. Simulated hydraulic heads for the hybrid case. The orange lines are waste boundaries and landfill boundaries.

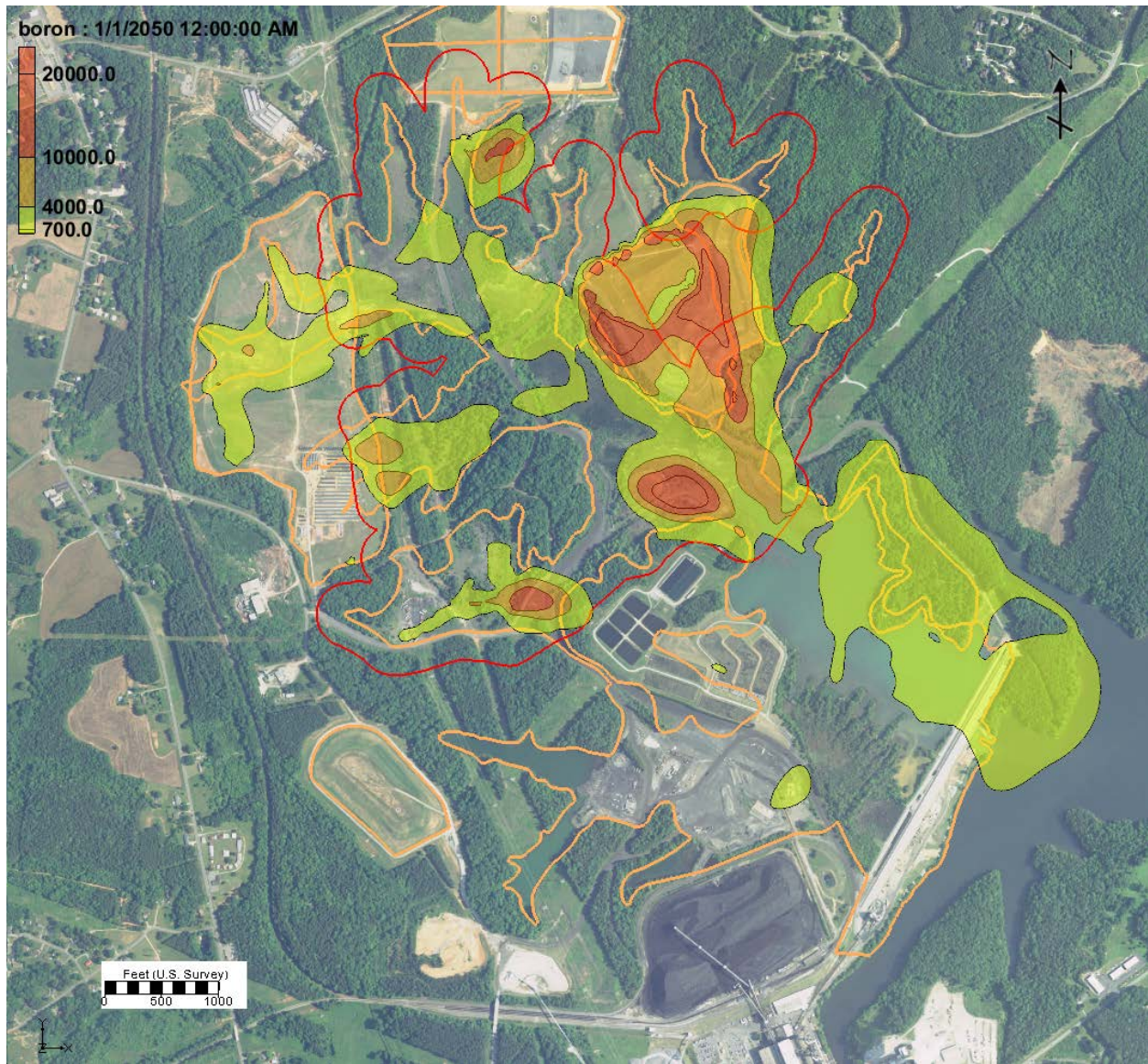


Figure 6-19a. Simulated boron concentrations in the transition zone (layer 8) in 2050 for the hybrid case. The red line is the potential compliance boundary and orange lines are waste boundaries and landfill boundaries.

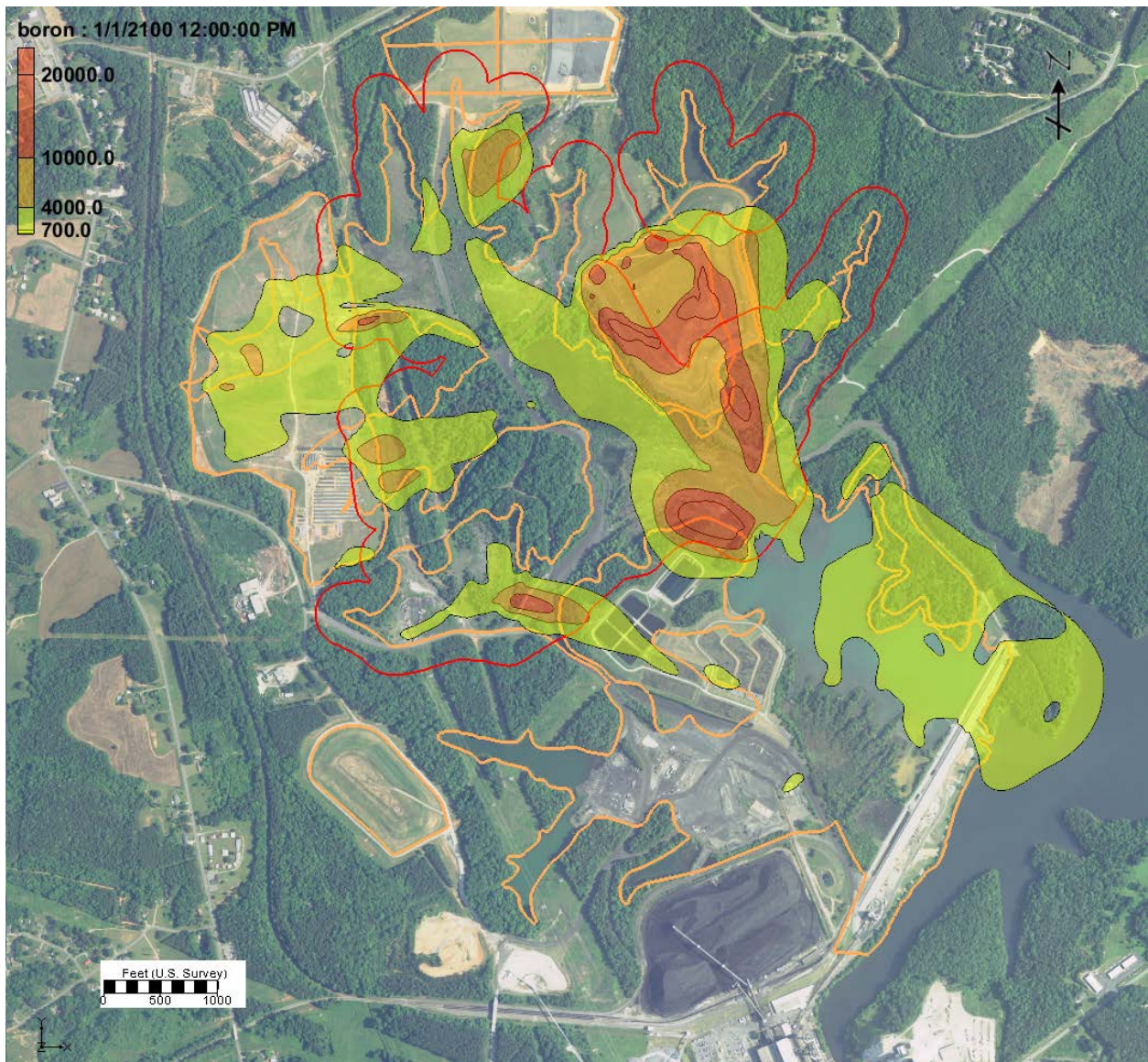


Figure 6-19b. Simulated boron concentrations in the transition zone (layer 8) in 2100 for the hybrid case. The red line is the potential compliance boundary and orange lines are waste boundaries and landfill boundaries.

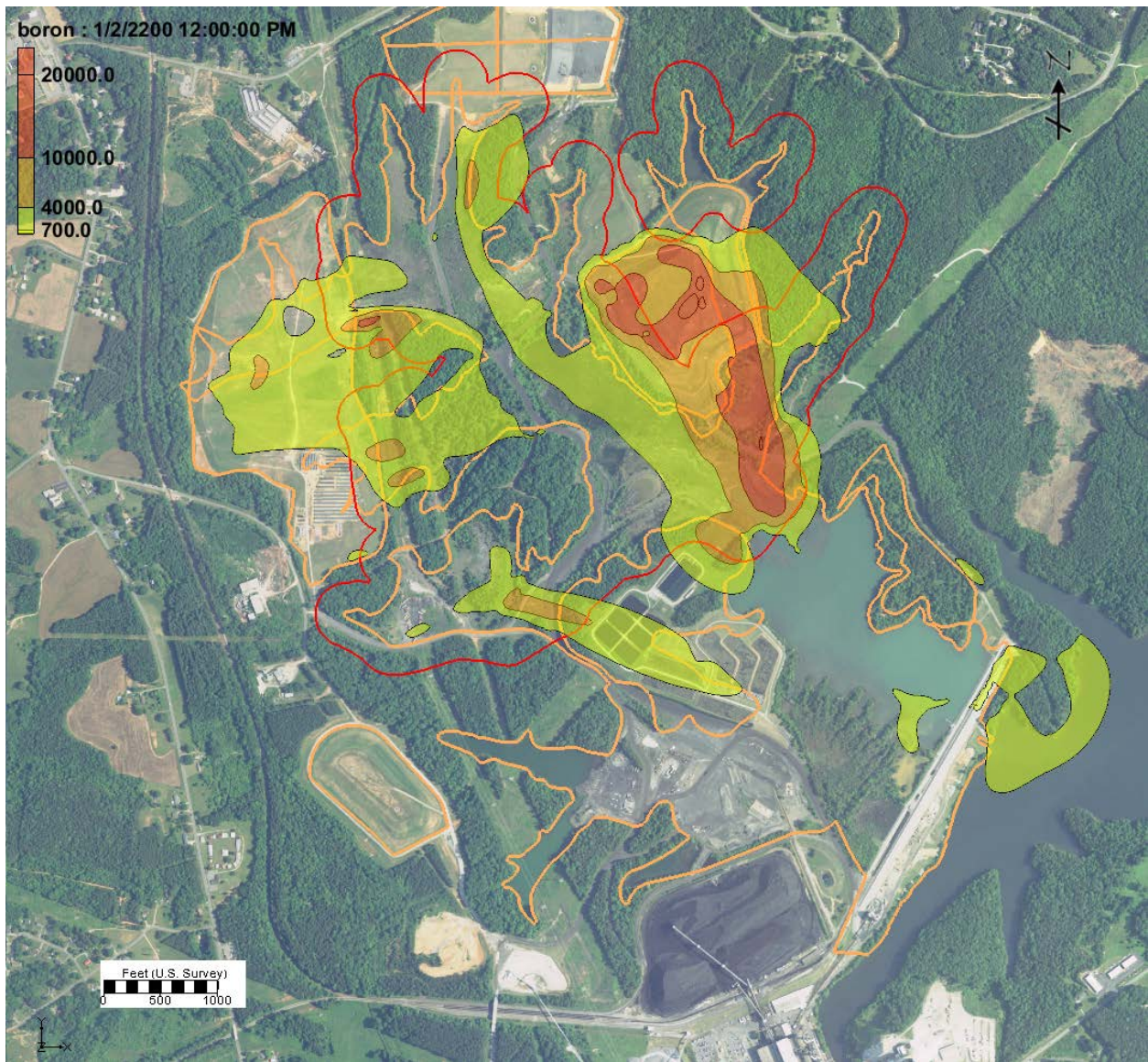


Figure 6-19c. Simulated boron concentrations in the transition zone (layer 8) in 2200 for the hybrid case. The red line is the potential compliance boundary and orange lines are waste boundaries and landfill boundaries.

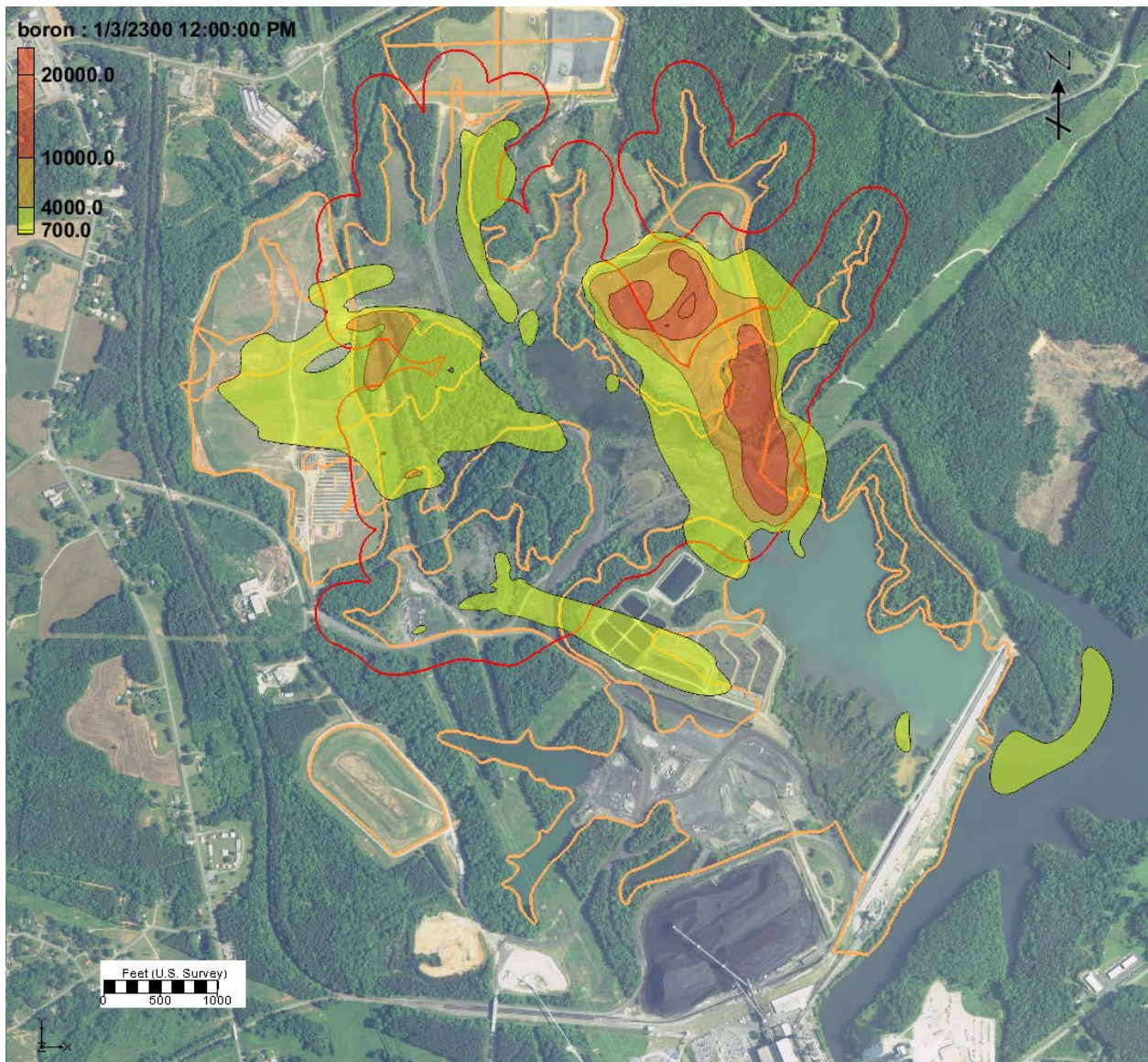


Figure 6-19d. Simulated boron concentrations in the transition zone (layer 8) in 2300 for the hybrid case. The red line is the potential compliance boundary and orange lines are waste boundaries and landfill boundaries.

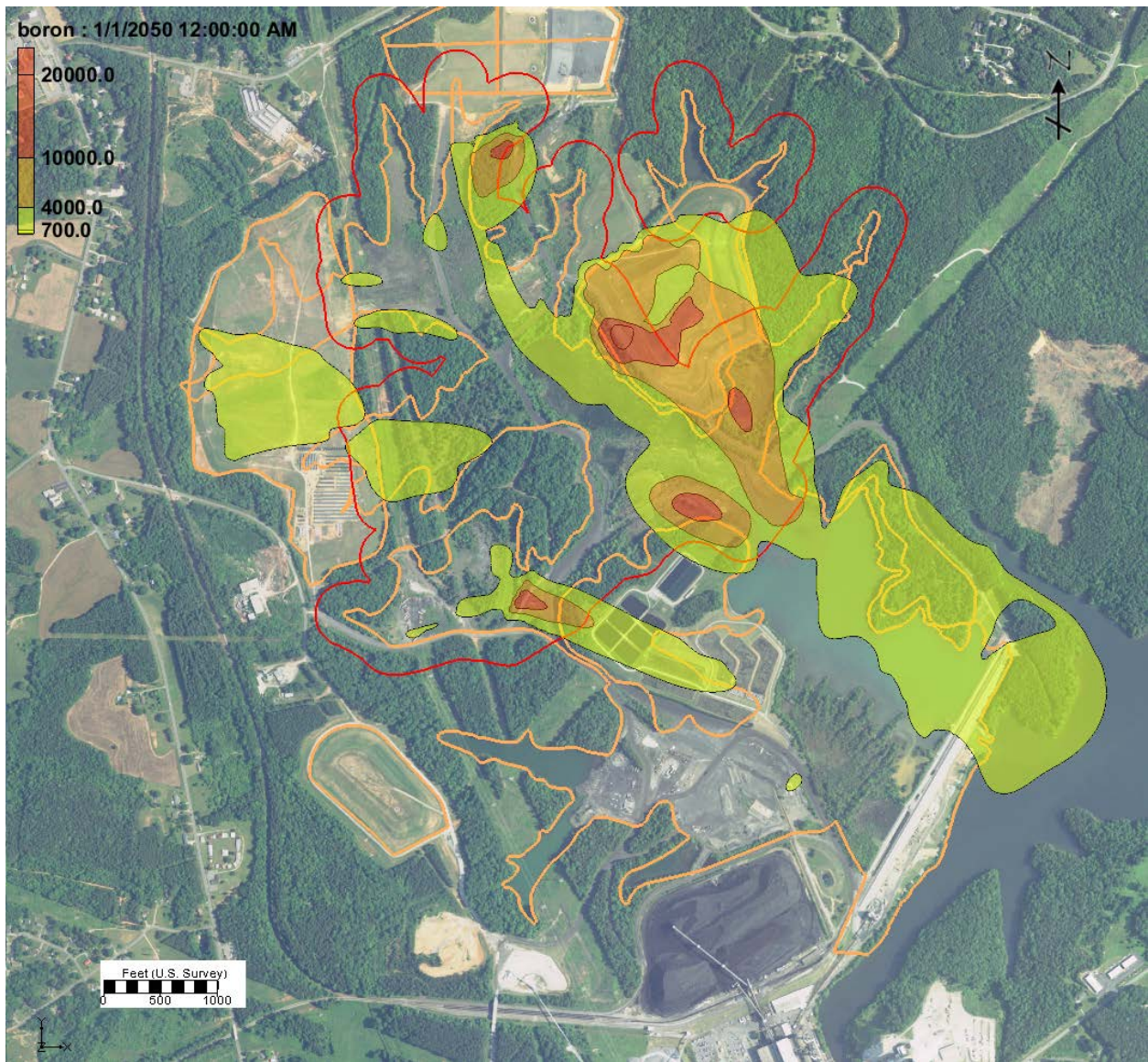


Figure 6-20a. Simulated boron concentrations in the upper bedrock (layer 9) in 2050 for the hybrid case. The red line is the potential compliance boundary and orange lines are waste boundaries and landfill boundaries.

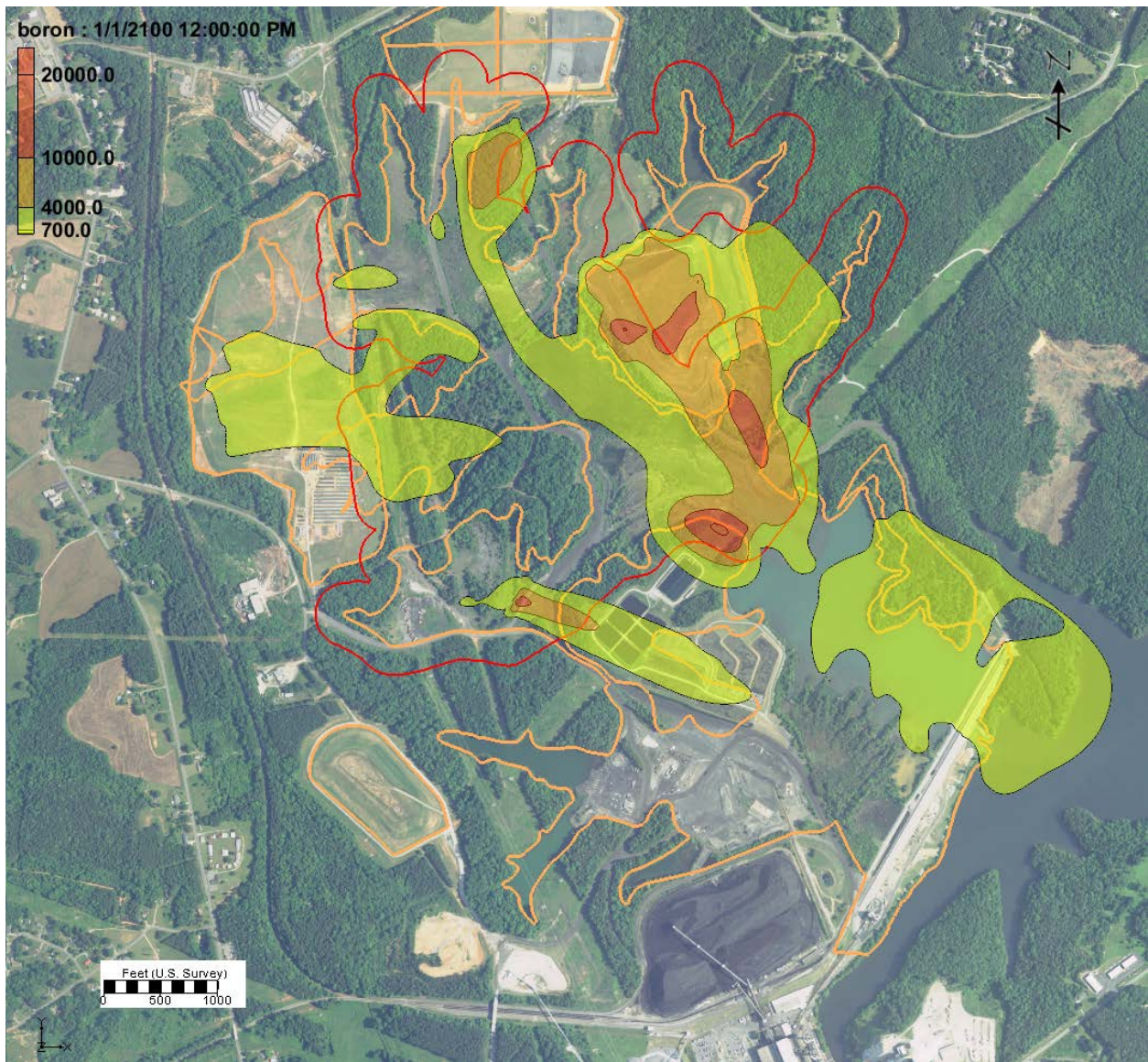


Figure 6-20b. Simulated boron concentrations in the upper bedrock (layer 9) in 2100 for the hybrid case. The red line is the potential compliance boundary and orange lines are waste boundaries and landfill boundaries.

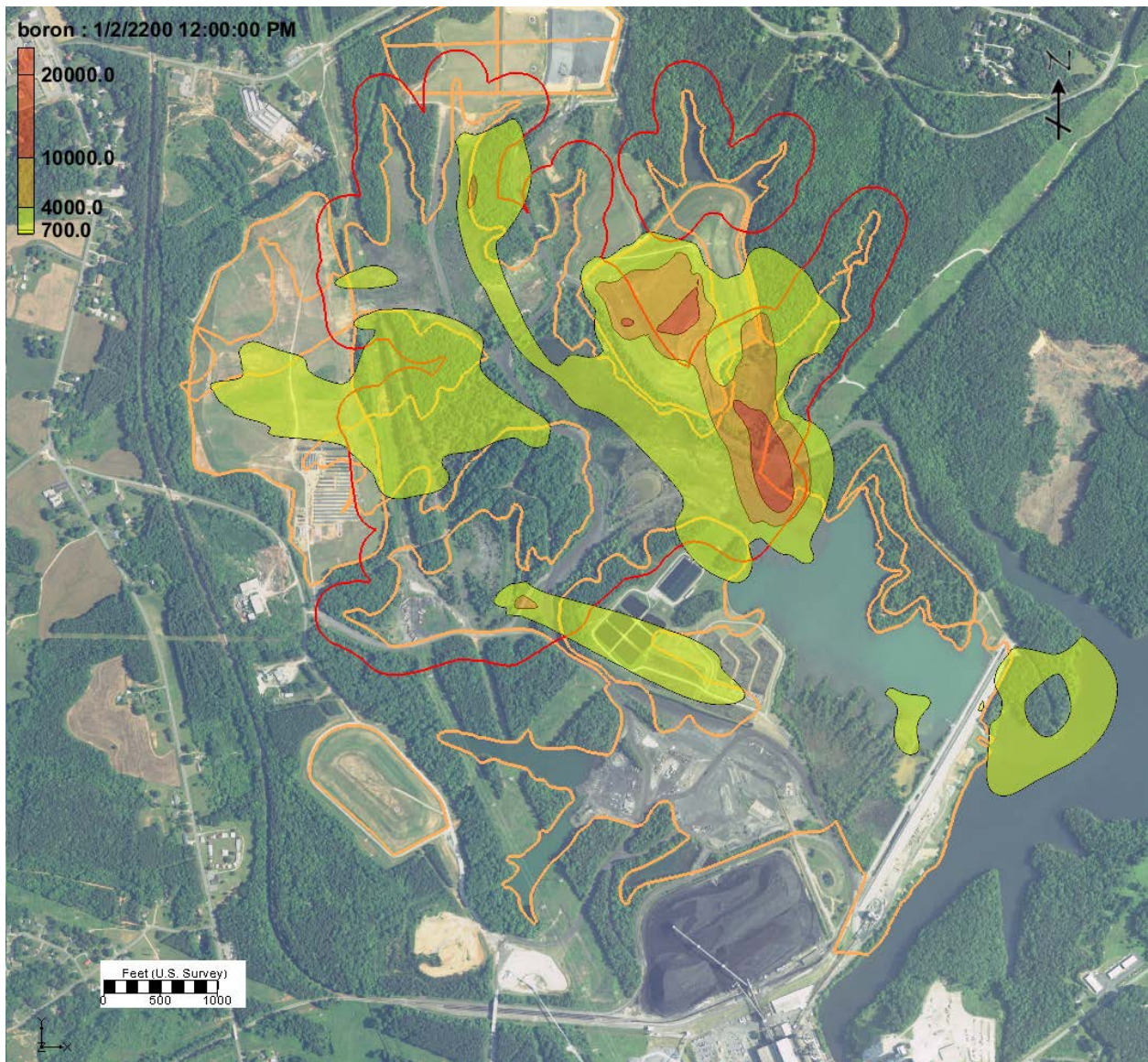


Figure 6-20c. Simulated boron concentrations in the upper bedrock (layer 9) in 2200 for the hybrid case. The red line is the potential compliance boundary and orange lines are waste boundaries and landfill boundaries.

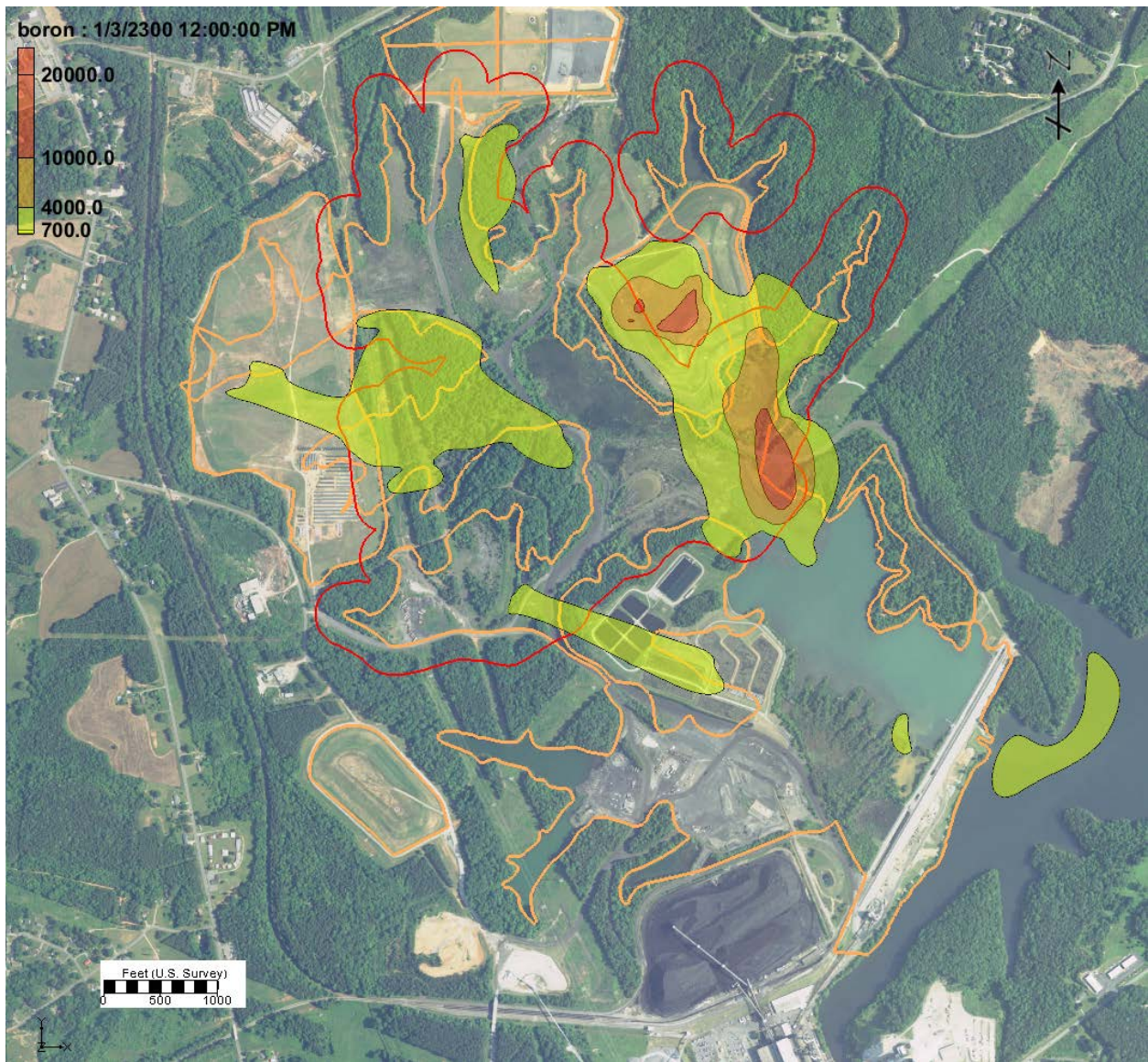


Figure 6-20d. Simulated boron concentrations in the upper bedrock (layer 9) in 2300 for the hybrid case. The red line is the potential compliance boundary and orange lines are waste boundaries and landfill boundaries.

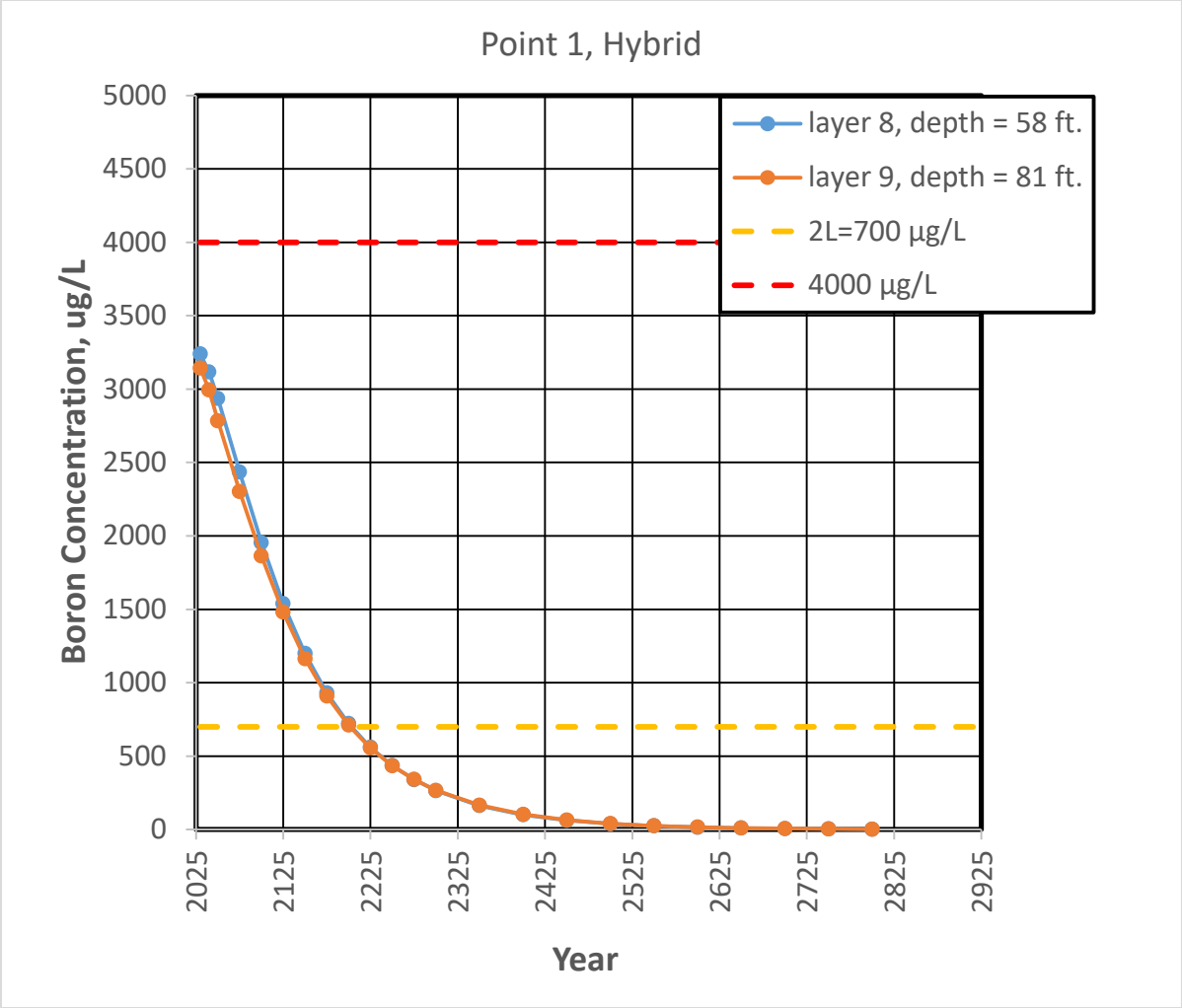


Figure 6-21. Predicted boron concentrations at point 1 near Lake Norman for the hybrid case.

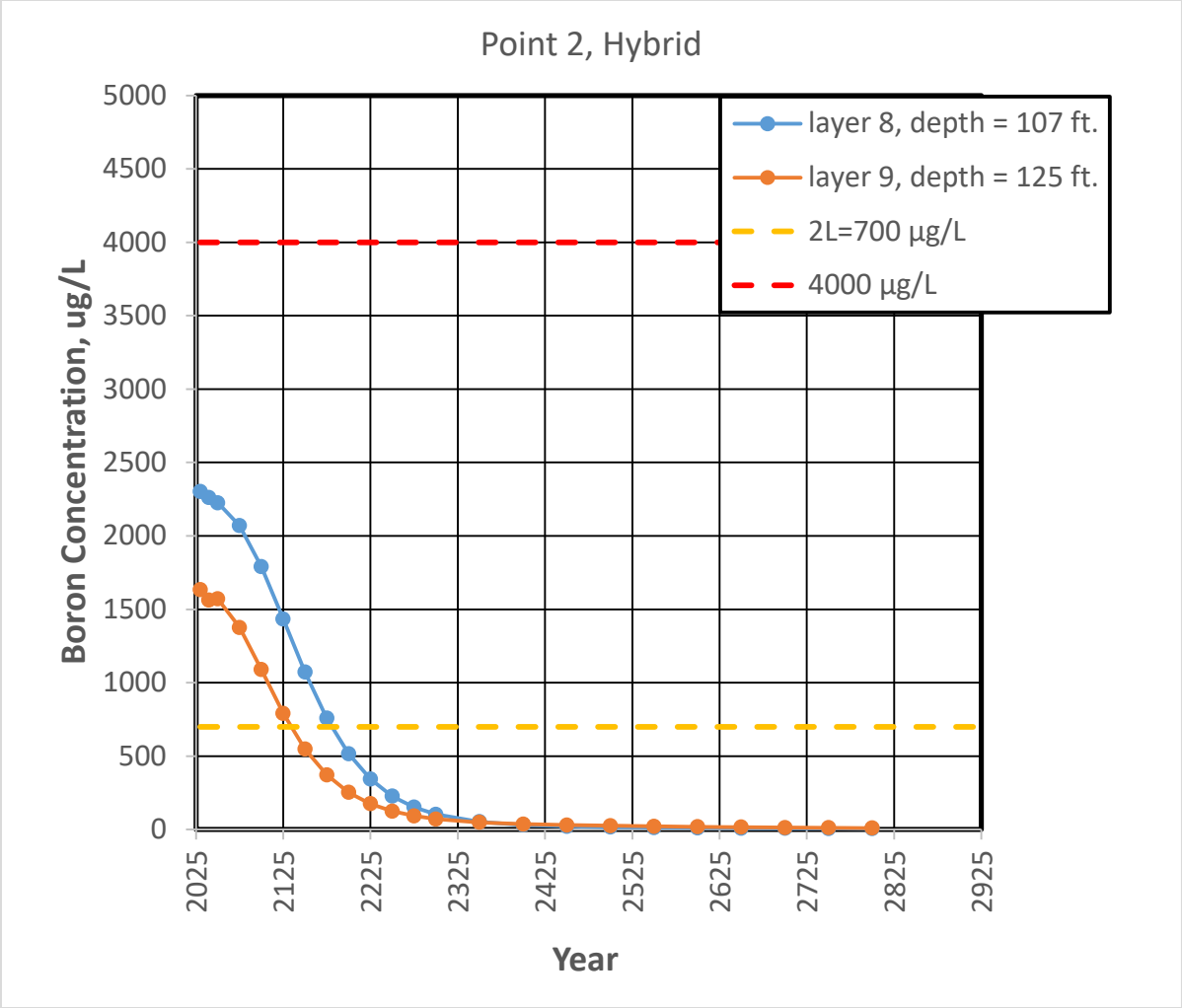
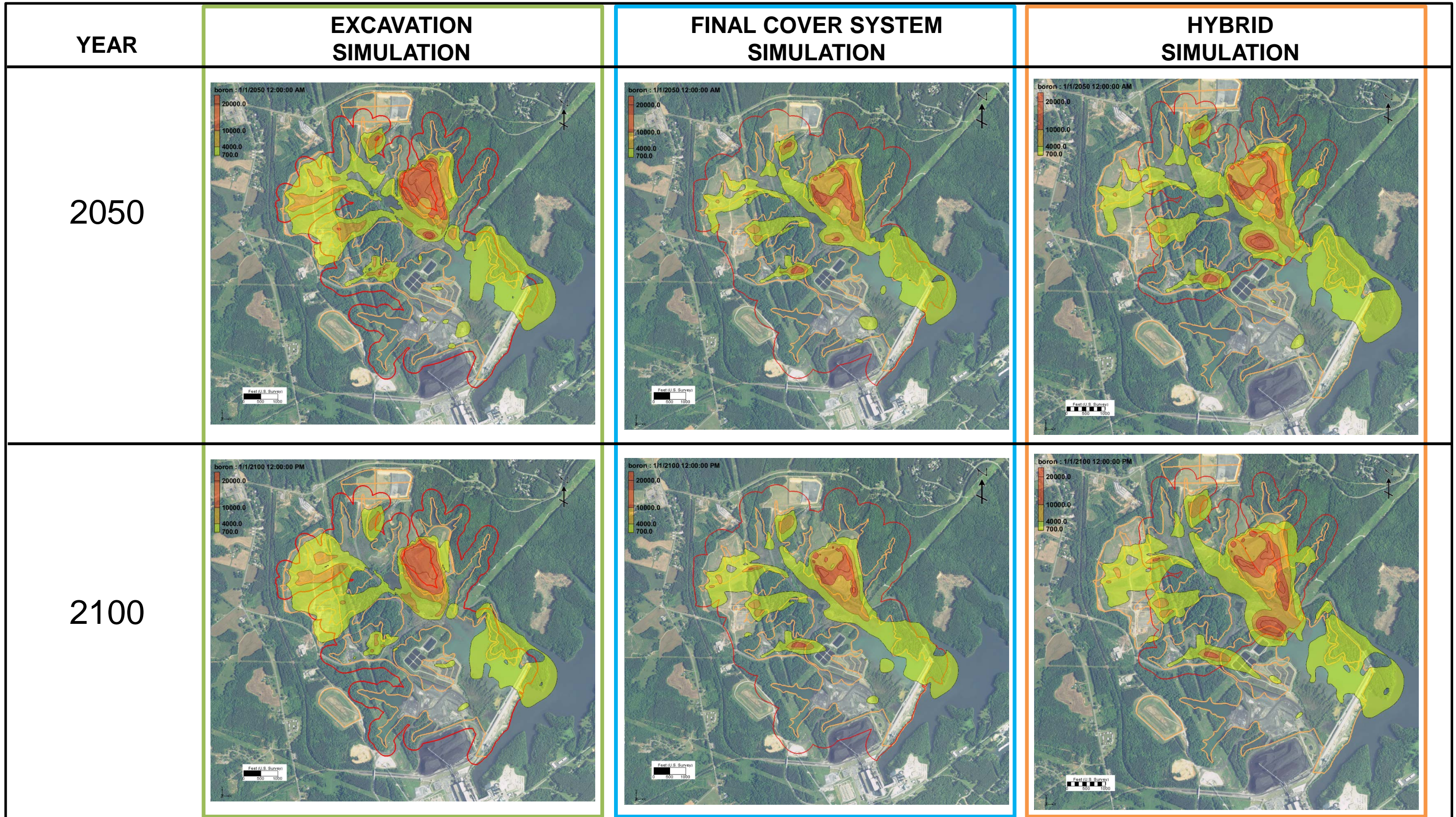


Figure 6-22. Predicted boron concentrations at location 2 east of the Phase I ash landfill for the hybrid case.

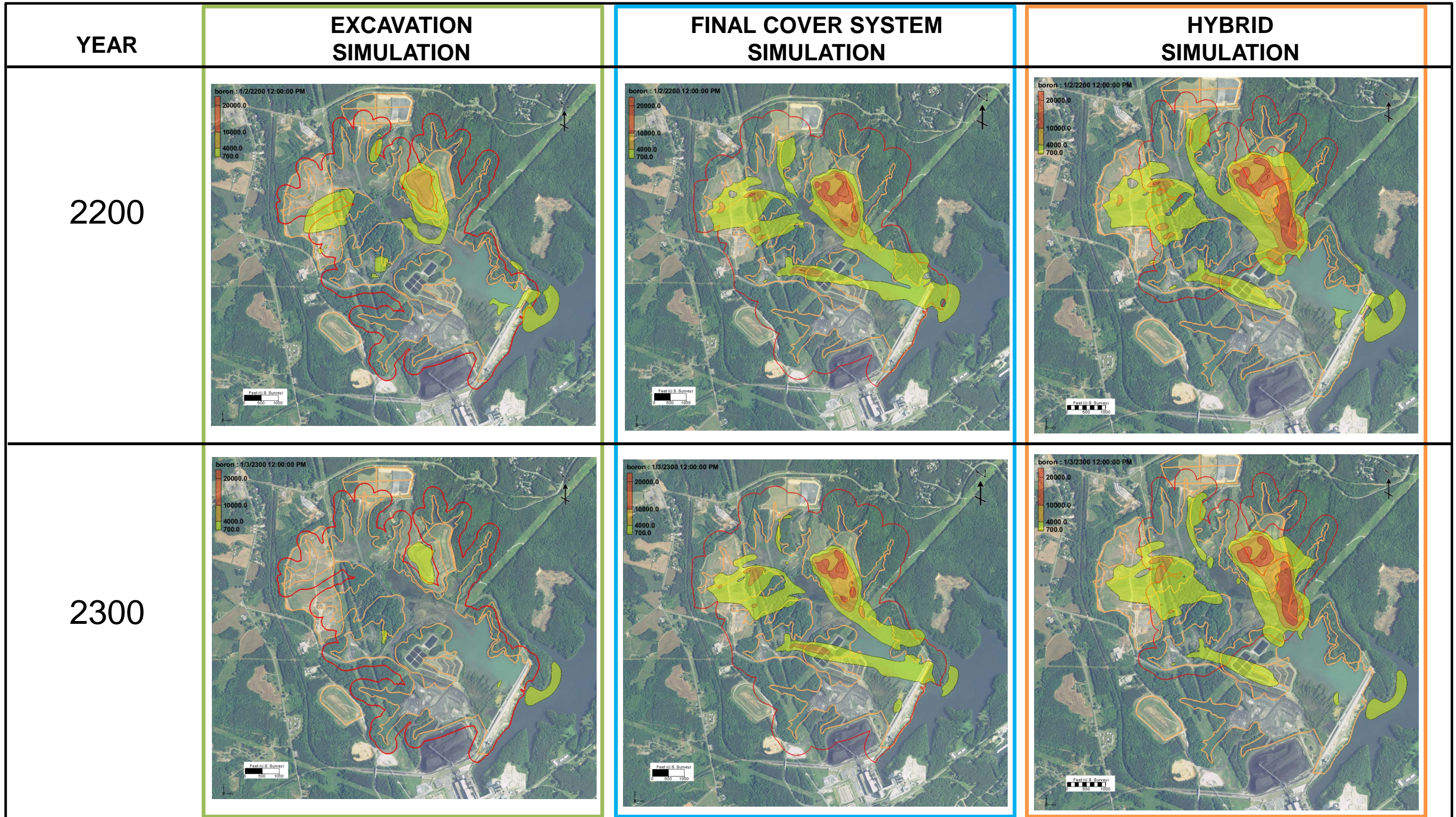


NOTES:
THE START DATES FOR THE THREE MODEL SCENARIOS ARE BASED ON THE COMPLETION DATES FOR THOSE ACTIVITIES. THESE DATES ARE:

- EXCAVATION – YEAR 2038
- FINAL COVER SYSTEM – YEAR 2030
- HYBRID – YEAR 2030

THE EXISTING AND POTENTIAL COMPLIANCE BOUNDARIES FOR THE DIFFERENT SIMULATION SCENARIOS ARE SHOWN IN RED, THE WASTE BOUNDARIES ARE SHOWN IN GOLD.

FIGURE 6-23
COMPARISON OF CLOSURE OPTIONS FOR THE
TRANSITION FLOW ZONE
MODEL YEARS 2050 AND 2100
MARSHALL STEAM STATION
DUKE ENERGY CAROLINAS, LLC
TERRELL, NORTH CAROLINA

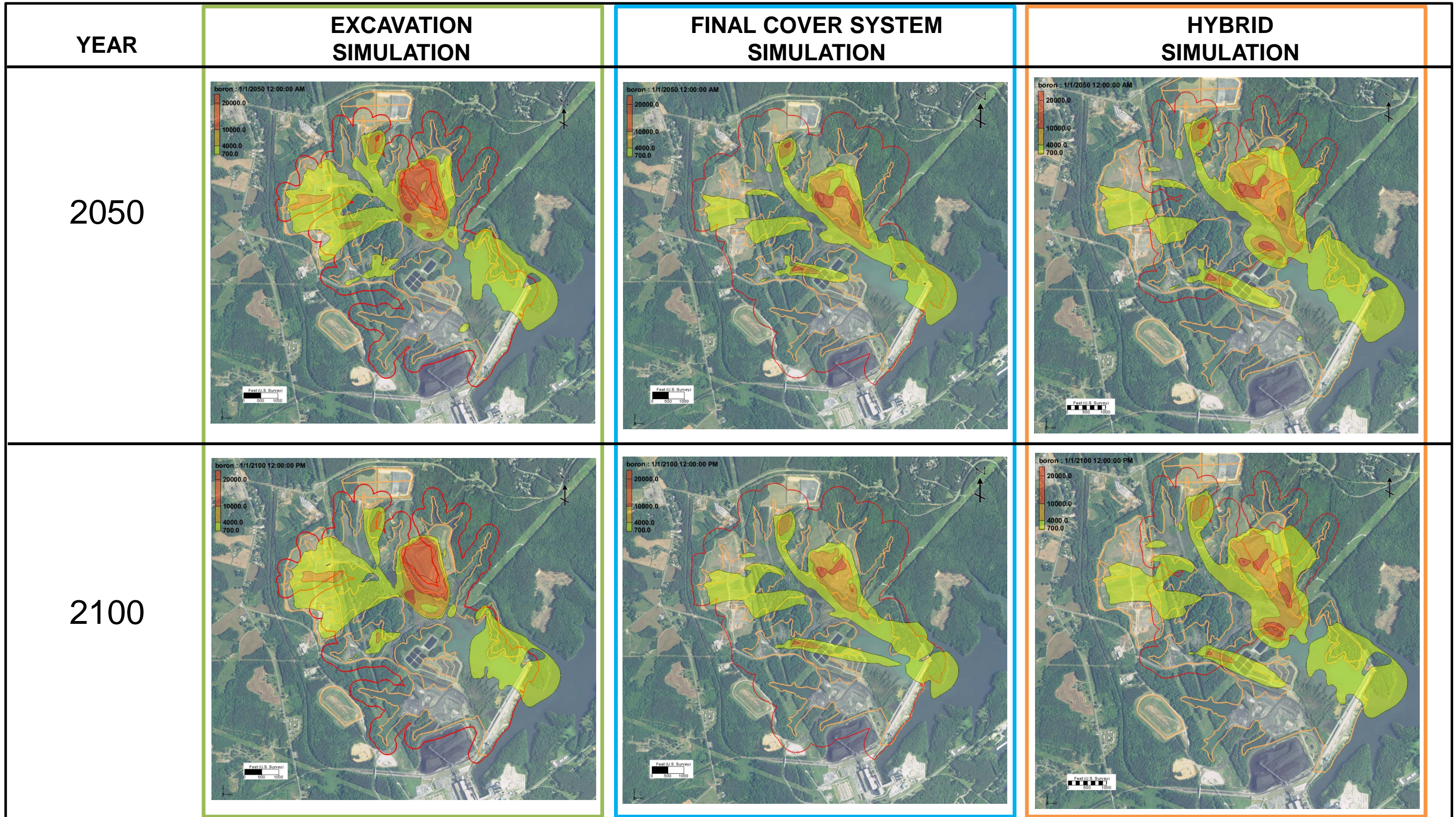


NOTES:
 THE START DATES FOR THE THREE MODEL SCENARIOS ARE BASED ON THE COMPLETION DATES FOR THOSE ACTIVITIES. THESE DATES ARE:

- EXCAVATION – YEAR 2038
- FINAL COVER SYSTEM – YEAR 2030
- HYBRID – YEAR 2030

THE EXISTING AND POTENTIAL COMPLIANCE BOUNDARIES FOR THE DIFFERENT SIMULATION SCENARIOS ARE SHOWN IN RED, THE WASTE BOUNDARIES ARE SHOWN IN GOLD.

FIGURE 6-24
COMPARISON OF CLOSURE OPTIONS FOR THE
TRANSITION FLOW ZONE
MODEL YEARS 2200 AND 2300
MARSHALL STEAM STATION
DUKE ENERGY CAROLINAS, LLC
TERRELL, NORTH CAROLINA

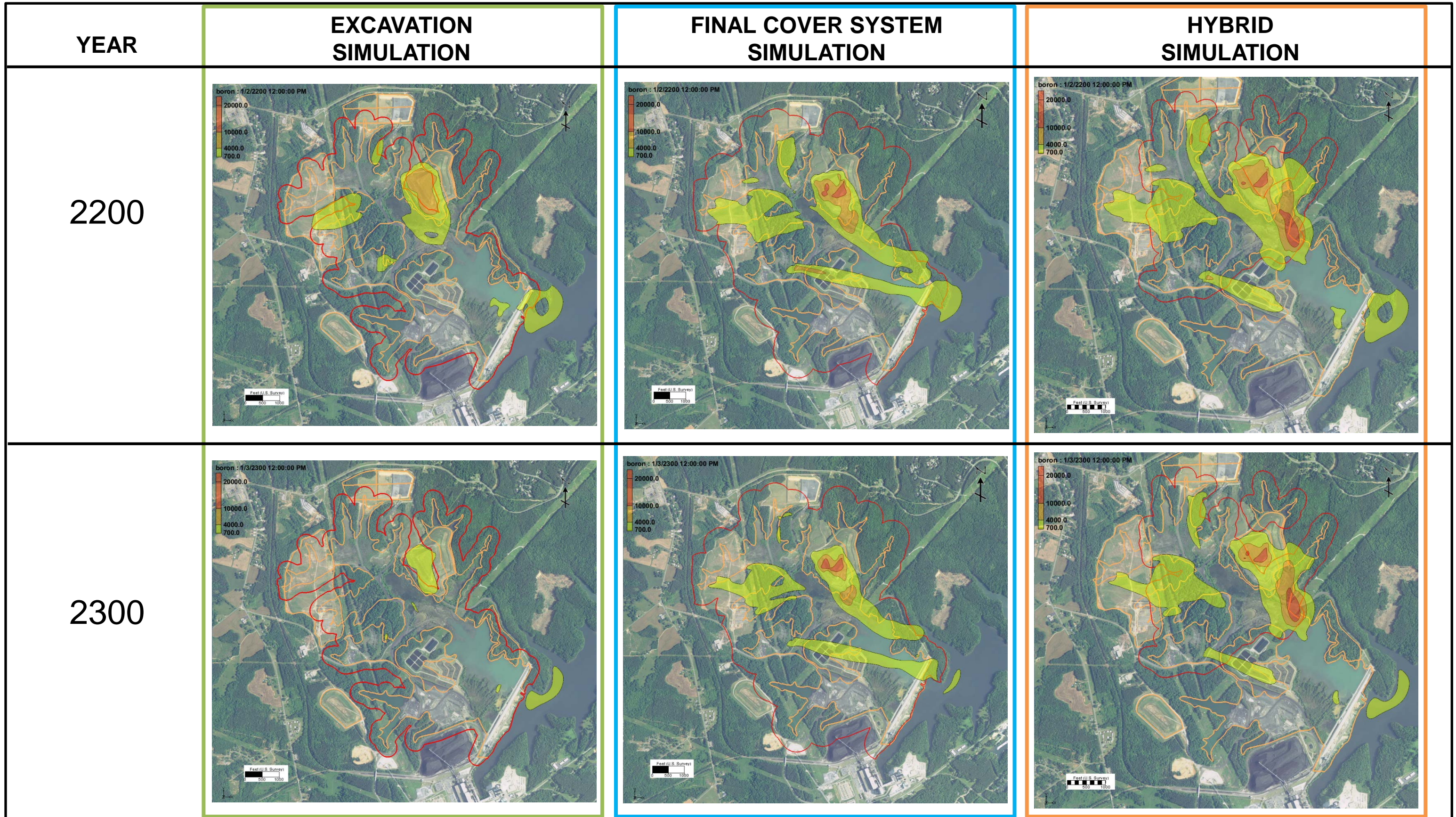


NOTES:
THE START DATES FOR THE THREE MODEL SCENARIOS ARE BASED ON THE COMPLETION DATES FOR THOSE ACTIVITIES. THESE DATES ARE:

- EXCAVATION – YEAR 2038
- FINAL COVER SYSTEM – YEAR 2030
- HYBRID – YEAR 2030

THE EXISTING AND POTENTIAL COMPLIANCE BOUNDARIES FOR THE DIFFERENT SIMULATION SCENARIOS ARE SHOWN IN RED, THE WASTE BOUNDARIES ARE SHOWN IN GOLD.

FIGURE 6-25
COMPARISON OF CLOSURE OPTIONS FOR THE
UPPER BEDROCK FLOW ZONE
MODEL YEARS 2050 AND 2100
MARSHALL STEAM STATION
DUKE ENERGY CAROLINAS, LLC
TERRELL, NORTH CAROLINA



NOTES:
THE START DATES FOR THE THREE MODEL SCENARIOS ARE BASED ON THE COMPLETION DATES FOR THOSE ACTIVITIES. THESE DATES ARE:

- EXCAVATION – YEAR 2038
- FINAL COVER SYSTEM – YEAR 2030
- HYBRID – YEAR 2030

THE EXISTING AND POTENTIAL COMPLIANCE BOUNDARIES FOR THE DIFFERENT SIMULATION SCENARIOS ARE SHOWN IN RED, THE WASTE BOUNDARIES ARE SHOWN IN GOLD.

FIGURE 6-26
COMPARISON OF CLOSURE OPTIONS FOR THE
UPPER BEDROCK FLOW ZONE
MODEL YEARS 2200 AND 2300
MARSHALL STEAM STATION
DUKE ENERGY CAROLINAS, LLC
TERRELL, NORTH CAROLINA